Synthesis, Molecular Docking Studies and Evaluation of Antibacterial and Antioxidant Activities Fluoroquinoline Derivatives

Mona Fekadu Abera

A Thesis Submitted to

The Department of Applied Chemistry

School of Applied Natural Sciences

Presented in Partial Fulfillment of the Requirement for the Degree of Master's in Applied Chemistry

Office of Graduate Studies

Adama Science and Technology University

July, 2021

Adama, Ethiopia

Synthesis, Molecular Docking Studies and Evaluation of Antibacterial and Antioxidant Activities of Fluoroquinoline Derivatives

Mona Fekadu Abera

Major Advisor: Yadessa Melaku (PhD)

Co-advisor: Anuradha Gayanty (PhD)

A Thesis Submitted to
The Department of Applied Chemistry
School of Applied Natural Sciences
Presented in Partial Fulfillment of the Requirement for the Degree of Master's in Applied Chemistry

Office of Graduate Studies
Adama Science and Technology University

July, 2021
Adama, Ethiopia

Approval Sheet

I/we, the advisors of the thesis entitled “Synthesis, Molecular Docking Studies and Evaluation of Antibacterial and Antioxidant Activities of Fluoroquinoline Derivatives” and developed by Mona Fekadu Abera hereby certify that the recommendation and suggestions made by the board of examiners are appropriately incorporated into the final version of the thesis.

Major Advisor	Signature	Date
Co-advisor	Signature	Date

We, the undersigned, members of the Board of Examiners of the thesis by Mona Fekadu Abera have read and evaluated the thesis entitled “Synthesis, Molecular Docking Studies and Evaluation of Antibacterial and Antioxidant Activities of Fluoroquinoline Derivatives” and examined the candidate during open defense. This is, therefore, to certify that the thesis is accepted for partial fulfillment of the requirement of the degree of Master of Science in Applied Chemistry.

Chairperson	Signature	Date
Internal Examiner	Signature	Date
External Examiner	Signature	Date

Final approval and acceptance of the thesis is contingent upon submission of its final copy to the Office of Postgraduate Studies (OPGS) through the Department Graduate Council (DGC) and School Graduate Committee (SGC).

Department Head	Signature	Date
School Dean	Signature	Date
Office of Postgraduate Studies, Dean	Signature	Date

Declaration

I hereby declare that this Master Thesis entitled “Synthesis, Molecular Docking Studies and Evaluation of Antibacterial and Antioxidant Activities of Fluoroquinoline Derivatives” is my original work. That is, it has not been submitted for the award of any academic degree, diploma or certificate in any other university. All sources of materials that are used for this thesis have been duly acknowledged through citation.

_____	_____	_____
Name of the student	Signature	Date

Recommendation

I/we, the advisors of this thesis, hereby certify that I/we have read the revised version of the thesis entitled “Synthesis, Molecular Docking Studies and Evaluation of Antibacterial and Antioxidant Activities of Fluoroquinoline Derivatives” prepared under my/our guidance by Mona Fekadu Abera submitted in partial fulfillment of the requirements for the degree of Masters of Science in Applied Chemistry. Therefore, I/we recommend the submission of revised version of the thesis to the department following the applicable procedures.

_____	_____	_____
Major Advisor	Signature	Date
_____	_____	_____
Co-advisor	Signature	Date

ACKNOWLEDGMENTS

First of all, I would like to thanks the almighty God, the most gracious and merciful who gave me the strength, health and patience with his handful blessing to complete this study. Second, I would like to express my deepest appreciation and sincere gratitude to my advisor, Dr. Yadessa Melaku for his kind encouragement, innovative ideas, guidance, support and supervisions, starting from proposal writing to the completion of this thesis.

I would also like to thanks my Co-Advisor Dr. Anuradha. G, for her continuous technical, constructive advice, useful discussion, continuous guidance, friendly treatment, encouragement, frequently visits to our laboratory and careful supervision from the starting to the end of works.

My Special thanks to Dr. Raja Laxamanan Eswarmoorthy for his guidance and help in the molecular docking studies.

I would like to thanks Haramaya University College of Health and Medical Science, School of Pharmacy for giving me the sponsorship opportunity to continue my post graduate study and Adama Science and Technology University, School of Applied Natural Science, Department of Chemistry to facilitating all necessary things and fund that access to NMR Spectrometer in Addis Ababa University for this research.

I would also like to extend my thanks to Oromia Public Health Research and referral laboratory center for their acceptance and kindness to the request for antibacterial Activity and completely helped me in all aspects.

My special thanks goes to my family, for providing me the infinite love and inducement during all steps of my life.

In my daily work I have been blessed with a friendly and cheerful group of fellow students. Words are inadequate to express my heartfelt gratitude to my colleagues; Digafie Zeleke (PhD), Mr. Beyan Abdi, Mr. Fitsum Lemilemu, Mr. Demis Zelelew, Mr. Mamaru Bitew and Mr. Tadewos Damena with whom I have spent many memorable occasions and who have been very helpful and supportive both in personal and academic. My sincere thanks to all others who gave me valuable suggestions, materials and Chemicals during the research work.

CONTENTS

ACKNOWLEDGMENTS iv
LIST OF TABLES viii
LIST OF FIGURES ix
LIST OF SCHEMES xi
LIST OF APPENDICES xii
LIST OF ABBREVIATIONS xiv
ABSTRACT xv
CHAPTER ONE 1
Introduction 1
1.1. Background 1
1.2. Statement of the problem 3
1.3. Objectives of the Study 4
1.3.1. General Objective 4
1.3.2. Specific Objectives 4
1.4. Significance of the Study 4
CHAPTER TWO 5
Literature Review 5
2.1. Synthesis of Quinoline Derivatives 5
2.1.1. Conrad-Limpach Quinoline Synthesis 6
2.1.2. Combes Quinoline Synthesis 7
2.1.3. Doebner-Miller Quinoline Synthesis 7
2.1.4. Skraup Quinoline Synthesis 7
2.1.5. Pfitzenger Quinoline Synthesis 8
2.1.6. The Knorr Quinoline Synthesis 8
2.1.7. Friedlander Quinoline Synthesis 9
2.1.8. Vilsmeier Haack Quinoline Synthesis 9
2.2. Biological Activities of Quinoline Derivatives 10
2.2.1. Antibacterial Activity 10
2.2.2. Anticancer Activity 14
2.2.3. Anti-inflammatory Activity 16
2.2.4. Antifungal Activity 17

2.2.5. Antiviral Activity 17
2.2.6. Antimalarial Activity 18
2.2.7. Anticonvulsant Activity 19
2.2.8. Antimycobacterial Activity 20
2.3. Radical Scavenging Activity 21
2.4. Molecular Docking Studies 22
2.5. *In silico* drug likeness prediction 23
CHAPTER THREE 25
Materials and Methods 25
3.1. General 25
3.2. Chemicals and equipment 25
3.3. Experimental Procedures 25
3.3.1. Synthesis of some derivatives of fluoroquinoline 25
3.3.1.1. Synthesis of 2-Chloro-6-fluoro quinoline-3-carbaldehyde (86) 25
3.3.1.2. Synthesis of 6-fluoro-2-methoxy quinoline-3-carbaldehyde (87) 26
3.3.1.3. Synthesis of 2-ethoxy-6-flouro- quinoline-3-carbaldehyde (88) 27
3.3.1.4. Synthesis of 6-fluoro-2-thiocyanatoquinoline-3-carbaldehyde (89) 27
3.3.1.5. Synthesis of 2-((2-hydroxyethyl) amino)-3-(-2-(ethylideneamino) ethanol quinoline (90) 28
3.3.1.6. Synthesis of 6-fluoro-N-phenyl-3-((phenylimino) methyl) quinolin-2-amine (91) 28
3.3.1.7. Synthesis of 2-methoxyquinoline-3-carboxylic acid (96) 28
3.3.1.8. Synthesis of methyl 2-chloroquinoline-3-carboxylate (97) 29
3.3.2. Characterization of synthesized compounds 30
3.3.3. Determination of Antibacterial Activity 30
3.3.4. DPPH Radical Scavenging Activity 30
3.3.5. Molecular Docking Analysis 31
CHAPTER FOUR 32
RESULTS AND DISCUSSIONS 32
4.1. Synthesis of the target compounds 32
4.2. Characterization of Synthesized Compounds 34
4.2.1. 2-Chloro-6-fluoroquinoline-3-carbaldehyde (86) 36
4.2.2. 6-Fluoro-2-methoxyquinoline-3-carbaldehyde (87) 37
4.2.3. 2-Ethoxy-6-fluoroquinoline-3-carbaldehyde (88) 39

4.2.4. 6-Fluoro-2-thiocyanatoquinoline-3-carbaldehyde (89) 40
4.2.5.2-((2-Hydroxyethyl) amino)-3-(-2-(ethylideneamino) ethanol quinoline (90) 42
4.2.6. 6-Fluoro-N-phenyl-3-((E)-(phenylimino) methyl) quinolin-2-amine (91) 44
4.2.7. 2-Methoxyquinoline-3-carboxylic acid (96) 46
4.2.8. Methyl 2-chloroquinoline-3-carboxylate (97) 48
4.3. Antibacterial Activity of Synthesized Compound 50
4.4. Molecular Docking Studies of the Synthesized Compounds 54
4.4.1. Molecular docking studies of synthesized compounds against *E.coli* DNA gyrase B 54
4.4.2. Molecular docking value of synthetic compounds against Human Topoisomerase IIα 56
4.5. *In silico* drug likeness prediction 70
4.6. Radical Scavenging Activity of the Synthesized Compounds 73
5. CONCLUSION AND RECOMMENDATION 76
5. 1. Conclusion 76
5.2. Recommendation 77
6. REFERENCES 79
7. APPENDICES 84

LIST OF TABLES

Table 1: Physical Characterization and % Yield of the synthesized compounds.....35
Table 2:^{1}H, ^{13}C-NMR and DEPT-135 spectral data of compound **86**.....37
Table 3:^{1}H, ^{13}C-NMR and DEPT-135 spectral data of compound **87**.....38
Table 4:^{1}H, ^{13}C-NMR and DEPT-135 spectral data of compound **88** 40
Table 5:^{1}H, ^{13}C-NMR and DEPT-135 spectral data of compound **89**.....41
Table 6:^{1}H, ^{13}C-NMR and DEPT-135 spectral data of compound **90**.....43
Table 7:^{1}H, ^{13}C-NMR and DEPT-135 spectral data of compound **91**.....45
Table 8:^{1}H, ^{13}C-NMR and DEPT-135 spectral data of compound **96**.....47
Table 9:^{1}H, ^{13}C-NMR and DEPT-135 spectral data of compound **97** 49
Table 10: Inhibition zone of synthesized compounds in mm (mean ± SD). 51
Table 11: Comparing inhibition zone (mm) of some synthesized compounds with similar compound from literature review 53
Table 12: Molecular Docking value of synthesized compounds against E.coli DNA gyrase B (PDB ID: 6F86): 55
Table 13: Molecular docking value of synthetic compounds against Human Topoisomerase IIα (PDB ID: 4fm9).....57
Table 14: Molecular docking value of synthetic compounds against human peroxidoxin (PDB ID: 1HD2).....58
Table 15: Drug-likeness predictions of compounds, computed by SwissADME.....71
Table 16: ADME predictions of compounds, computed by SwissADME and PreADMET 72
Table 17: Toxicity prediction of compounds, computed by Pro-Tox II and OSIRIS Property Explorer. 73
Table 18: Percentage inhibition of compound and ascorbic acid and IC_{50} 74
Table 19: Radical scavenging activity comparism of synthesized compounds with similar compounds from literature 75

LIST OF FIGURES

Figure 1: Chemical Structure of Quinoline 2
Figure 2: Quinoline derivatives with bactericidal effects 12
Figure 3: Quinoline derivatives with antibacterial activity 13
Figure 4: Series of quinoline derivatives with their IZ 14
Figure 5: Quinoline derivatives with anticancer activity 15
Figure 6: Quinolines with anticancer activities against HeLa, HT29, and C6 tumor cell lines 15
Figure 7: C-2-substituted quinolines having anticancer activity 15
Figure 8: Anti-breast cancer agents from substituted quinolines 16
Figure 9: Quinoline derivatives having anti-inflammatory activity 16
Figure 10: Quinoline derivatives having antifungal activity 17
Figure 11: Quinoline scaffold with antiviral activity 18
Figure 12: Structures of quinoline and common quinolone with antimalarial. 19
Figure 13: Quinoline derivatives having anticonvulsant activity 20
Figure 14: Anti mycobacterial of quinoline derivatives 20
Figure 15:2-Mercapto/2-selenobenzoih] quinoline-3-carbaldehyde derivatives 22
Figure 16: Structure of 1, 1-diphenyl-1-picrylhydrazyl (DPPH) 22
Figure 17:2-Chloro-6-fluoroquinoline-3-carbaldehyde (**86**) 36
Figure 18:6-Fuoro-2-methoxyquinoline-3-carbaldehyde (**87**) 37
Figure 19: 2-Ethoxy-6-fluoroquinoline-3-carbaldehyde (**88**) 39
Figure 20:6-Fluoro-2-thiocyanatoquinoline-3-carbaldehyde (**89**) 40
Figure 21:2-((2-Hydroxyethyl) amino)-3-(-2-(ethylideneamino) ethanol quinoline (**90**) 42
Figure 22:6-Fluoro-N-phenyl-3-((E)-(phenylimino) methyl) quinolin-2-amine (**91**) 44
Figure 23:2-Methoxyquinoline-3-carboxylic acid (**96**) 46
Figure 24: Methyl 2-chloroquinoline-3-carboxylate (**97**) 48
Figure 25: Inhibition zone (mm) of synthesized compounds at 200µg/mL.Error bar indicates standard deviation. 52
Figure 26: The binding interactions compound **86** against Human Topoisomerase IIα (PDB ID: 4fm9). 59

Figure 27: The binding interactions compound **87** against Human Topoisomerase IIα (PDB ID: 4fm9). 60
Figure 28: The binding interactions compound **88** against Human Topoisomerase IIα (PDB ID: 4fm9). 61
Figure 29: The binding interactions compound **89** against Human Topoisomerase IIα (PDB ID: 4fm9). 62
Figure 30: The 2D and 3D binding interactions of compound **89** against Human peroxiredoxin 5 (PDB ID: 1HD2). 63
Figure 31: The 2D and 3D binding interactions of Ascorbic Acid against Human peroxiredoxin 5 (PDB ID: 1HD2). 64
Figure 32: The binding interactions compound **90** against Human Topoisomerase IIα (PDB ID: 4fm9). 65
Figure 33: The binding interactions compound **91** against Human Topoisomerase IIα (PDB ID: 4fm9) 66
Figure 34: The binding interactions compound **96** against Human Topoisomerase IIα (PDB ID: 4fm9). 67
Figure 35: The binding interactions compound **97** against Human Topoisomerase IIα (PDB ID: 4fm9). 68
Figure 36: The binding interactions of vosaroxin against Human Topoisomerase IIα (PDB ID: 4fm9). 69
Figure 37: The percentage inhibition of the compounds and standard(Ascorbic acid) 74

LIST OF SCHEMES

Scheme 1: Synthesis of nalidixic acid 5
Scheme 2: Conrad Limpach Quinolines Synthesis 6
Scheme 3: Combes Quinoline Synthesis 7
Scheme 4: Doebner-Miller of Quinoline Synthesis 7
Scheme 5: Skraup Quinoline Synthesis 7
Scheme 6: Pfitzinger Quinoline Synthesis 8
Scheme 7: The Knorr Quinoline Synthesis 9
Scheme 8: Freidlander Quinoline Synthesis 9
Scheme 9: Vilsmeier Haack Quinoline Synthesis 10
Scheme 10: Synthesis of Quinoline by Vilsmeier Reaction 32
Scheme 11: Synthesis of fluoroquinoline derivatives 33
Scheme 12: Synthesis of quinoline derivatives 34

LIST OF APPENDICES

Appendix 1: ^{1}H NMR spectrum (400 MHz, $CDCl_3$) of 2-chloro-6-fluoroquinoline-3-carbaldehyde (**86**) 84

Appendix 2: ^{13}C NMR spectrum (100 MHz, $CDCl_3$) of 2-chloro-6-fluoroquinoline-3-carbaldehyde (**86**) 85

Appendix 3: The DEPT-135 NMR spectrum of 2-chloro-6-fluoroquinoline-3-carbaldehyde (**86**) 86

Appendix 4: ^{1}H NMR spectrum (400 MHz, $CDCl_3$) of 6-fluoro-2-methoxyquinoline-3-carbaldehyde (**87**) 87

Appendix 5: ^{13}C NMR spectrum (100 MHz, $CDCl_3$) of 6-fluoro-2-methoxyquinoline-3-carbaldehyde (**87**) 88

Appendix 6: DEPT-135 NMR spectrum of 6-fluoro-2-methoxyquinoline-3-carbaldehyde (**87**) . 89

Appendix 7: ^{1}H NMR spectrum (400 MHz, $CDCl_3$) of 2-ethoxy-6-fluoroquinoline-3-carbaldehyde (**88**) 90

Appendix 8: ^{13}C NMR spectrum (100 MHz, $CDCl_3$) of 2-ethoxy-6-fluoroquinoline-3-carbaldehyde (**88**) 91

Appendix 9: DEPT-135 NMR spectrum of 2-ethoxy-6-fluoroquinoline-3-carbaldehyde (**88**) 92

Appendix 10: ^{1}H NMR spectrum (400 MHz, $CDCl_3$) of 6-fluoro-2-thiocyanatoquinoline-3-carbaldehyde (**89**) 93

Appendix 11: ^{13}C NMR spectrum (100 MHz, $CDCl_3$) of 6-fluoro-2-thiocyanatoquinoline-3-carbaldehyde (**89**) 94

Appendix 12: DEPT-135 NMR spectrum of 6-fluoro-2-thiocyanatoquinoline-3-carbaldehyde (**89**) 95

Appendix 13: ^{1}H NMR spectrum (400 MHz, $CDCl_3$) of 2-((2-hydroxyethyl) amino)-3-(-2-(ethylideneamino) ethanol quinoline (**90**) 96

Appendix 14: ^{13}C NMR spectrum (100 MHz, $CDCl_3$) of 2-((2-hydroxyethyl) amino)-3-(-2-(ethylideneamino) ethanol quinoline (**90**) 97

Appendix 15: DEPT-135 NMR spectrum of 2-((2-hydroxyethyl) amino)-3-(-2-(ethylideneamino) ethanol quinoline (**90**) 98

Appendix 16: ^{1}H NMR spectrum (400 MHz, $CDCl_3$) of 6-fluoro-N-phenyl-3-((phenylimino) methyl) quinolin-2-amine (**91**) 99
Appendix 17: ^{13}C NMR spectrum (100 MHz, $CDCl_3$) of 6-fluoro-N-phenyl-3-((phenylimino) methyl) quinolin-2-amine (**91**) 100
Appendix 18: DEPT-135 NMR spectrum of 6-fluoro-N-phenyl-3-((phenylimino) methyl) quinolin-2-amine (**91**) 101
Appendix 19: ^{1}H NMR spectrum (400 MHz, $CDCl_3$) of 2-methoxyquinoline-3-carboxylic acid (**96**) 102
Appendix 20: ^{13}C NMR spectrum (100 MHz, $CDCl_3$) of 2-methoxyquinoline-3-carboxylic acid (**96**) 103
Appendix 21: DEPT-135 spectrum of 2-methoxyquinoline-3-carboxylic acid (**96**) 104
Appendix 22: ^{1}H NMR spectrum (400 MHz, $CDCl_3$) methyl 2-chloroquinoline-3-carboxylate (**97**) 105
Appendix 23: ^{13}C NMR spectrum (100 MHz, $CDCl_3$) of methyl 2-chloroquinoline-3-carboxylate (**97**) 106
Appendix 24: DEPT-135 spectrum of methyl 2-chloroquinoline-3-carboxylate (**97**) 107

LIST OF ABBREVIATIONS

ADMET:	Absorption, Distribution, Metabolism, Excretion, and Toxicity
DNA:	Deoxyribonucleic acid
DPPH:	1, 1-diphenyl-2-picryl hydrazyl
DVM:	Doebner-Von Miller quinoline synthesis
ED50:	Effective dose 50
GI50:	Concentration 50% growth inhibition
HBA:	H-bond acceptors
HBD:	H-bond donors
IC_{50}:	Inhibitory Concentration inhibiting 50% of growth
MD:	Molecular dynamics
MRSA:	Methicillin-resistant Staphylococcus aureus
MES:	Maximal electroshock test
NSAIDs:	Non-steroidal anti-inflammatory drugs
NMR:	Nuclear Magnetic Resonance
PDB:	Protein Data base
PfCRT:	P. falciparum resistance transporter
PI:	Protective index
PK/PD:	Pharmacokinetics/Pharmacodynamics
PLC:	Private Limited Company
Ro5:	Rule of Five
ROS:	Reactive oxygen species
SDR:	Single-drug-resistant
TD50:	Toxic dose 50
TLC:	Thin Layer Chromatography
VR:	Vilsmeier Reagents

ABSTRACT

*Quinoline is a ubiquitous structural feature that occurs in several natural compounds and pharmacologically active substances displaying a broad range of biological activities such as anti-bacterial, anti-malarial, anti-microbial, ant-inflammatory, anti-convulsant, anti-cancer and anti-mycobacterial activity. The aim of this project was to synthesize and evaluate antibacterial and antioxidant activities of the quinoline derivatives. In this project 8 quinoline derivatives were synthesized. The characterization of the synthesized compounds were carried out by melting point and spectroscopic technique ((UV-Vis, ^{1}H, ^{13}C and DEPT-135 NMR). The synthesized compounds were screened for their antibacterial activities by disc diffusion method against E. coli, S. aureus, S.pyogene and P. aeruginosa. Ciprofloxacin and DMSO were used as reference drugs and negative control, respectively. Compounds **86**, **87**, **88** and **89** showed antibacterial activity with IZ of 14.7±0.04 mm, 13.0±0.53mm, 13.2±0.3mm, and 12.9±0.33mm against S. pyogene, respectively, whereas compounds **90**, **96** and **97** showed IZ value of 10.4±0.66mm, 7.9±0.45mm, and 8.0±0.55mm against P. aeruginosa at 200 µg, respectively. Compound **91** showed IZ value of 11.1±0.07mm against E. coli at 200 µg all compared to ciprofloxacin with IZ of 18.2±0.34mm against S.pyogene, 10.0±0.45mm against P. aeruginosa and 11.1±0.07mm against E.coli at the same concentration. Molecular docking of synthesized compounds was assessed against DNA gyrase B and Human Topoisomerase IIα. The synthesized compounds were found to have binding affinity ranging from -6.8 to -7.5 (kcal/mol) with best result achieved for **87** (-7.2 kcal/mol), **88** (-7.2 kcal/mol), **91** (-7.4 kcal/mol) and **96** (-7.5 kcal/mol). Radical scavenging activity of synthesized compounds was evaluated using DPPH. Compounds **86, 87,88,89,90** and **91** have strong antioxidant activity with 62.5%, 61.43%, 71.12%, 73.32%, 57.78% and 66.09% respectively, compared to ascorbic acid 87.06%. From these compounds compound **89(**73.32 %,) was strong. IC_{50} varies from 5.31 µg/mL for compound **89** to 16.71 µg/mL for compound **96**. Compound **89 (**5.31 µg/mL) showed strong antioxidant activity. Hence compound **87, 88, 91** and **96** might be used for further studies.*

Keywords: *Quinoline, NMR, antioxidant, antibacterial, molecular docking, DNA gyrase B, Human Topoisomerase IIα*

CHAPTER ONE

Introduction

Quinolines are a new class of synthetic antibiotics with potent bactericidal, broad-spectrum activity against many clinically important pathogens which are responsible for variety of infections (Huang, 2019). The initial preparation of quinolines was applied as new drugs for antimicrobial activity. However, the structure modification and preparation of some derivatives from quinolines, allowed the discovery of new drugs for different diseases (Horta, 2019). This class of compounds are developed according to the structure development of designed drugs, like quinoline synthetic derivatives (Edijane, 2017). A number of researchers have synthesized and evaluated the biological activities of quinolines, showing its importance to obtaining new drugs (Clinton, 2015).

1.1. Background

Bacterial infections, which represent a significant health threat throughout the world, which are responsible for acquired infections and mortality in turn leads burden on global healthcare systems (Gao *et al*., 2019). While different therapies were used for the treatment of these infection, the introduction of antibiotic agents opened new avenues for the treatment of bacterial infections (Faisal *et al*., 2018).

Antimicrobial agent is an effective weapon to treat bacterial infections, while the dramatic increase in human-pathogenic bacteria that are resistant to one or multiple antibiotics is a grave threat to the global health. This problem is exacerbated by long-term use, abuse of antibiotics as well as a lack of development of new antibacterial agents (Gao *et al*., 2019). Quinolines are a group of compounds derived from a bicyclic aromatic fused six-membered heterocyclic nucleus containing one to four nitrogen atoms (Horta, 2019).

Quinolines and their derivatives are very important in medicinal chemistry because of their broad spectrum activities. In addition to the medicinal applications, quinolines have been employed in the study of bioorganic and bioorganometallic processes (Kaur, 2019).

Quinoline derivatives represent the major class of heterocycles, and a number of preparations have been known since the late 1800s. The quinoline ring system occurs in various natural products,

especially in alkaloids. The quinoline skeleton is often used for the design of many synthetic compounds with diverse pharmacological properties (Adam, 2019).

Quinoline is an important heterocyclic derivatives that serves as building block for many pharmacological synthesized compounds and possess various activities (Riahifard *et al*., 2017). The synthesis of the quinoline ring has been the subject of continued interest as several derivatives of this heterocyclic unit have been found to possess useful biological and pharmacological activities. Quinoline derivatives are very important in medicinal chemistry because of their wide occurrence in natural products and drugs. It is well known that replacement of hydrogen with fluorine frequently confers bioactivity to organic molecules (Alkadir *et al*, 2017).

Quinolines are heterocyclic aromatic compounds and are characterized by a double-ring structure composed of a benzene and a pyridine ring fused at two adjacent carbon atoms. The simplest member of the quinoline family is quinoline itself, a compound with molecular structure C_9H_7N represented in Figure 1 (Giardinieri *et al*., 2017)**.** The quinoline skeleton is often used for the design of many synthetic compounds with diverse pharmacological properties (Kouznetsov *et al*., 2018).

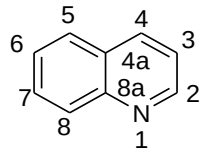

1

Figure 1: Chemical Structure of Quinoline

1.2. Statement of the problem

Public health has become a major concern due to the population explosion, an increase in endemic and epidemic diseases and microbial resistance.

The increase in resistance to many commercially produced synthetic antimicrobial agents by microorganisms has been increasing with time. This resulted by prolonged use of antimicrobials and antibiotics for therapeutic use. In spite the existence of a number of drugs that are used for the treatment of bacterial infections, the mortality and morbidity caused by microbes are increasing due to the increasing number of multidrug-resistant. Because of this treatment of microbial infection is a major emerging health issue. This has led to the search for new, cheap and effective antimicrobial agents with least side effects that can combat the increasing resistance by the pathogenic microbes (Harold, 2019).

Inspired by wide spectrum biological activities of quinoline derivatives as antibacterial and antioxidant agents, this project is intended towards synthesis, molecular docking studies and evaluation of antibacterial and antioxidant activities of fluoroquinoline derivatives.

1.3. Objectives of the Study

1.3.1. General Objective

The general objective of this project was to synthesize and evaluate *in silico* molecular docking studies, antibacterial and antioxidant activities of fluoroquinoline derivatives.

1.3.2. Specific Objectives

- ✓ To synthesize 6- fluoroquinoline derivatives
- ✓ To characterize the synthesized compounds using melting point, UV-Vis and NMR (^{1}H-NMR, ^{13}C-NMR).
- ✓ To evaluate antibacterial activity of the synthesized compound using disk diffusion method against selected Gram-negative, *Escherichia coli* and *Pseudomonas aeruginosa* and Gram positives, *Staphylococcus aureus* and *Streptococcus pyogenes.*
- ✓ To evaluate radical scavenging activity of synthesized compounds using DPPH assay.
- ✓ To conduct molecular docking studies of synthesized compounds against Human Topoisomerase IIα and DNA gyrase B by AutoDock Vina.

1.4. Significance of the Study

This study might be strongly built convenient synthetic routes leading to quinoline derivatives. Synthesis of the various bioactive molecules might be used as a references for researchers who intend to do research on a related synthetic protocol. It might be provide information about antibacterial, antioxidant and *in silico* molecular docking studies activities of synthesized derivatives. The research might also be useful in searching for drug lead candidates for further studies.

CHAPTER TWO

Literature Review

2.1. Synthesis of Quinoline Derivatives

Number of established protocols are there for the synthesis of quinoline ring, which can be well modified to prepare a number of differently substituted quinolines (Marella *et al*., 2017). There are many various synthetic routes for the formation of quinolines, but the great majority of that have been prepared by ring formation, rather than by transformation from other quinoline derivatives (Giardinieri *et al*., 2017).

The initial research with quinolines was the synthesis of the nalidixic acid in 1962, which presents very good antibacterial activity with gram-negatives bacteria (Kouznetsov *et al*., 2018).

Nalidixic acid **7,** 1-ethyl-1, 4-dihydro-7-methyl-4-hydroxy-1,8-naphthiridin-3-carboxilic acid, is synthesized method depicted in the Scheme 1. In the first stage reaction of 2-amino-6-methylpyridine **2** and diethyl ethoxymethylenemalonate **3** forms the substituted product **4,** which when heated cyclizes to ethyl ester of 4-hydroxy -7- methyl 1,8-naphtiridin -3-carboxilic acid **5.** Hydrolyzing the resulting product with base gives corresponding acid **6.** Alkylating this with ethyl iodide in the presence of sodium hydroxide gives nalidixic acid **7** (Mohammed *et al*., 2018).

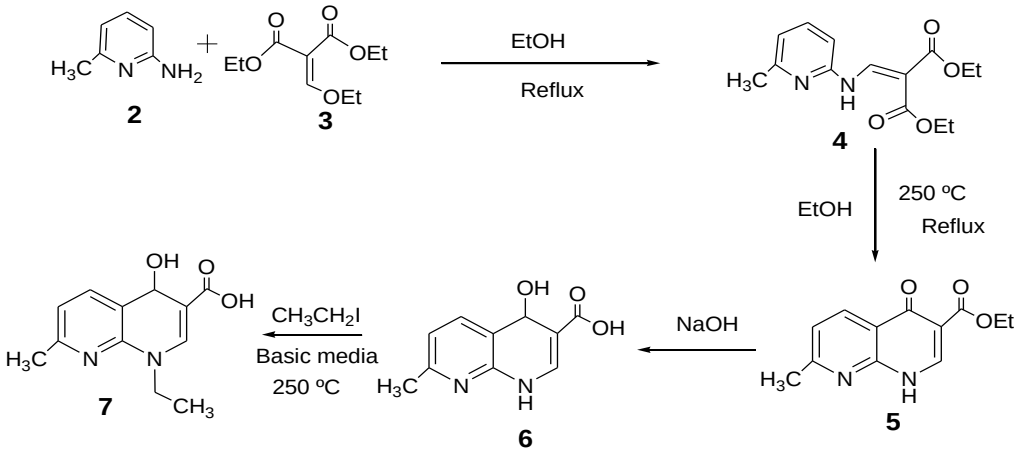

Scheme 1: Synthesis of nalidixic acid

After the discovery of nalidixic acid **7**, new compound was developed by substitution of the ethyl group bounded to the nitrogen atom and with modifications of the aromatic ring, affording several new drugs with antimicrobial activity. These new compounds were very efficient antimicrobial agents with more potent activity against the many number of gram-positive and gram-negative microorganisms (Andersson, 2018)

2.1.1. Conrad-Limpach Quinoline Synthesis

The original Conrad and Limpach synthesis, with one major modification, has been more widely used compared to any other route to quinolines. Limpach at first used paraffin oil as the cyclization medium, but then boiling diphenyl ether or a mixture of diphenyl ether with diphenyl (Dowtherm) has been reported as superior (Andersson, 2018). For Conrad-Limpach method of Quinoline synthesis reaction a minimum time at high temperature, such as 260-280℃ is required. Furthermore the common practice has been to add a solution of the amino-acrylate to preheated cyclization medium, preferably maintaining high dilution, after that cyclization is completed in a few minutes. Older procedures using acid catalysts or heating without solvents gave much poorer yields (Giardinieri *et al*., 2017). The method Conrad-Limpach to obtain quinolines carried out as shown in scheme 2 with condensation of primary aniline **8** with acetoacetic ester **9** to yield a Schiff base intermediate **10** and following the reaction is executed at high temperature in acidic media to obtain the hyrdoxy quinolines **12** (Edijane *et al*, 2017).

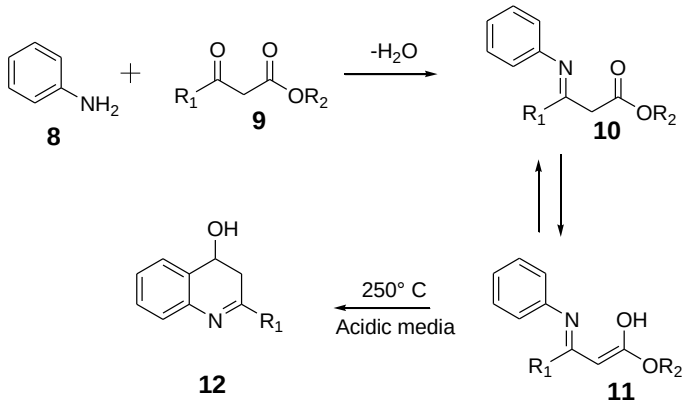

Scheme 2: Conrad Limpach Quinolines Synthesis

2.1.2. Combes Quinoline Synthesis

It is acid catalyzed condensation reaction of anilines **8** and *β* diketones **13** to assembles quinolines **14** as shown in scheme 3 (Jabeen *et al*., 2019).

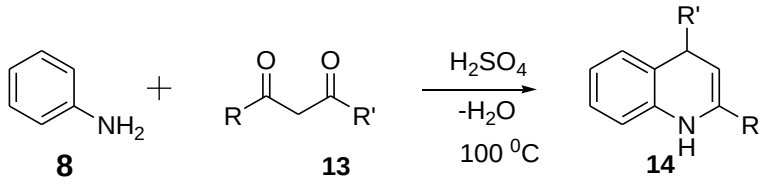

Scheme 3: Combes Quinoline Synthesis

2.1.3. Doebner-Miller Quinoline Synthesis

It is organic reaction of aniline with α, *β* unsaturated carbonyl compounds to form quinolines as shown in scheme 4 (Ladani *et al*., 2020)**.**

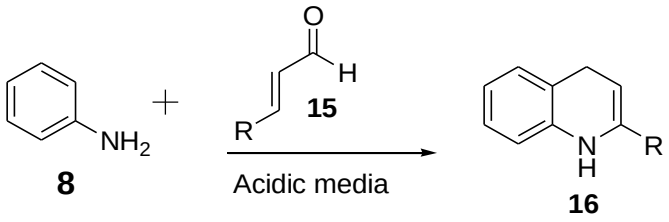

Scheme 4: Doebner-Miller of Quinoline Synthesis

2.1.4. Skraup Quinoline Synthesis

It is named after the Czech chemist Zdenko Hans Scraup(1850-1910). In this reaction aniline is heated with sulfuric acid, glycerol and an oxidizing agent such as nitrobenzene to yield quinoline as shown in scheme 5 (Kumar *et al*., 2016)**.**

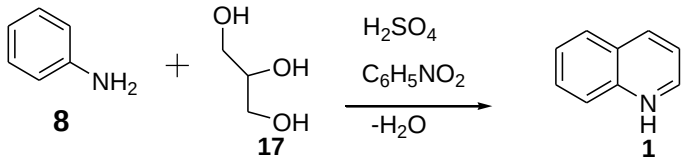

Scheme 5: Skraup Quinoline Synthesis

2.1.5. Pfitzenger Quinoline Synthesis

This is a chemical reaction first discovered at the end of the nineteenth century by Pfitzingerin which isatin **18** with base and a carbonyl compound yield substituted quinoline-4-carboxylic acid called cinchoninic acid. Pfitzinger Synthesis is the most widely used modification of the Friedlander reaction and it is characterized by simplicity of the procedure, and the high yields of product(Giardinieri *et al*., 2017). It is chemical reaction of isatin with base and carbonyl compounds to yield substituted quinolone -4- carboxylic acid as shown in scheme 6 (Ishak *et al.*, 2018).

Reaction involves the conversion of isatin **18** by the action of a strong nucleophiles, such as sodium hydroxide or potassium hydroxide, into the salt of isatoic acid **19**, which condenses with ketones **20** with the release of water, forming another salt **21.** The latter undergoes cyclization through the -CO and -CH_2 groups and is converted into the salt of 4-quinolinecarboxylic acid **22**, the treatment of which with acids, usually acetic, gives the required final compounds **23** shown in scheme 6

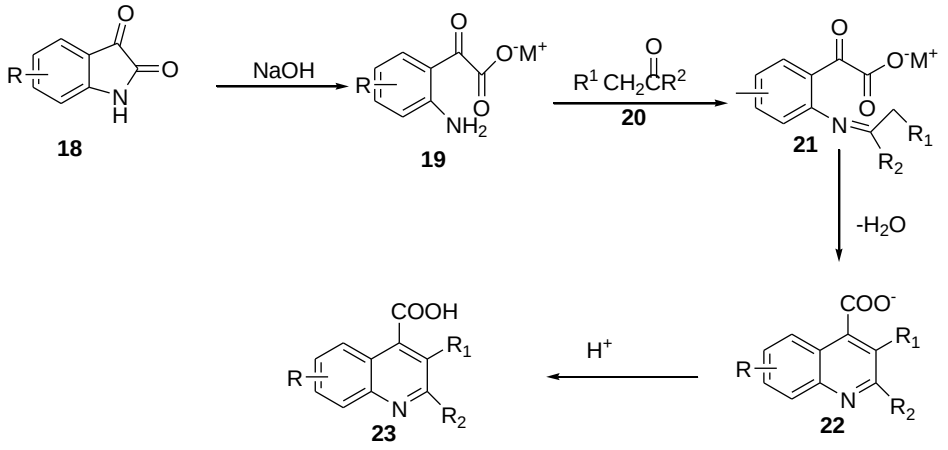

Scheme 6: Pfitzinger Quinoline Synthesis

2.1.6. The Knorr Quinoline Synthesis

This reaction, discovered by Knorr in 1886, provide 2-hydroxyquinoline ring by the treatment of *β*-ketoester with arylamine above 100℃. The mechanism, represented in Scheme 7, involves at first the reaction between the amino group **8** with *β*-ketoester **24** that furnishes anilide **25** and

successively the cyclization of the latter in presence of acid by the loss of water molecule to afford quinoline derivative **29** (Giardinieri *et al*., 2017).

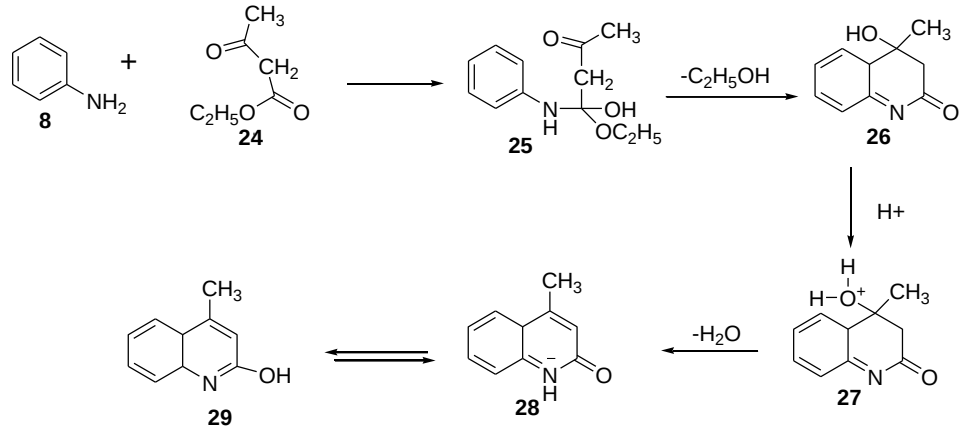

Scheme 7: The Knorr Quinoline Synthesis

2.1.7. Friedlander Quinoline Synthesis

Friedlander synthesis using 2-aminobenzaldehyde **30** and acetaldehyde **31** in particular the starting materials are o-aminoaryl aldehydes or ketones and a ketone possessing an α-methylene group under basic or acidic condition as depicted in Scheme 8 (P.Kaur *et al*, 2019)

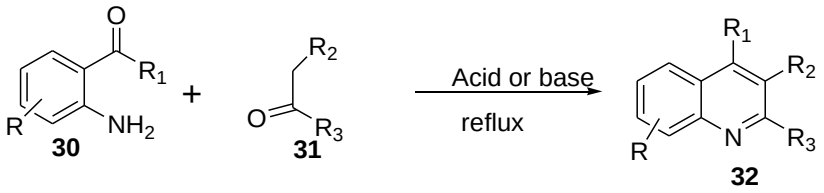

Scheme 8: Freidlander Quinoline Synthesis

2.1.8. Vilsmeier Haack Quinoline Synthesis

Substituted quinolines are very simply, efficiently and conveniently synthesized in less time and high yield with less amount of raw material under mild condition with the help of Vilsmeier-Haack reagent and substituted acetanilide. Formylation of heterocyclic compounds may be achieved by heating heterocyclic compound with Vilsmeier reagent. The intermediate is hydrolyzed in the

presence of mild base give 2-*o*-substituted heterocyclic compound. This reaction is known as Vilsmeier-Haack reaction (As & Sal, 2017).

Synthesis of 2-Chloro-8-methyl-3-formyl quinoline **34** can be done by adding dimethyl formamide (DMF) that was cooled to 0 °C temperature in a flask equipped with a drying tube with $POCl_3$ (Phosphorous oxychloride) that was added drop wise with stirring to it. *Ortho* methyl acetanilide **35** was added and the reaction was refluxed for 6-8 hours using air condenser and the temperature of reaction mixture is maintained between 80-90 °C. After completion of requiring duration, the reaction mixture was cooled and poured in 100 ml beaker containing ice-cold water and stirred about half an hour then filter precipitated quinoline **36** and wash with water and dried, recrystallized from ethyl acetate (As & Sal, 2017).

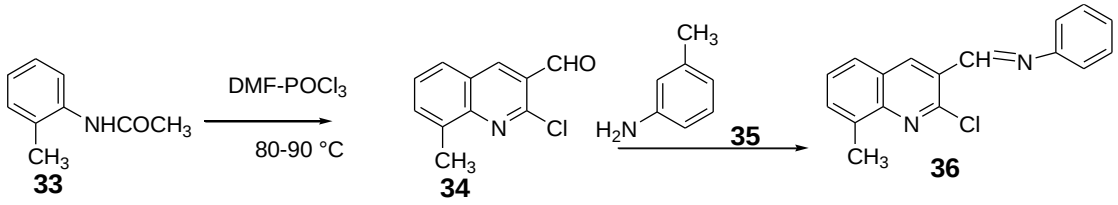

Scheme 9: Vilsmeier Haack Quinoline Synthesis

2.2. Biological Activities of Quinoline Derivatives

2.2.1. Antibacterial Activity

Currently resistance to first-line antibiotic agents is a severe problem. Infections caused by these resistant microbes fail to respond to treatment resulting in prolonged illness and greater risk of death. The alarming rates of emerging and remerging microbial threats coupled with increasing antibacterial resistance, particularly in regard to multi drug-resistant Gram-positive bacteria, are major concerns to the public health as well scientific communities worldwide. These trends have emphasized the pressing need for new, more effective and safe antibacterial agents and which in turn has opened up a new area of research for the scientists (Parminder & Rajwant, 2019).

Quinoline derivatives containing 1, 2, 4-triazole moiety from derivatives of 4-hydroxy-8-(triflouromethyl) quinoline-3-carbohydrazide through multistep reaction were evaluated for their *in vitro* antibacterial activities. Preliminary result indicates that the most of the compounds such

as **37, 38** and **39,** shown in (Figure 2) demonstrate the very good antimicrobial activity(Adam, 2019).

A series of 2-oxopyrimido[4,5]-, 2-thio[4,5]-, 1-(p-tosyl)pyrazolo[3,4]and 1-(2',4'-dinitrophenyl)pyrazolo[3,4]-quinolines were synthesized by environmentally benign solvent free microwave-induced techniques and evaluated for their anti-bacterial activity. Most of the compounds **40** and **41** (Figure 2) showed the best activity against *E. coli* and *P. aeruginosa* (Parminder & Rajwant, 2019).

The most naturally occurring and synthesized quinolines were tested for antibacterial against a range of Gram-positive and Gram-negative bacteria, including a hospital isolate of Methicillin-resistant *S. aureus* (MRSA). In particular, 4-hydroxy-3-iodo-quinol-2-one **35** showed good activity against an Irish hospital MRSA-1 strain and a distinct MRSA strain as well as a non-type able MRSA strain, the values are comparable with the antibiotic Vancomycin used in the treatment of MRSA infections (Divo, 2018).

Series of quinoline-based chalcones **44** (Figure) were synthesized and screened for anti-microbial activities against *E.coli, P. aeruginosa, B. subtiles, K. aerogeues, S. albus, A. flavus, A. niger, R.larubera, L. opofera and C. albicans*(Parminder & Rajwant, 2019).

Pyrazolo[3,4]quinoline derivatives were synthesized by cyclization of the intermediate 2-chloroquinoline-3-carbonitrile, namely 3-amino-1H-pyrazolo[3,4]quinoline, 3-amino-1-phenyl/(p-substituted)phenyl/-1H-pyrazolo[3,4]quinolone **45**. Furthermore, 3-[(3-aryl-4-oxothiazolidin-2-ylidene)amino]-1H-pyrazolo[3,4]quinolines **46** and 3-[(3-aryl-4-oxothiazin-2-ylidene)amino]-1H-pyrazolo[3,4]quinolines **47** (Figure 3) were synthesized. The antimicrobial activity was evaluated and good for most of the prepared compounds (Ishak *et al*., 2018).

A series of 3-((6-(2, 6-dichloroquinolin-3-yl)-4-aryl-1, 6-dihydro-pyrimidin-2-yl)thio) propane nitriles and subjected to molecular properties prediction and drug-likeness model score by Molinspiration property calculation toolkit and MolSoft software, respectively. Compounds **48, 49** and **50** (Figure 3) displayed broad spectrum antibacterial activity against all the bacterial strains (Parminder & Rajwant, 2019).

Synthesized a new series of substituted 1, 2, 3-triazoles from 4-azido-2, 8-bistrifluoromethylquinoline and were evaluated *in vitro* for their antibacterial activity. Among that

most active compound was **51** (Figure 3), which contained the 3-methylthien-2-yl moiety and showed a broad spectrum of antimicrobial activity against all the strains used for testing. Compounds **52** (Figure 3) showed significant antimicrobial activity at the concentration of 6.25µg/mL (Ladani *et al*., 2020).

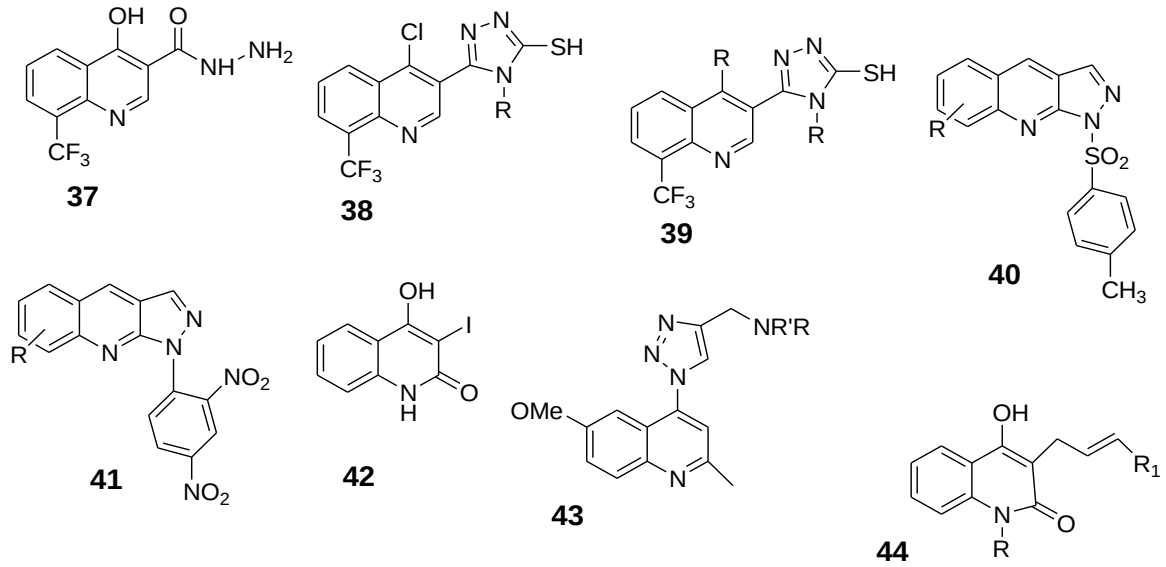

Figure 2: Quinoline derivatives with bactericidal effects

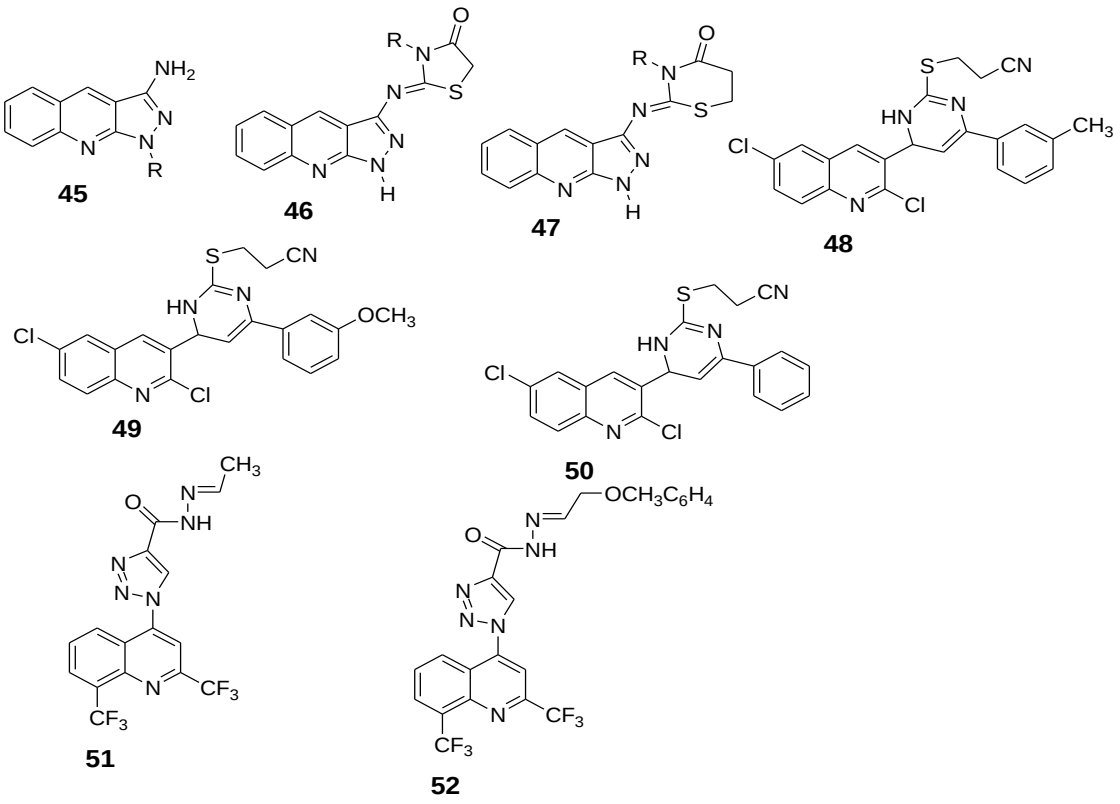

Figure 3: Quinoline derivatives with antibacterial activity

Quinolines derivatives **49, 50, 51, 52** and **53** (Figure 3) are also pharmacologically active compounds against selected bacterial strain. In an attempt to find out lead compounds against bacteria, a series of quinoline derivatives have been synthesized and subsequently evaluated for their antibacterial activities against various strains of bacterial pathogen (Secrieru, 2020).

Series of quinoline derivatives have been synthesized and evaluated for their antibacterial activities against various strains of bacterial pathogens. Compound **53** displayed 6.67±0.89mm, 7.0± 0.67mm, and 9.0 ±0.67mm at 500µg/mL against *E. coli, S.aureus* and *P. aeruginosa* respectively. Compound **54** displayed no activity, 6.33±0.44mm and 9.33±0.44 at 500µg/mL against *E. coli, S.aureus* and *P. aeruginosa* respectively. Compound **55** displayed no activity, 7.67±0.44mm and 9.67±1.11 at 500µg/mL against *E. coli, S.aureus* and *P. aeruginosa* respectively. Compound **56** displayed 11.33±1.11, 6.33±0.44mm and 8.33±0.44 at 500µg/mL against *E. coli, S.aureus* and *P. aeruginosa* respectively. ±0.44mm and 9.67±1.11 at 500µg/mL against *E. coli, S.aureus* and *P. aeruginosa* respectively. Compound **57** displayed no activity, 7.33±0.44mm and 6.33±0.44 at 500µg/mL against *E. coli, S.aureus* and *P. aeruginosa* respectively(Zeleke *et al*., 2020).

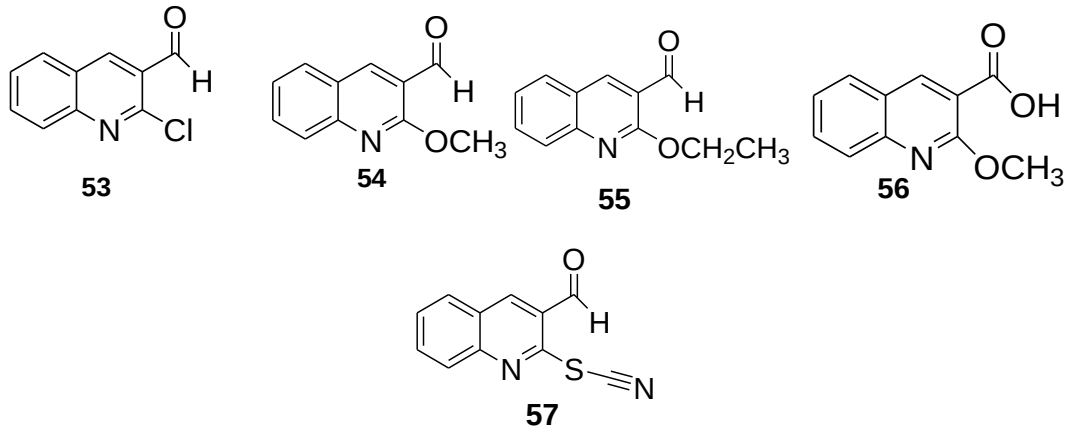

Figure 4: Series of quinoline derivatives with their IZ

2.2.2. Anticancer Activity

Cancer, rapid unregulated pathological proliferation of abnormal cells, is the second leading cause of death in humans after cardiovascular diseases. According to data from the World Health Organization, of the 58 million deaths occurred worldwide in 2008, 7.6 million (13%) were due to cancer. The pathologies that contribute most to mortality are lung (1.3 million annual deaths), stomach (740.000 deaths per year), liver (662.000 deaths annually), colon (655.000 deaths annually), and breast cancer (502.000 deaths per year). It is expected that the global number of cancer deaths will continue to rise around the world and will reach 9 million by the year 2015 and 11.4 million by 2030. The most common cancers in the world are, in order of mortality in men - lung, stomach, liver, colon and rectum, esophagus and prostate and in women -breast, lung, stomach; colon and rectum, and cervix. The search for new anticancer agents is an important and challenging task of scientist (Parminder & Rajwant, 2019).

The series 11-subsituted 6H-indolo derivatives were prepared from the commercially available 1, 4-dihydroxyquinoline through alkylation, chlorination, nucleophilic reaction, and ring cyclization. The *in-vitro* anti-cancer assay indicated 5-methylated derivatives **58, 59** and **60** depicted in Figure 4 are cytotoxic.

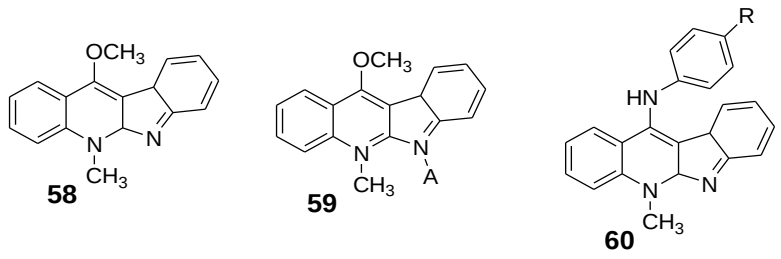

Figure 5: Quinoline derivatives with anticancer activity

The anticancer activities of compounds against HeLa, HT29, and C6 tumor cell lines were tested, and 6,8-dibromo-1,2,3,4-tetrahydroquinoline **61** and 6,8-dimethoxyquinoline **62** shown in Figure 5 showed significant anticancer activities against the tumor cell lines (Parminder & Rajwant, 2019).

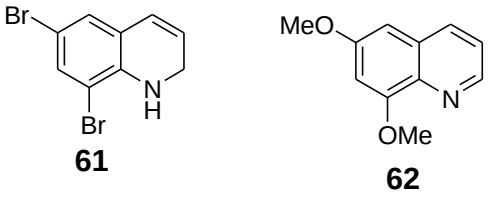

Figure 6: Quinolines with anticancer activities against HeLa, HT29, and C6 tumor cell lines

C-2-substituted quinolines in both human cancer cell lines (MCF-7, H-460 and SF-268) and normal cell lines (Vero and THP-1). Preliminary results indicate that 2-α-furyl-and 2-β-pyridinylquinoline derivatives **63** and **64** shown in Figure 6, are active against three human cancer cell lines and, at the same time, were devoid of cytotoxic effect on normal cells. Biological activity and SAR results were compared with different molecular descriptors determined *in silico* using online available software, in an attempt to show a relationship with the possible mode of action of this quinoline derivative (Parminder & Rajwant, 2019)

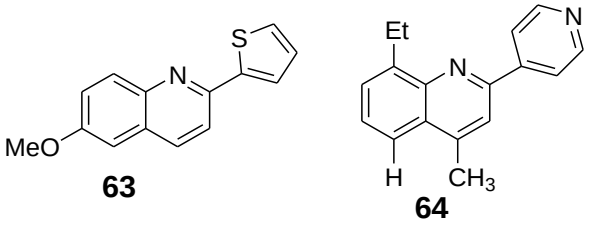

Figure 7: C-2-substituted quinolines having anticancer activity

The quinolines were readily synthesized from a sequence of reactions starting from 4-acetamidoanisole. Effects of the substituted quinolines on breast cancer cells using try pan blue exclusion assay were examined. The results showed that the IC_{50} value of 6-methoxy-8-[(2-furanylmethyl)amino]-4-methyl-5-(3-trifluoromethylphenyloxy)quinolone **65** shown in Figure 7 was 16 ± 3 nm, the lowest IC_{50} out of all the quinolines tested (Rajwant *et al.,* 2019)

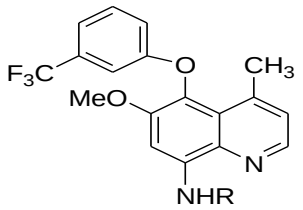

65

Figure 8: Anti-breast cancer agents from substituted quinolines

2.2.3. Anti-inflammatory Activity

Non-steroidal anti-inflammatory drugs (NSAIDs) are useful tools in the treatment of acute and chronic inflammation, pain, and fever. However, long term clinical usage of NSAIDs is associated with significant side effects of gastro-intestinal lesions, bleeding, and nephrotoxicity. Therefore thediscovery of new and safer anti-inflammatory drugs represents a challenging goal for such a research area (Edijane *et al* , 2017). Synthesized the series of tetrazolo [1,5-a]quinolone derivatives by the condensation of various compounds. The newly synthesized compounds were evaluated for their anti-inflammatory and antimicrobial activities. Compounds **66** shown in Figure 8 (ED50 values range 8.50–9.84 μmol) have anti-inflammatory activity comparable to that of indomethacin (ED50 value 9.28 μmol) (Huang *et al*, 2019).

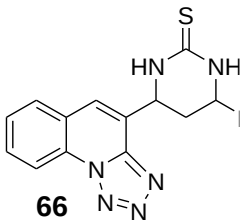

66

Figure 9: Quinoline derivatives having anti-inflammatory activity

2.2.4. Antifungal Activity

Fungal infections have emerged as a current serious global public health problem. The main problem involving these infections is the expansion of multidrug resistance. Therefore, the prospection of new compounds with efficacy antifungal becomes necessary. Thus, this study evaluated the antifungal profile and toxicological parameters of quinolines derivatives against Candida spp. and dermatophyte strains (Monte *et al*., 2020).

Compounds **67** and **68** shown in Figure 9 were tested against some strains of fungus. Thus, the compounds were submitted to the broth micro dilution assay to determine their minimum inhibitory concentration (MIC). Each compound was tested at 100μg/ml, with concentrations ranging from 0.09 to50μg/ml in the assay (Monte *et al*., 2020).

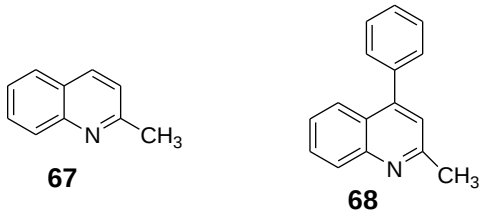

Figure 10: Quinoline derivatives having antifungal activity

2.2.5. Antiviral Activity

Several antiviral drugs such as saquinavir **69,** Simprevir, **70** shown in Figure 10 containing quinoline scaffold are marketed these days but still this area is widely unexplored. Drugs acting specifically on virus targets are available but only for some viral infections. Various molecules have been developed but they are usually associated with drug resistance, cytotoxicity that by there is an urge to develop more efficient antiviral drugs (Kumar *et al*, 2021).

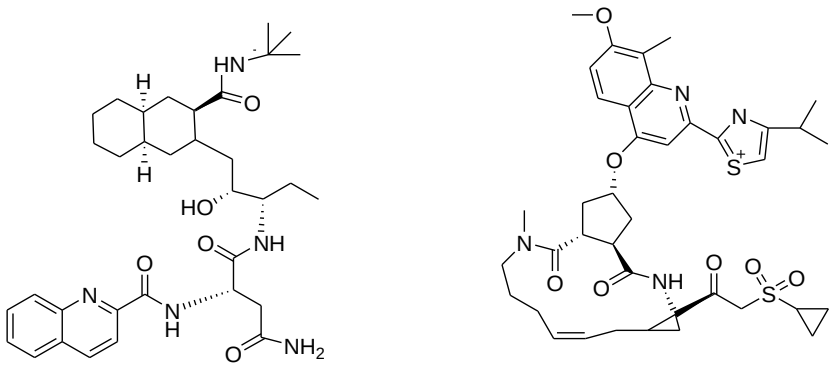

69 **70**

Figure 11: Quinoline scaffold with antiviral activity

2.2.6. Antimalarial Activity

Malaria is one of the most widespread and deadliest diseases that resulted in 212 million clinical cases and 429,000 deaths in 2015 alone, especially among children (in Africa, 78% of deaths apply to children under the age of five) and pregnant women according to the World Health Organization (WHO)(Hu *et al*., 2017). Malaria is usually caused by protozoan parasites of the genus *Plasmodium* including *P. Falciparum, P. vivax, P. malariae, P. ovale and P. knowlesi* species of human malaria parasite. In particular, *P. falciparum* is the most fatal one, which is responsible for 95% of the case of death (Patel *et al*., 2021).

Quinoline and its derivatives, exhibited antimalarial properties. Quinoline-containing anti-malarials, such as quinine **71**, chloroquine **72**, amodiaquine **73**, mefloquine **74** and primaquine **75** shown in Figure 11 are mainstays of chemotherapy against malaria which have long been used clinically. Among them**, 72** has been used in the treatment as well as prophylaxis of almost all forms of malaria owing to its highly effective, safe, well-tolerated and reasonably low cost (Secrieru *et al*, 2020)

The human malaria parasite *P. falciparum* is able to regulate its genes and results in strains resistant to almost all the antimalarial, especially toward **72**. Resistance to **72** is associated with mutations in the gene encoding the digestive vacuole membrane protein *P. falciparum* resistance transporter (PfCRT), which appears to result in reduced drug concentration at the target without altering the

target itself. In this case, the target remains vulnerable and the organism is susceptible to drug action if access and binding to the target can be achieved (Beteck *et al*., 2019).

To overcome the drug resistance, great efforts have been under-taken. Numerous of studies revealed that modification of the basic amine side chain of quinoline-contained antimalarial can keep activities against drug-resistant *P*. *falciparum* strains, but it has generally been assumed that changes to the quinoline nucleus itself will not (Hu *et al*., 2017)

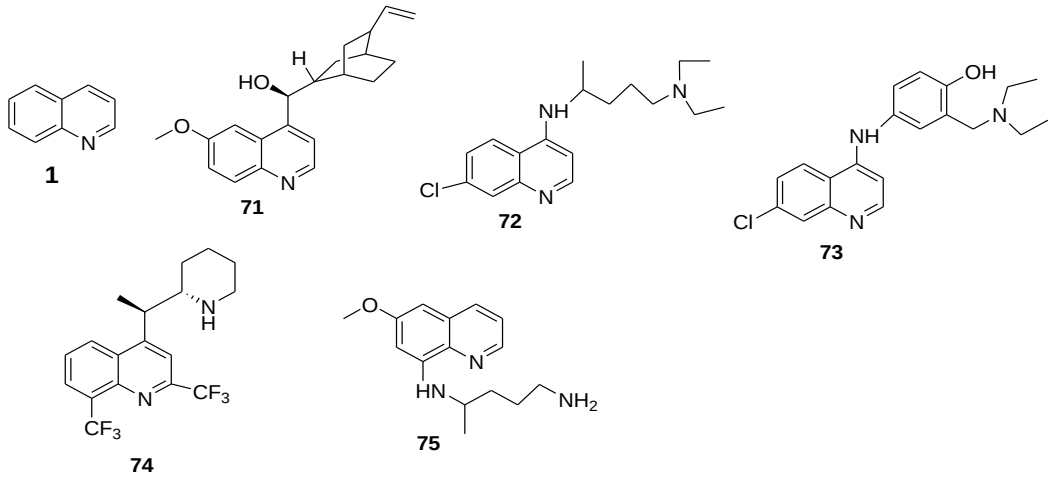

Figure 12: Structures of quinoline and common quinolone with antimalarial.

2.2.7. Anticonvulsant Activity

Epilepsy, a ubiquitous disease characterized by recurrent seizures, inflicts more than 60 million people worldwide according to epidemiological studies (Edijane, 2017). For epilepsy treatment, nearly 95 percent of clinically available drugs were approved before 1985 and they could provide satisfactory seizure control for 60-70percent of patients. These drugs, however, also cause notable adverse side effects such as drowsiness, ataxia, gastrointestinal disturbance, hepatotoxicity and megaloblastic anemia, and even life threatening conditions. Research to find more effective and safer anticonvulsant drugs are therefore a challenging task (Parminder & Rajwant, 2019).

Synthesized a series of 5-alkoxy-[1, 2, 4] triaolo [4, 3] quinoline derivatives were evaluated by the maximal electroshock test (MES) and their neurotoxicity's were measured by the rotarod test. The results of these tests demonstrated that 5-ethoxy-[1, 2, 4] triazolo [4, 3] quinoline **76** was the most potent anticonvulsant, with median effective dose (ED50) of 19.0 mg/kg and protective index

(PI=TD50/ED50) values of 5.8 in the MES test. Compound 5-methoxy-[1, 2, 4] triazolo [4, 3] quinoline **77** possessed lower neurotoxicity with PI vale of 12.0, which was safer than marketed drug Carbamazepine. To explain the possible mechanism of anticonvulsant activity, compound **77** was tested in penteylenetetrazole test, isoniazoid test, thiosemicarbazide test, 3-mercaptopropionic acid and strychnine test (R. Kaur & Kumar, 2021)

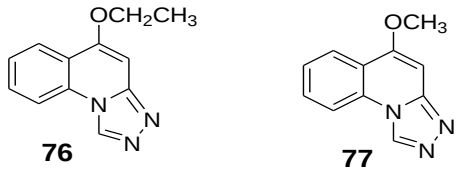

Figure 13: Quinoline derivatives having anticonvulsant activity

2.2.8. Antimycobacterial Activity

Tuberculosis is a worldwide pandemic caused by different species of mycobacteria. The latest statistics reveals that around 2 million people throughout the world die annually from tuberculosis and there are around 8 million new cases each year. Among HIV-infected people with weakened immune system, TB is leading killer epidemic. Every year about 2 million people living with HIV/AIDS die from TB (Valadbeigi, 2019).

In vitro anti-mycobacterial properties of ring-substituted quinolines constituting many analogues against drug-sensitive and drug-resistant M. tuberculosis H37Rv strains. The most effective compounds have exhibited an MIC value of 1 μg/mL against drug-sensitive M. tuberculosis H37Rv strain that is comparable to first line anti-tuberculosis drug, isoniazid. Selected analogues **78** and **79** shown in Figure 11 have MIC: ⩽6.25 μg/mL) upon further evaluation against single-drug-resistant (SDR) strains of M. tuberculosis H37Rv have produced potent efficacy in the range between 6.25 and 50 μg/mL (R. Kaur & Kumar, 2021)

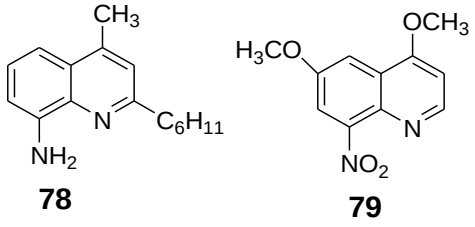

Figure 14: Anti mycobacterial of quinoline derivatives

2.3. Radical Scavenging Activity

A free radical can be defined as any molecular species capable of independent existence that contains an unpaired electron in an atomic orbital. The presence of an unpaired electron results in certain common properties that are shared by most radicals. Many radicals are unstable and highly reactive. They can either donate an electron to or accept an electron from other molecules, therefore behaving as oxidants or reductants (El-Gazzar *et al*., 2019). The most important oxygen-containing free radicals in many disease states are hydroxyl radical, superoxide anion radical, hydrogen peroxide, oxygen singlet, hypochlorite, nitric oxide radical, and peroxynitrite radical. These are highly reactive species, capable in the nucleus, and in the membranes of cells of damaging biologically relevant molecules such as DNA, proteins, carbohydrates, and lipids.

Free radicals attack important macromolecules leading to cell damage and homeostatic disruption. Targets of free radicals include all kinds of molecules in the body. Among them, lipids, nucleic acids, and proteins are the major targets (Matada *et al*., 2019). Radical scavenging activity is very important due to the hazardous role of free radicals in biological systems. Reactive oxygen species (ROS) derived from pollution, radiation, food ingredients or produced endogenously in the human body from the metabolic reactions is responsible for oxidative damage to vital macromolecules such as DNA, proteins and lipids. It is reported to play a key role in the pathogenesis of many chronic diseases .Various different methods are presently used to assess antioxidant activity (Zhang *et al*., 2020). Antioxidant covers a wide range of molecules (atoms bound together by chemical bonds) that protect other molecules from a chemical process called oxidation. Oxidation can damage vital molecules in our cells, including DNA and proteins, which are responsible for many body processes. Molecules such as DNA are needed for cells to function properly, so if too many are damaged, the cell can malfunction or die. This is why antioxidants are important.

They can prevent or reduce this damage. In the body, uncontrolled oxidation is typically caused by highly reactive molecules known as free radicals (Matada *et al.*, 2019)

Naik *et al*, have identified a variable and useful novel access to different scaffold of biologically important 2-mercapto **80** or 2-selenobenzo[h]quinoline-3-carbaldehydede devatives **81** shown in **figure 14.** These compounds have strong antioxidant activity, wound healing activity and high

protection potential to oxidative DNA damage from hazardous of free radical reactions (Orhan Puskullu *et al*., 2013).

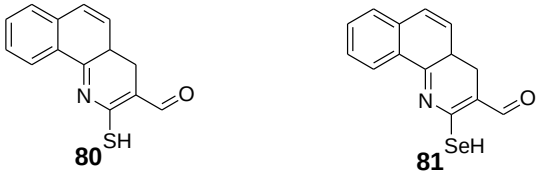

Figure 15:2-Mercapto/2-selenobenzoih] quinoline-3-carbaldehyde derivatives

Free radical scavenging ability of the compounds tested by DPPH radical scavenging assay. The hydrogen atom donating ability of the compounds are determined by the decolonization of methanol solution of 2,2-diphe-nyl-1-picrylhydrazyl (DPPH). DPPH produces violet/purple color in methanol solution and fades to shades of yellow color in the presence of antioxidants. The absorbance of the mixture measured spectrophotometrically at 517 nm. Percentage DPPH radical scavenging activity was calculated by the following equation:

% DPPH radical scavenging activity = $\frac{A_{0-A_1}}{A_0} \chi_{100}$

Where A_0 is the absorbance of the control, and A_1 is the absorbance of the extractives/standard. Then % of inhibition was plotted against concentration, and from the graph IC_{50} was calculated (Rahman *et al*., 2015).

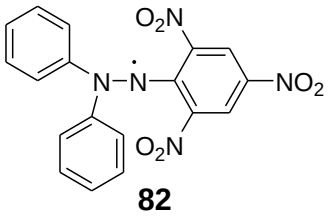

Figure 16: Structure of 1, 1-diphenyl-1-picrylhydrazyl (DPPH)

Compound **53, 54, 55, 56 and 57** displayed 32.64, 31.53, 35.44, 67.02 and 33. 76 percentage inhibition respectively (Zeleke *et al*., 2020).

2.4. Molecular Docking Studies

Molecular Docking is the computational modeling of the structure of complexes formed by two or more interacting molecules. The goal of molecular docking is the prediction of the three

dimensional structures. Docking itself only produces plausible candidate structures. These candidates are ranked using methods such as scoring functions to identify structures that are most likely to occur in nature (Gaba *et al*., 2015).

Docking is a computational procedure of searching for an appropriate ligand that fits both energetically and geometrically the protein's binding site. In other words, it is a study of how two or more molecules e.g. ligand and protein, fit together. The problem is like solving a 3D puzzle. Molecular Docking is an effective and competent tool for *in silico* screening. It is playing important and ever increasing role in rational drug design(Azam & Abbasi, 2013).

In the field of molecular modeling, molecular docking is a method which predicts the preferred orientation of one molecule to a second when bound to each other to form a stable complex(Mura & McAnany, 2014). Docking consists of two parts, sampling method to general trial and a scoring system to evaluate a pose by assigning it a value that presumably reflects its accuracy(Gaba *et al*., 2015). Compounds **53, 54, 55, 56** and **57** have -6.2 kcal/mol, -6.2 kcal/mol, -6.2 kcal/mol and -6.2 kcal/mol binding affinity respectively.

2.5. *In silico* drug likeness prediction

The terms such as 'drug-likeness,' 'PK/PD study,' and 'ADMET profiling' are addressed by researchers interchange-ably many times, but they are different and each has a crucial role to play in drug discovery. The ideas about PK/PD, drug-likeness, lipophilicity, water solubility, and toxicity are considered under the term ADMET profiling in a broader sense. In the profiling of drug metabolism, human cytochrome P450 (CYP450) enzyme inhibition prediction is extremely crucial for drug toxicity. Combining the efforts of molecular dynamics (MD) simulations and *in silico* prediction for CYP inhibition has improved the safety of the drugs up to many fold (Kadam & Roy, 2017).

The concept of drug-likeness, established from the analyses of the physiochemical properties and structural features of existing small organic drugs and drug candidates, has been widely used to filter out compounds with undesirable properties, especially poor ADMET (absorption, distribution, metabolism, excretion, and toxicity) profiles. Various approaches for drug-likeness evaluations, including simple rules/filters based on molecular properties and quantitative prediction

models based on sophisticated machine learning methods, and provide a comprehensive review of recent advances in this field (Suhud *et al*., 2019).

Approaches with open access *in silico* tools have revolutionized disease management due to early prediction of the absorption, distribution, metabolism, excretion, and toxicity (ADMET) profiles. The choice of *in silico* tools is important for drug discovery and the accuracy of ADMET prediction. The accuracy depends on the types of data set, the algorithm used, the quality of the model, the available endpoints for prediction, and user requirement (Kar & Leszczynski, 2020). Lipinski and coworkers developed the "Rule of Five" which is defined as combined parameters that are capable of identifying a potential drug candidate that might present problems with absorption and permeability. According to the rule, poor oral bioavailability is more likely when there are more than 5 H-bond donors (HBD), 10 H-bond acceptors (HBA), the molecular weight (MW) is greater than 500 and the calculated Log P (CLog P – calculated logarithm of partition coefficient between *n*-octanol and water) is greater than 5 (B. Fernandes *et al*., 2016).

CHAPTER THREE

Materials and Methods

3.1. General

Melting points were determined in an open capillaries using digital melting point apparatus (Thiele tube) expressed in ºC. Reaction progress was checked on TLC plates and spots were visualized using UV light at 254 nm. Silica gel (60-120 mesh, Merck grade) has been used for column chromatography. The synthesized compounds were characterized on the basis of physical and spectral analysis. The UV-Vis spectra of synthesized compounds were recorded on Double-beam UV-Vis spectrophotometer using DCM and MeOH as blank solvents and λ_{max} values were expressed by nm. The ^{1}H and ^{13}C NMR spectra of the compounds were recorded on Bruker avance 400 MHz NMR spectrophotometer using Chloroform-*d* or Methanol-d_4 as the solvent and the values are expressed in δ ppm.

3.2. Chemicals and equipment

All solvents and chemicals were obtained commercially from fine chemicals PLC (Addis Ababa). All solvents and reagents were used as received without further purification. *n*-hexane, ethyl acetate, methanol, ethanol, dichloromethane, silica gel (60-120 mesh), Phosphorous oxychloride, normal aniline, 4-flouro aniline, DMF, sulfuric acid, acetic acid, glacial acetic acid, acetic anhydride, zinc powder, potassium carbonate, ethanolamine, potassium thiocyanate, potassium permanganate, oxalic acid and sodium hydroxide were chemicals used in this work.

3.3. Experimental Procedures

3.3.1. Synthesis of some derivatives of fluoroquinoline

3.3.1.1. Synthesis of 2-Chloro-6-fluoro quinoline-3-carbaldehyde (86)

In 250 mL round bottom flask, 4-fluoro aniline (15 mL), acetic anhydride (22 mL), zinc powder (0.1 g), and glacial acetic acid (23 mL) were added. The mixture was boiled under reflux using water condenser for 2 hour. Then, it was cooled to room temperature and poured into 200 mL of

crushed ice water. The solid product, *N*-(4-flouro phenyl) acetamide was collected by suction filtration. White crystal; yield 19.69g (81.2%), mp 154–156°C. Then after, *N*,*N*-dimethylformamide (29.9 mL) was added to a 100 mL round-bottom flask guarded with drying tube; it was cooled to 0 °C using ice bath. Then, phosphorus oxychloride (84.3 mL) was added dropwise to it from dropping funnel guarded by drying tube while being stirred by magnetic stirrer. This addition was done for 30 minutes. Then *N*-(4-flouro phenyl) acetamide (19.69 g) was added to it. After 5 minutes, the dropper funnel was replaced by air condenser with guarding tube at its end, and the mixture was heated for 22 hours on oil bath at 85–90 °C. Then it was cooled to room temperature, poured into a beaker containing 400 mL crushed ice water, and stirred for 20 minutes. The yellow solid product was collected by suction filtration and washed with 100 mL cold water. The crude yield was 16.4 g (60.8%) and was recrystallized from ethyl acetate. yellow crystal; mp 160-162 °C; yield 15.5 g (57.5%); Rf = 0.72 (*n*-hexane : EtOAc= 4 :1; ^{1}H NMR (400 MHz, $CDCl_3$) δ 10.44 (1H, s, H-9), 8.70 (1H, s, H-4), 8.08 (1H, d, *J*=7.2 Hz, H-8), 7.63 (1H ,d, *J* = 2.7 Hz, H-5), 7.27 (1H, dd, *J* = 8.7 Hz, H-7); ^{13}C NMR (101 MHz, $CDCl_3$) δ 189.0(C-9), 162.2(C-6), 148.6(C-2), 143.9(C-8a), 139.7 (C-4), 130.77 (C-8), 130.0(C-4a), 127.6(C-3), 123.8(C-7), 111.2(C-5).

3.3.1.2. Synthesis of 6-fluoro-2-methoxy quinoline-3-carbaldehyde (87)

100 mL two-neck round-bottom flask was charged with methanol (10 mL), *N*,*N*-dimethylformamide (13 mL), 2-Chloro-6-flouro quinoline-3-carbaldehde (0.5 g), and potassium carbonate (0.57 g); the mixture was refluxed using water condenser for 4 hours; and the progress of reaction was monitored with TLC. After completion of the reaction, methanol was removed by distillation, allowed to cool to room temperature, and then added to 100 mL ice-cold water. The solid product was collected by fractional distillation and washed with excess ice-cold water. Yellow powder; yield 75.2%; mp 158–160°C;Rf=0.78 (*n*-hexane: EtOAc=4:1; ^{1}H NMR (400 MHz, $CDCl_3$) δ 10.46 (1H, s, H-9), 8.50 (s, 1H,H-4), 8.03 (1H, d, *J* = 8.5 Hz, H-8), 7.85 (d, 1H, *J* =2.6, H-5), 7.48 (1H, dd, *J* = 8.6, H-7), 7.28, 4.17 (3H, s, H-11); ^{13C} NMR (101 MHz, $CDCl_3$) δ 189.1 (C-9), 160.7(C-2), 158.0(C-6), 145.8(C-8a), 139.0 (C-4), 129.4 (C-8), 124.6(C-4a), 122.2 (C-7), 120.5(C-3), 112.6 (C-5), 53.8(C-11).

3.3.1.3. Synthesis of 2-ethoxy-6-flouro- quinoline-3-carbaldehyde (88)

100 mL two-neck round-bottom flask was charged with 2-Chloro-6-flouro quinoline-3-carbaldehyde (0.5g), potassium carbonate (0.6 g), ethanol (10 mL), and *N*,*N*-dimethylformamide (10 mL), and the necks were fitted with water condenser and stopper. The mixture was refluxed for 4 hours and the progress of the reaction was monitored with TLC. At the end, the ethanol was removed by distillation, and the remaining cooled mixture was poured into 100 mL crushed ice water. The solid mass was collected by suction filtration. Yield 72.3%; white powder; mp 184–186°C, Rf=0.64 (*n*-hexane: EtOAc=4:1; ^{1}H NMR (400 MHz, $CDCl_3$) δ 10.50 (1H, s, H-9), 8.52 (1H, s, H-4), 7.84 (1H, d, *J* = 8.8 Hz, H-8), 7.49 (1H ,d, *J*=2.8 Hz H-5), 7.34 (1H, dd, *J* = 8.9 Hz, H-7), 4.64 (2H, q, *J* = 7.1 Hz, H-10), 1.52 (3H, t, *J* = 7.1 Hz, H-11); ^{13}C NMR (101 MHz, $CDCl_3$) δ 189.3 (C-9), 160.6(C-2), 158.0(C-6), 145.9(C-8a), 138.7(C-4), 129.3(C-8), 124.6(C-4a), 122.1 (C-7), 120.4(C-3), 112.6(C-5), 62.4 (C-10), 14.4(C-11).

3.3.1.4. Synthesis of 6-fluoro-2-thiocyanatoquinoline-3-carbaldehyde (89)

Potassium thiocyanate (0.24 g), 2-chloro-8-methyl quinoline-3-carbaldehyde (0.4 g),and potassium carbonate (0.65 g) were added to 100 mL two-neck round-bottom flask containing *N*,*N*-dimethylformamide (20 mL). A water condenser was placed on one of its neck, and the other was closed with glass stopper and then refluxed for 5 hours, and the progress of the reaction was followed by TLC. The system was cooled to room temperature and crushed into 50 mL crushed ice water. The solid product was collected with suction filtration and washed with 10 mL cold water. Yield 67%; Gray powder; mp 156–158°C;Rf=0.49 (DCM with drop of methanol). ^{1}H NMR (400 MHz, DMSO) δ 10.24 (1H, s, H-9), 8.48 (1H, s, H-4), 7.82 (1H, d, *J* = 8.87 Hz, H-8), 7.60 (1H, d, *J* = 2.9 Hz , H-5), 7.56 (1H, d, *J* = 9.4 Hz, H-7); ^{13}C NMR (101 MHz, DMSO) δ 190.2(C-9), 161.6(C-2), 158.7(C-6), 141.9(C-8a), 141.9 (C-4), 122.5(C-8), 122.3(C-4a), 119.1(C-3), 117.8(C-7), 115.6(C-5), 115.3(C-10).

3.3.1.5. Synthesis of 2-((2-hydroxyethyl) amino)-3-(-2-(ethylideneamino) ethanol quinoline (90)

2-Chloroquinoline-3-carbaldehyde (0.5g) was added to ethanolamine (8 mL) in 100 mL round bottom flask and heated in oil bath at 100 °C for 2 hr. after cooled to ambient temperature, it was poured into 100 mL crushed ice water the precipitate was collected by sunction filtration and allowed to dry in air. Yield 63.6%; yellow powder; mp 150–152°C;Rf=0.57 (DCM with drop of methanol). ; ^{1}H NMR (400 MHz, DMSO) δ 9.49 (1H ,s, H-4), 8.48 (1H, d, *J*=8.6 Hz, H-8), 8.18 (1H ,t, *J*=2.3 Hz, H-9), 7.52 (2H, H-5(d) and H-7(dd), *J*=8.9 Hz), 4.88 (1H, t, J=7.5 Hz, H-14), 4.73 (2H, td, *J*=9.4 Hz, H-16), 3.68 (2H, td, *J*=9.4 Hz, H-12), 3.41 (2H, td, *J*=9.2 Hz H-15), 2.50 (2H, s, H-13 and 17); ^{13}C NMR (101 MHz, DMSO) δ 163.6(C-2), 158.3 (C-9), 155.0(C-6), 145.3(C-8a), 142.2(C-4), 127.8(C-8), 122.2(C-4a), 122.1(C-3), 120.6 (C-7), 111.9 (C-5), 63.6 (C-11), 61.2 (C-16), 60.3 (C-12), 43.4(C-15).

3.3.1.6. Synthesis of 6-fluoro-N-phenyl-3-((phenylimino) methyl) quinolin-2-amine (91)

2-Chloroquinoline-3-carbaldehyde (0.5g) was added to aniline (8mL) and of acetic acid (9 mL) reflux for 25 min in 100 mL round bottom flask. After cooled to ambient temperature, it was poured into 100mL crushed ice water the precipitate was collected by sunction filtration and allowed to dry in air. Yield 1.09 g (70%); Yellow powder; mp 162-164°C;Rf=0.5 (*n*-hexane:EtOAc=4 :1) ; ^{1}H NMR (400 MHz, DMSO) δ 9.93 (1H, s, H-4), 7.83 (1H, d, *J*= 7.2 Hz, H-8), 7.60 (1H, s, H-9), 7.32 (1H, m, *J*=8.2, H-12,13,14,15,15), 7.27 (1H, d, *J*= 2.2 Hz, H-5), 7.26 (1H, dd, *J*=7.6 Hz, H-7), 7.04 (2H, ddd, *J*=9.1Hz ,H-20 and 22), 7.02 – 6.99 (1H, m, *J*=10.2 Hz ,H-21), 6.58 – 6.54 (2H, m, *J*= 7.8 Hz, H-19 and 23), 3.97 (H, s, ,H-17); ^{13}C NMR (101 MHz, DMSO) δ 168.7(C-9), 139.7(C-18), 129.2(C-13,15), 129.1(C-20,22), 123.4(C-4a, 8,12,14,16), 119.4(C-7,21),(C-19,23)

3.3.1.7. Synthesis of 2-methoxyquinoline-3-carboxylic acid (96)

Sodium hydroxide solution (1mL,10%) was added to a suspensions of 2-chloroquinoline-3-carbaldehyde (0.5 g) in water (20 mL). Then, saturated solution potassium permanganate in water

was added dropwise until a definite purple color remains after shaking the solution. The mixture was acidified with 10% of sulfuric acid, and oxalic acid was added to destroy the excess permanganate solution. The carboxylic acid precipitate was collected by sunction filtration. 60.1% yield, white powder, mp 205-207 °C; Rf=0.71 (*n*-hexane: EtOAc=4:1) and then A 100 mL two-neck round-bottom flask was charged with methanol (10 mL) *N*,*N*-dimethylformamide (13 mL), 2-chloroquinoline-3-carboxylic acid (0.5 g) and potassium carbonate (0.57 g); the mixture was refluxed using water condenser for 5 hours; and the progress of reaction was monitored with TLC. After completion of the reaction, methanol was removed by distillation, allowed to cool to room temperature, and then added to 100 mL ice-cold water. The solid product was collected by fractional distillation and washed with excess ice cold water. The amount of product was 0.42 g. White powder; yield 76.2%; mp 192-194 °C; Rf=0.75 (*n*-hexane: EtOAc=4:1; ^{1}H NMR (400 MHz, $CDCl_3$) δ 11.02 (1H, s, H-9), 9.12 (1H, s, H-4), 8.42 (1H, dd, *J* = 11.3 Hz, H-8), 8.39 (1H, d, *J*=7.0 Hz, H-5), 8.29 (1H, ddd, *J* = 8.2 Hz, H-7), 7.99 (1H, ddd, *J* = 8.2 Hz, H-6), 4.75 (3H, s, H-10); ^{13}C NMR (101 MHz, $CDCl_3$) δ 185.3(C-9) 157.1(C-2), 144.9(C-8a), 135.9 (C-4), 128.5 (C-7), 125.7(C-5), 123.2(C-8), 121.0(C-6), 120.3(C-4a), 115.9(C-3), 49.8(C-10).

3.3.1.8. Synthesis of methyl 2-chloroquinoline-3-carboxylate (97)

A 100 mL two-neck round-bottom flask was charged with methanol (6 mL), 2-chloroquinoline-3-carbaldehyde (0.5 g), and Sulfuric acid (2mL) the mixture was refluxed using water condenser for 2 hours; and the progress of reaction was monitored with TLC. After completion of the reaction, methanol was removed by distillation, allowed to cool to room temperature, and then added to 100 mL ice-cold water. The solid violet product was collected and washed with excess ice cold water. The amount of product was 0.37 g. yellow powder; yield 60.7%; mp196–198°C;Rf=0.66 (DCM in drop methanol); ^{1}H NMR (400 MHz, $CDCl_3$) δ 9.50 (H, s, H-4), 8.16 (1H, dd, *J*=10.5 Hz, H-8), 7.85 (1H, dd, *J*=7.8 Hz, H-5), 7.65 (1H, ddd, *J*=8.6 Hz, H-7), 7.27 (1H, ddd, J=8.6 Hz, H-6), 3.90 (3H s, H-10); ^{13}C NMR (101 MHz, $CDCl_3$) δ 166.2(C-9), 142.0(C-2), 134.8(C-8a), 132.3(C-40, 126.8(C-7), 123.3(C-5, 8) 119.4(C-3,C-4a).

3.3.2. Characterization of synthesized compounds

Characterizations of the synthesized compounds were done by spectroscopic techniques (^{1}H NMR, ^{13}C NMR and DEPT-135).

3.3.3. Determination of Antibacterial Activity

The reference strains for human pathogenic bacteria were representing Gram negatives, *E.coli (*ATCC 25922) and *Pseudomonas aeruginosa (*ATTC 27853) and Gram positives, *Staphylococcus aureus (*ATCC 6538) and *streptococcus pyogenes* (ATTC 19615) were obtained from Adama regional microbiology laboratory. *In vitro* antibacterial activities of synthesized compounds were done against the bacterial species *S. aureus, E. coil, S. pyogene* and *P. aeruginosa.* The bacterial cultures were inoculated into the nutrient broth (inoculation medium) and incubated overnight at 37 ºC. Inoculated medium containing 24 hrs grown culture were added aseptically to the nutrient medium and mixed thoroughly to get a uniform distribution. The solution was poured approximately 20 mL of sterile MHA in sterile culture plates and allowed to attain room temperature. Sterile agar-disc diffusion previously soaked in a known concentration (100 and 200 µg /mL per disc) synthesized compounds and standard drugs was prepared in DMSO using nutrient agar tubes and carefully placed at the center of the labeled seeded plate. The zones of growth inhibition around the disks were measured after 24 hrs. of incubation at 37 °C for bacteria. The inhibition zones were measured with a ruler and compared with the positive control disk (disk containing Ciprofloxacin)

3.3.4. DPPH Radical Scavenging Activity

The radical scavenging activity of the synthesized compounds was evaluated with 1, 1-diphenyl-2-picryl hydrazyl (DPPH). In the process, 4 mg/100 mL solution of DPPH in methanol was prepared. Likewise each samples was dissolved in methanol and serially diluted with the DPPH solution to furnish four different concentrations (10, 5, 2.50, 1.25µg/mL). The mixtures were shaken and allowed to stand at 37°C for 30 min in dark oven, and absorbance was recorded at 517 nm using double beam UV-Vis spectrophotometer. Ascorbic acid was used for reference standard in similar concentration as above. Percentage inhibition of DPPH radical was determined using the following equation:

$$\text{Percentage inhibition} = \frac{A_0 - A_1}{A_0} x_{100}$$

Where Ao is the absorbance of control reaction and A_1 is the absorbance in presence of test or standard sample (Zeleke *et al*, 2020).

3.3.5. Molecular Docking Analysis

AutoDock Vina with standard protocol was used to dock the proteins (PDB ID: 6F86; PDB ID: 2XCT) and synthesized compounds incorporate into the active site of proteins. The chemical structures of compounds were drawn using ChemOffice tool (ChemDraw 16.0) assigned with proper 2D orientation, and energy of each molecule was minimized using ChemBio3D. The energy-minimized ligand molecules were then used as input for AutoDock Vina, in order to carry out the docking simulation. The crystal structures of receptor molecule *E.coli* gyrase B (PDB ID: 6F86) complex with ciprofloxacin and DNA (PDB ID: 2XCT) were downloaded from protein data bank. The protein preparation was done using the reported standard protocol by removing the cocrystallized ligand, selected water molecules, and cofactors; the target protein file was prepared by leaving the associated residue with protein using Auto preparation of target protein file Auto Dock 4.2(MGLTools 1.5.6). The graphical user interface program was used to set the grid box for docking simulations. The grid was set so that it surrounds the region of interest in the macromolecule. The docking algorithm provided with AutoDock Vina was used to search for the best docked conformation between ligand and protein. During the docking process, a maximum of nine conformers were considered for each ligand. The conformations with the most favorable (least) free binding energy were selected for analyzing the interactions between the target receptor and ligands by Discovery Studio Visualizer and PyMOL. The ligands are represented in different color; H-bonds and the interacting residues are represented in ball and stick model representation(Zeleke *et al*., 2020).

CHAPTER FOUR

RESULTS AND DISCUSSIONS

4.1. Synthesis of the target compounds

In the process of synthesizing fluoroquinoline and other quinoline derivatives scaffolds Vilsmeier-Haack reaction were used. *N*-(4-fluorophenyl) acetamide **85** and *N*-phenylacetamide **93** were synthesized by refluxing 4-flouro aniline **83** and corresponding normal aniline **92** in acetic acid and acetic anhydride **84** mixtures. Then 2-chloro-6-fluoroquinoline-3-carbaldehyde **86** and 2-chloroquinoline-3-carbaldehyde **94** were prepared from *N*-(4-fluorophenyl) acetamide **85** and *N*-phenylacetamide 93 by Vilsmeier-Haack reaction methods respectively, by using DMF and $POCl_3$. The chlorine in position 2 of quinolines was substituted by nucleophiles by refluxing 2-chloro-6-fluoroquinoline-3-carbaldehyde and 2-chloroquinoline-3-carbaldehyde in *N,N* dimethylformamide with nucleophiles in basic medium. The carbaldehyde functional group was oxidized to carboxylic acid by potassium permanganate and subsequently converted to ester by using Methanol in sulfuric acid. Over all sequence of reaction used in synthesizing the compounds were illustrated in scheme 11 and 12. Structural elucidation of synthesized compounds was accomplished with spectroscopic methods.

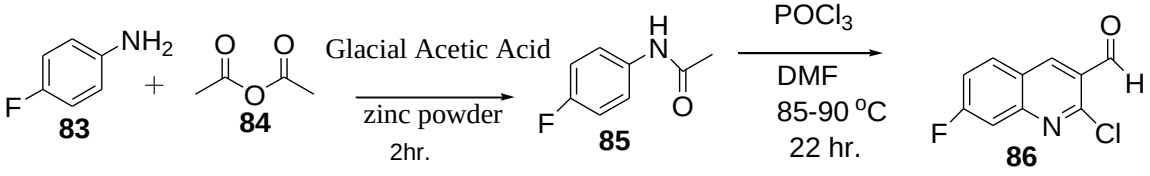

Scheme 10: Synthesis of Quinoline by Vilsmeier Reaction

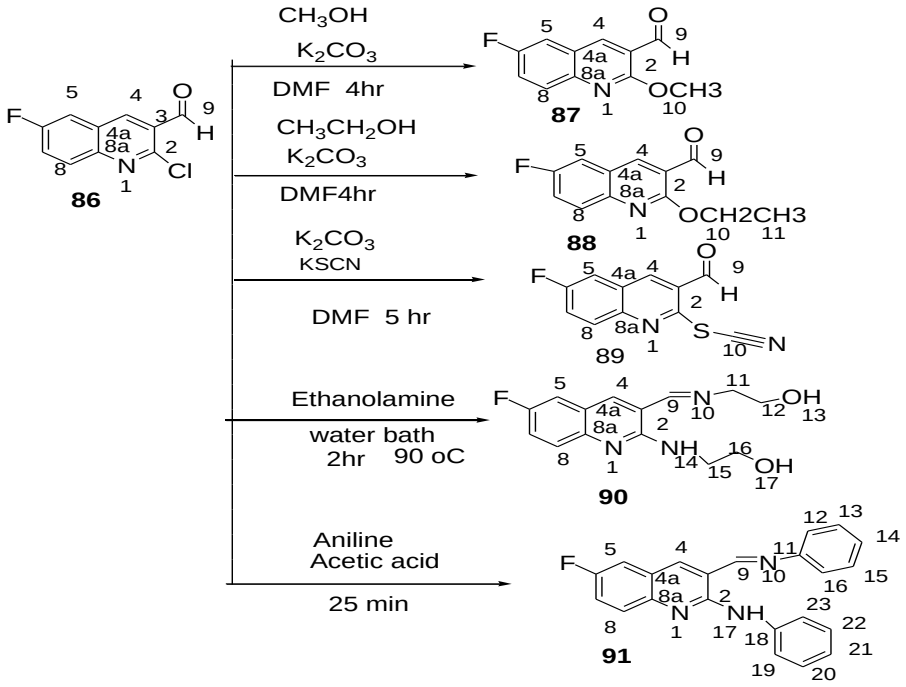

Scheme 11: Synthesis of fluoroquinoline derivatives

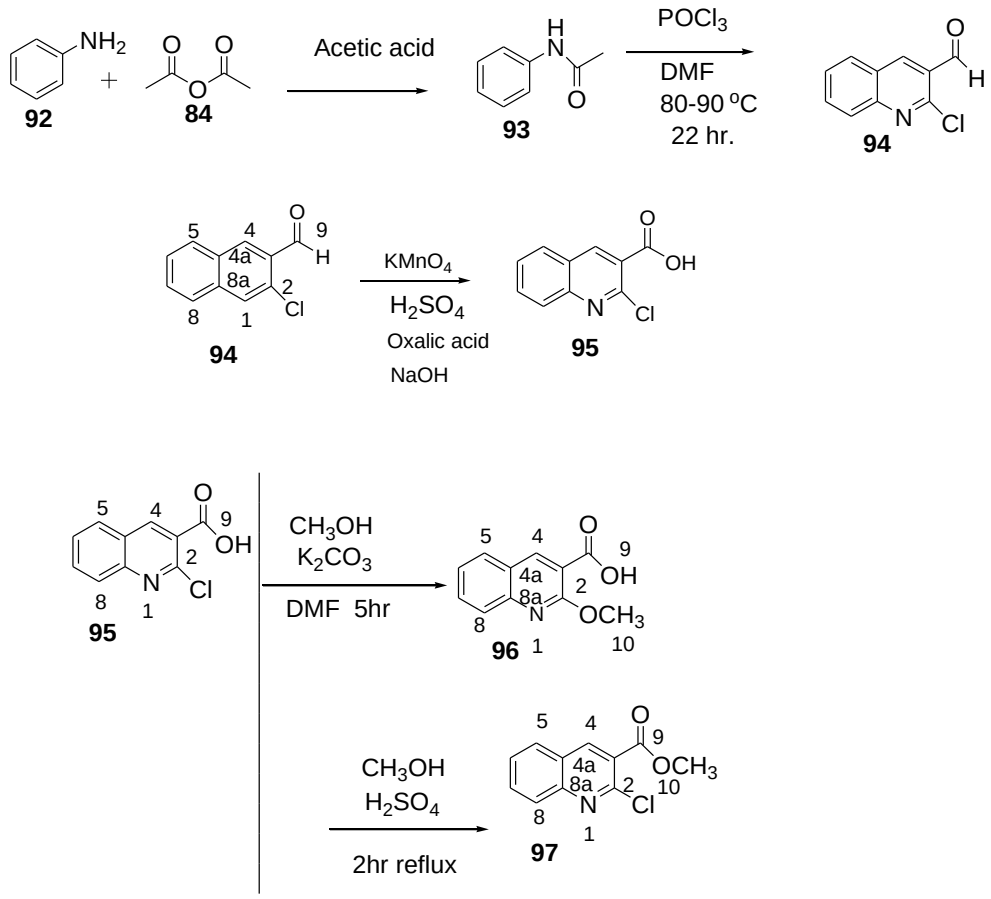

Scheme 12: Synthesis of quinoline derivatives

4.2. Characterization of Synthesized Compounds

In the course of this project, 8 compounds were synthesized and the structures of these compounds were carried out using spectroscopic methods (^{1}H NMR, ^{13}C NMR and DEPT-135). The details were presented below

Physical constants and percent yield of the synthesized compounds are presented in Table 1. Progress of the reactions were monitored using TLC. The Rf values for each of the synthesized compounds were calculated (Table 1). The spots on the TLC plate were visualized using UV lamp at 254 nm.

Table 1: Physical Characterization and % Yield of the synthesized compounds.

Compound	Color	m.p(°C)	Yield (%)	Rf values
86	Yellow	160-162	57.5%	0.72 (*n*-hexane/ EtOAc (4:1)
87	Yellow	158-160	75.2%	0.78 (*n*-hexane/ EtOAc (4:1)
88	White	184-186	72.3%	0.64 (*n*-hexane/ EtOAc (4:1)
89	Gray	156-158	67.4%	0.49 (DCM in drop of methanol)
90	Yellow	150-152	63.6%	0.57 (DCM in drop of methanol)
91	Yellow	162-164	70.0%	0.55 (*n*-hexane/ EtOAc(4:1)
96	White	192-194	76.2%	0.75 (*n*-hexane/ EtOAc (4:1)
97	Yellow	196-198	60.7%	0.66 (DCM in drop of methanol)

The % yield was estimated on the basis of initial weight of the raw materials taken and the final weight of the quinoline derivatives after purification from column chromatography. It was observed that % yield of compounds **96** (76.2% and **87** (75.2%), and **88** (72.3%) was higher as compared to other.

The target compounds were synthesized in moderate to excellent yield (57.5-76.2%). The synthesized compounds such as **86, 87 88** and **89** were readily soluble in both chloroform and DMSO whereas compounds **91, 96 and 97** were soluble in methanol and DMSO**.** Chemical structures of the synthesized compounds were fully characterized based on ^{1}Hand ^{13}C-NMR recorded data.

4.2.1. 2-Chloro-6-fluoroquinoline-3-carbaldehyde (86)

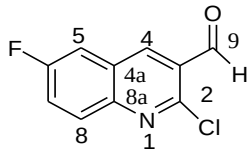

86

Figure 17:2-Chloro-6-fluoroquinoline-3-carbaldehyde (**86**)

Compound **86** was obtained in 57.5% yield as a yellow crystalline with melting point of 160-162 °C. TLC showed spot at Rf 0.72 using *n*-hexane/EtOAc (4:1) as a mobile phase. The ^{1}H NMR spectrum (400 MHz, $CDCl_3$) of compound **86** (Table 2, Appendix 1) showed singlet signal at δ 10.44 (1H) presumably due to aldehyde protons. The two doublet peaks observed at δ 8.08 (1H, d, J=7.2Hz, H-8) and 7.63 (d, J=2.3Hz, 1H, H-5) coupled with doublet of doublet observed at δ 7.27(1H, dd, J=8.7, 2.3Hz, H-7) suggest the presence of ABX pattern in ring B of quinoline moiety. The downfield chemical shift value of singlet aromatic proton at δ 8.70 (1H, s, H-4) suggest peri effect due to carbonyl at C-3 position.

The proton decoupled ^{13}C NMR spectrum (101 MHz, $CDCl_3$) of compound 86 with the aid of DEPT-135 (Appendix 3) showed the presence of ten carbon resonances. Among these five of which are methine and the remaining are quaternary carbon. The most down field signal at δ 189.0 is attributed to aldehyde carbon (C-9). The signal observed at δ 162.2 indicates fluorine containing quaternary aromatic carbon (C-6) **(**Appendix 2). The other signals were observed at **δ** 148.6 (C-2), 143.9(C-8a), 139.7 (C-4), 130.77 (C-8), 130.0(C-4a), 127.6(C-3), 123.8(C-7), 111.2(C-5).

Table 2:^{1}H, ^{13}C-NMR and DEPT-135 spectral data of compound **86**

Position	Compound **86**		
	^{1}H	^{13}C	DEPT-135
1	-	-	
2	-	148.6	
3	-	127.6	
4	8.70 (1H,s)	139.7	139.7
5	7.63 (1H, d)	111.2	111.2
4a	-	130.0	
6	-	162.2	
7	7.27 (1H, dd, *J* = 8.7 Hz)	123.8	123.8
8	8.08 (1H, d, *J*=7.2 Hz)	130.77	130.77
8a	-	143.9	
9	δ 10.44 (1H, s)	189.0	189.0

Therefore the spectral data generated here was good agreement with the structure suggested in Figure 16.

4.2.2. 6-Fluoro-2-methoxyquinoline-3-carbaldehyde (87)

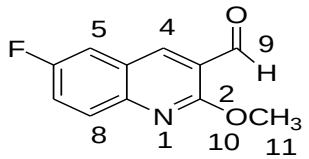

87

Figure 18:6-Fuoro-2-methoxyquinoline-3-carbaldehyde (**87**)

Compound **87** was obtained as yellow crystalline in 75.2 % yield with melting point of 158-160 ^{o}C. TLC showed spot at Rf 0.78 in *n*-hexane/EtOAc (4:1) solvent system as mobile phase. The ^{1}H NMR spectrum (400 MHz, $CDCl_3$) of compound **87** (Table 3, Appendix 4) showed singlet signal at δ 10.46 (1H) apparently due to aldehyde protons. The two doublet peaks observed at δ 8.03 (1H,d,J=8.5Hz), δ7.85 (1H, d, J=2.6 Hz) coupled with doublet of doublet signal at δ 7.48 (d, J=8.6,

Hz, 1H) suggest the presence of ABX pattern in ring B of quinoline moiety The downfield chemical shift value of singlet aromatic proton at δ 8.50 (1H,s, H-4) suggest peri effect due to carbonyl at C-3 position. The presence of methoxy signal is evident at δ 4.17.

The proton decoupled ^{13}C NMR spectrum (101 MHz, $CDCl_3$) of compound **87** (Table 3, Appendix 5) showed peak at δ 189.0 attributed to aldehyde carbon (C-9). The signal observed at δ160.7 indicates aromatic carbon containing methoxy group (C-2). This was further confirmed by the appearance of a signal at δ 53.8 (C-11). The ^{13}C-NMR spectrum together with DEPT-135 revealed the presence of five methine protons at δ139.0 (C-4), 112.6(C-5), 122.2(C-7), 129.4(C-8) and 189.1(C-9) and five quaternary carbon five quaternary carbon 158.0(C-6), 145.8(C-8a), 124.6(C-4a), 120.5(C-3). The other carbon is CH_3 carbon at ***δ* 53.8** (C-11).

Table 3:^{1}H, ^{13}C-NMR and DEPT-135 spectral data of compound **87**

Position	Compound **87**		
	^{1}H	^{13}C	DEPT-135
1	-	-	
2	-	160.7	
3	-	120.5	
4	8.50 (1H, s)	139.0	139.0
5	7.85 (1H, d, J =2.6)	112.6	112.6
4a	-	124.4	
6	-	158.0	
7	7.48 (1H, d, J = 8.6 Hz)	122.2	122.2
8	8.03 (1H, d, J = 8.5 Hz)	129.4	129.4
8a	-	145.8	
9	δ 10.46 (1H, s)	189.1	189.1
10	-	-	
11	4.17 (s, 3H)	53.8	

Therefore the spectral data generated here was good agreement with the structure suggested in Figure 17.

4.2.3. 2-Ethoxy-6-fluoroquinoline-3-carbaldehyde (88)

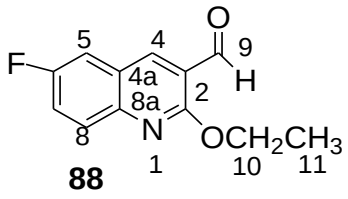

88

Figure 19: 2-Ethoxy-6-fluoroquinoline-3-carbaldehyde (**88**)

Compound **88** was obtained as white powder in 72.3 % yield with melting point of 90-91 ºC. TLC showed spot at Rf 0.64 in *n*-hexane/EtOAc (4:1) solvent system as mobile phase.

The ^{1}H NMR spectrum (400 MHz, $CDCl_3$) of compound **88** (Table 4, Appendix 7) showed singlet signal at δ 10.46 (1H) apparently due to aldehyde protons. The two doublet peaks observed at δ 7.49 (1H, d, J=2.8 Hz) and 7.84 (1H, d, J = 8.8 Hz) confirms presence of aromatic ring. The doublet of doublet signal at δ 7.34 (1H, dd, J = 8.9 Hz) due to H-7 shows *ortho* and *meta* coupled proton present on aromatic ring. The singlet at δ 9.49 (1H), H-4 appeared downfield compared to other aromatic protons due to peri effect of the carbonyl at C-3 position in compounds. Triplet signal at δ 1.52 is due to H-11. The presence quartet at δ 4.64 is evidence of methylene proton next to methyl group. Compounds have ABX pattern in ring B of quinoline moiety and a singlet in ring A of quinoline moiety.

The proton decoupled ^{13}C NMR spectrum (101 MHz, $CDCl_3$) of compound **88** (Table 4, Appendix 8) showed peak at δ 189.0 attributed to aldehyde carbon (C-9). The signal observed at δ160.6 indicates aromatic carbon containing ethoxy group (C-2). This was further confirmed by the appearance of a signal at δ 62.4 (C-10) and 14.4(C-11). The ^{13}C-NMR spectrum together with DEPT-135 revealed the presence of five methine protons at δ 138.7 (C-4), 112.6 (C-5), 122.1(C-7), 129.3 (C-8) and 189.3(C-9) and one methyl at δ 14.4. Downward signal on DEPT-135 at δ 62.4 revealed presence of methylene group.

Table 4: ^{1}H, ^{13}C-NMR and DEPT-135 spectral data of compound **88**

Position	Compound **88**		
	^{1}H	^{13}C	DEPT-135
1	-	-	
2	-	160.6	
3	-	120.4	
4	8.52 (1H, s)	138.7	138.7
5	7.49 (1H ,d, *J*=2.8 Hz)	112.6	111.2
4a	-	124.6	
6	-	158.0	
7	7.34 (1H, dd, *J*= 8.9 Hz)	122.1	122.1
8	7.84 (1H, d, *J* = 8.6 Hz)	129.3	129.3
8a	-	145.9	
9	δ 10.50 (s, 1H)	189.3	189.0
10	4.64 (2H, q, *J* = 7.1 Hz)	62.4	62.4
11	1.52 (3H, t, *J* = 7.1 Hz)	14.4	14.4

Therefore the spectral data generated here was good agreement with the structure suggested in Figure 18.

4.2.4. 6-Fluoro-2-thiocyanatoquinoline-3-carbaldehyde (89)

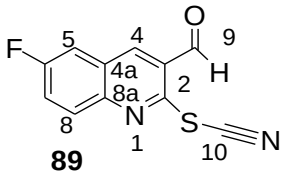

89

Figure 20:6-Fluoro-2-thiocyanatoquinoline-3-carbaldehyde (**89**)

Compound **89** was obtained as gray powder in 67.4 %yield with melting point of 156-158 ºC. TLC showed spot at Rf 0.49 in (DCM in drop of methanol) solvent system as mobile phase. The ^{1}H NMR spectrum (400 MHz, $CDCl_3$) of compound **89** (Table 4, Appendix 10) showed singlet signal at δ 10.24 (1H) apparently due to aldehyde protons. The two doublet peaks observed at δ 7.60 (1H, d, *J* = 2.9 Hz and 9 .82 (1H, d, *J* = 8.87 Hz) confirms presence aromatic ring. The other doublet of

doublet signal at δ 7.56 (1H, d, J = 9.4 Hz) due to H-7 showed *ortho* and *meta* coupled protons on aromatic ring. The singlet at δ 9.49 (1H), H-4 appeared downfield compared to other aromatic protons due to peri effect of the carbonyl at C-3 position in compounds. Compounds have ABX pattern in ring B of quinoline moiety and a singlet in ring A of quinoline moiety.

The proton decoupled ^{13}C NMR spectrum (101 MHz, $CDCl_3$) of compound **89** (Table 5, Appendix 11) showed peak at δ 190.2 due to aldehyde carbon (C-9). The signal observed at δ 161.6 indicates aromatic carbon having thiocyanate group (C-2). This was confirmed by the appearance of a signal at δ 115.3 (C-10). The ^{13}C-NMR spectrum together with DEPT-135 shows presence of five methine protons at δ 141.9 (C-4), 115.6 (C-5), 117.8 (C-7), 117.8 (C-8) and 190.2(C-9).

Table 5:^{1}H, ^{13}C-NMR and DEPT-135 spectral data of compound **89**

Position	Compound **89**		
	^{1}H	^{13}C	DEPT-135
1	-	-	
2	-	161.6	
3	-	119.1	
4	8.48 (1H, s)	141.9	141.9
5	7.60 (1H, d, J = 2.9 Hz	115.6	115.6
4a	-	122.3	
6	-	158.7	
7	7.56 (1H, dd, J = 9.4 Hz)	117.8	117.8
8	9 .82 (1H, d, J = 8.87 Hz)	122.5	122.5
8a	-	141.9	
9	δ 10.24 (1H, s, H-9),	190.2	190.2
10		115.3	-

The spectral data generated here was good agreement with the structure suggested in Figure 19.

4.2.5.2-((2-Hydroxyethyl) amino)-3-(-2-(ethylideneamino) ethanol quinoline (90)

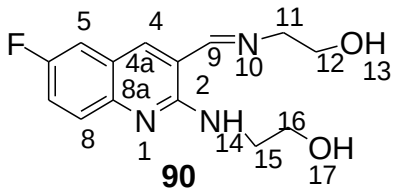

90

Figure 21:2-((2-Hydroxyethyl) amino)-3-(-2-(ethylideneamino) ethanol quinoline (**90**)

Compound **90** was obtained as yellow crystalline in 63.6 %yield with melting point of 150-152 ºC. TLC showed spot at Rf 0.57 (DCM in drop of methanol) solvent system as mobile phase. The ^{1}H NMR spectrum (400 MHz, $CDCl_3$) of compound **90** (Table 6, Appendix 13) showed singlet signal at δ 8.18 (1H) apparently due to imine protons. The two doublet peaks observed at δ 7.52 (d, J = 9.4 Hz, 1H) and 8.48 (1H, d, J=8.6 Hz, H-8) confirms presence of protons on aromatic ring. The singlet at δ9.49 (1H), H-4appeared downfield compared to other aromatic protons due to peri effect of the carbonyl at C-3 position in compounds. The other singlet at δ 2.50 (2H) shows presence of hydroxyl group. Triplet signal at δ 3.41 (2H), 3.68 (2H) and 4.73 (2H) shows presence of methylene next to another methylene. Compounds have ABX pattern in ring B of quinoline moiety and a singlet in ring A of quinoline moiety.

The proton decoupled ^{13}C NMR spectrum (101 MHz, $CDCl_3$) of compound **90** (Table 5, Appendix 14) showed peak at δ 158.3 attributed to imine carbon (C-9). The signal observed at δ 163.6 indicates attributed to quaternary aromatic carbon containing NH substituent(C-2). Peak at δ 155.07(C-6) shows quaternary aromatic carbon containing fluorine substituent. The ^{13}C-NMR spectrum together with DEPT-135 revealed the presence of five methine carbon at δ 142.2 (C-4), 111.9 (C-5), 120.6 (C-7), 127.8 (C-8) and 158.3(C-9) and four methylene at δ 63.6(C-11), 60.3 (C-12), 43.4(C-15), 61.2(C-16).

Table 6:^{1}H, ^{13}C-NMR and DEPT-135 spectral data of compound **90**

Position	Compound **90**		
	^{1}H	^{13}C	DEPT-135
1	-	-	-
2	-	163.6	-
3	-	122.1	-
4	9.49 (1H ,s)	142.2	142.2
5	7.52 (1H, d, *J*=8.9 Hz)	111.9	111.9
4a	-	122.2	-
6	-	155.6	-
7	7.52 (1H, dd, *J*=8.9 Hz)	120.6	120.6
8	8.48 (1H, d, *J*=8.6 Hz,	127.8	127.8
8a	-	145.3	-
9	8.18 (1H ,t, *J*=2.3 Hz)	158.3	158.3
10	4.64 (q, *J* = 7.1 Hz, 2H)	115.3	115.3
11	1.5(t,2H)	63.6	-
12	3.68 (2H, td, *J*=9.4 Hz)	60.3	60.3
13	2 2.50 (2H, s)	-	-
14	4.88 (1H, t, J=7.5 Hz	-	-
15	3.41 (2H, td, *J*=9.2 Hz)	43.4	43.4
16	4.73 (2H, td, *J*=9.4 Hz)	61.2	61.2
17	2.50 (2H, s)	-	-

Therefore the spectral data generated here was good agreement with the structure suggested in Figure 20.

4.2.6. 6-Fluoro-N-phenyl-3-((E)-(phenylimino) methyl) quinolin-2-amine (91)

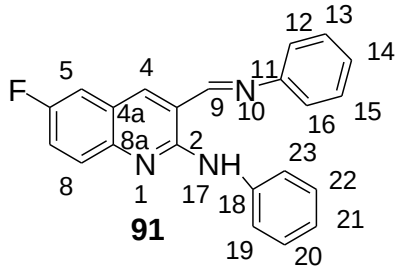

Figure 22:6-Fluoro-N-phenyl-3-((E)-(phenylimino) methyl) quinolin-2-amine (**91**)

Compound **91** was obtained as yellow crystalline in 70.0% yield with melting point of 162-164 ºC. TLC showed spot at Rf 0.55 in *n*-hexane/EtOAc (4:1) solvent system as mobile phase. The ^{1}H NMR spectrum (400 MHz, $CDCl_3$) of compound **91** (Table 7, Appendix 16) showed singlet signal resonates at δ 7.60 (1H, s, H-9), presence of imine proton and δ 9.93 (1H, s, H-4), 7.83 (1H, d, *J*= 7.2 Hz, H-8), 7.27 (1H, d, *J*= 2.2 Hz, H-5), 7.26 (1H, dd, *J*=7.6 Hz, H-7) indicates aromatic ring proton ring. Compounds have ABX pattern in ring B of quinoline moiety and a singlet in ring A of quinoline moiety.

The proton decoupled ^{13}C NMR spectrum (101 MHz, $CDCl_3$) of compound **91** (Table 5, Appendix 17) showed peak at δ 168.7(C-9) indicates imine carbon **(**Table 7**,** Appendix 17**).**The DEPT-135 NMR spectrum suggests the presence aromatic methine **(**Table 7, Appendix 18).

Table 7:^{1}H, ^{13}C-NMR and DEPT-135 spectral data of compound **91**

Position	Compound **91**		
	^{1}H	^{13}C	DEPT-135
1	-	-	-
2	-	163.6	-
3	-	122.1	-
4	9.93 (1H, s)	142.2	142.2
5	7.27 (1H, d, *J*= 2.2 Hz)	111.9	111.9
4a	-	123.4	-
6	-	155.6	-
7	7.26 (1H, dd, *J*=7.6 Hz)	119.4	119.4
8	7.83 (d, *J* = 2.9 Hz, 1H)	123.4	123.4
8a	-	145.3	-
9	7.60 (1H, s)	168.7	168.7
10	4.64 (q, *J* = 7.1 Hz, 2H)	115.3	115.3
11	-	63.6	-
12	7.32 (1H, m, *J*=8.2)	123.4	123.4
13	7.32 (1H, m, *J*=8.2)	129.2	129.2
14	7.32 (1H, m, *J*=8.2)	123.4	123.4
15	7.32 (1H, m, *J*=8.2)	129.2	129.2
16	4.73 (td, 2H)	123.4	123.4
17	3.97 (H, s)	-	-
18	-	139.7	-
19	6.58 – 6.54 (2H, m, *J*= 7.8 Hz)	119.4	-
20	7.04 (2H, ddd, *J*=9.1Hz)	129.1	129.1
21	7.02–6.99 (1H,m, *J*=10.2 Hz)	119.4	119.4
22	7.04 (2H, ddd, *J*=9.1Hz)	129.1	129.1
23	6.58–6.54 (2H, m,*J*= 7.8 Hz)	119.4	119.4

Therefore the spectral data generated here was good agreement with the structure suggested in Figure 21.

4.2.7. 2-Methoxyquinoline-3-carboxylic acid (96)

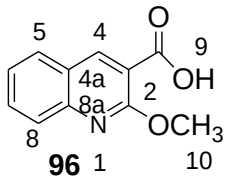

Figure 23:2-Methoxyquinoline-3-carboxylic acid (**96**)

Compound **96** was obtained as white crystalline in 76.2 %yield with melting point of 96-98 ºC. TLC showed spot at Rf 0.75 in *n*-hexane/EtOAc (4:1) solvent system as mobile phase. The ^{1}H NMR spectrum (400 MHz, $CDCl_3$) of compound **96** (Table 8, Appendix 19) showed singlet signal at δ 11.02 (1H) apparently due to carboxylic acid proton. The two doublet of doublet peaks observed at δ 8.42 (1H, dd, J = 11.3 Hz, H-8), and 8.39 (1H, dd, J=7.0 Hz, H-5), confirms presence of protons on aromatic ring. The other multiplet signal at δ 7.99 (1H, ddd, J = 8.2 Hz) and 8.29 (1H, ddd, J = 8.2 Hz) are due to H-7 and H-6 respectively. This shows aromatic ring has no any substituents at carbon 6. Singlet signal at δ 4.75 (3H) is evidence for methoxy substituent. Compounds have ABX pattern in ring B of quinoline moiety and a singlet in ring A of quinoline moiety.

The proton decoupled ^{13}C NMR spectrum (101 MHz, $CDCl_3$) of compound **96** (Table 8, Appendix 20) showed peak at δ 185.30 attributed to carboxylic acid carbon (C-9). The signal observed at δ157.6 indicates aromatic carbon containing methoxy group (C-2). This was further confirmed by the appearance of a signal at δ 49.8 (C-10). The ^{13}C-NMR spectrum together with DEPT-135 revealed the presence of five methine protons at δ 135.9 (C-4), 125.7 (C-5), 121.0(C-6) 128.5 (C-7) and 123.2 (C-8) and methyl at δ 49.8.

Table 8:^{1}H, ^{13}C-NMR and DEPT-135 spectral data of compound **96**

Position	Compound **96**		
	^{1}H	^{13}C	DEPT-135
1	-	-	-
2	-	157.1	-
3	-	115. 9	-
4	9.12 (1H, s)	135.9	135.9
5	8.39 (1H, d, *J*=7.0 Hz)	125.7	125.7
4a	-	120.3	-
6	7.99 (1H, ddd, *J* = 8.2 Hz)	121.0	121.0
7	8.29 (1H, ddd, *J* = 8.2 Hz)	128.5	128.5
8	8.42 (1H, dd, *J* = 11.3 Hz)	123.2	123.2
8a	-	144.9	-
9	δ 11.02 (1H, s)	185.3	-
10	4.75 (3H, s)	49.8	49.8

Therefore the spectral data generated here was good agreement with the structure suggested in Figure 22.

4.2.8. Methyl 2-chloroquinoline-3-carboxylate (97)

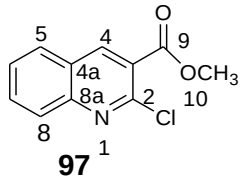

97

Figure 24: Methyl 2-chloroquinoline-3-carboxylate (**97**)

Compound **97** was obtained as yellow crystalline in 60.7 %yield with melting point of 196-198 ºC. TLC showed spot at Rf 0.66 (DCM in drop of methanol) solvent system as mobile phase. The ^{1}H NMR spectrum (400 MHz, $CDCl_3$) of compound **97** (Table 9, Appendix 22) showed singlet signal at δ 3.90 (3H) apparently due to methoxy of ester proton. The two doublet of doublet peaks observed at δ 8.16 (1H, dd, *J*=10.5 Hz, H-8), 7.85 (1H, dd, *J*=7.8 Hz, H-5), confirms presence of protons on aromatic ring. The multiplet signal at δ 7.27 (1H, ddd, J=8.6 Hz, H-6) and 7.65 (1H, ddd, *J*=8.6 Hz, H-7), are due to H-6 and H-7 respectively. This shows aromatic ring has no any substituents at carbon 6. Compounds have ABX pattern in ring B of quinoline moiety and a singlet in ring A of quinolone moiety.

The proton decoupled ^{13}C NMR spectrum (101 MHz, $CDCl_3$) of compound **97** (Table 8, Appendix 23) showed peak at δ 166.2 attributed to esteric carbon (C-9). This was further confirmed by the appearance of a signal at δ 52.9 (C-10). The ^{13}C-NMR spectrum together with DEPT-135 revealed the presence of five methine protons at δ 132.3 *(*C-4), 123.3 (C-5), 124.3 (C-6) 126.8 (C-7) and 123.3 (C-8) and methyl at δ 52.9.

Table 9: ^{1}H, ^{13}C-NMR and DEPT-135 spectral data of compound **97**

Position	Compound **97**		
	^{1}H	^{13}C	DEPT-135
1	-	-	-
2	-	142.0	-
3	-	119.4	-
4	9.50 (H, s)	132.3	132.3
5	7.85 (1H, dd, *J*=7.8 Hz)	123.3	123.3
4a	-	119.4	-
6	7.27 (1H, ddd, J=8.6 Hz)	124.3	124.3
7	7.65 (1H, ddd, *J*=8.6 Hz)	126.8	126.8
8	8.16 (1H, dd, *J*=10.5 Hz)	123.3	123.3
8a	-	134.8	-
9		166.2	-
10	3.90 (3H s)	52.9	52.9

Therefore the spectral data generated here was good agreement with the structure suggested in Figure 23.

4.3. Antibacterial Activity of Synthesized Compounds.

Quinoline derivatives show high antimicrobial activity against various microbial infections and used to treat various type of disease(Narwal *et al*., 2017). All synthesized compounds were evaluated for their *in-vitro* antibacterial activities against *S. aureus, E. coli, S. pyogene* and *P. aeruginosa* using disk diffusion method. The zone of inhibition values indicated that all the compounds exhibited a varied range of 6-14.7 mm (Table 10). The data in Table 10 shows that all synthesized compound displayed good activity against two or more bacterial strain. The mean inhibition zone ranged from the lowest (6.34±0.01 mm at 100µg/mL) to the highest (14.7±0.04 at 200µg/mL) for compound **96** against *P.aeruginosa* and compound **86** against *S. pyogene* respectively.

Six of eight synthesized compounds; **86, 87, 88, 89,90 and 91** have good activities against *E.coli* with compounds **86,89** and **90** displayed inhibition zone of 11.9±0.41 mm**,** 12.2±0.32mm and 11.2±0.13 mm at 200µg/mL respectively. Compound **90** had no activity against *S.aureus.* Compounds, **86, 87 and 89** exhibited good activity against *S.aureus* with IZ of 12.0±0.01mm**,** 10.4±0.60mm**,** and 11.0±0.56 mm at 200µg/mL respectively. On the other hand compounds **86, 87, 88, 89, 90** displayed inhibition zone of 13.7±0.98mm, 11.8±0.71mm 10.5±0.79mm, 11.9±0.41mm and 10.4±0.66mm respectively against *P. aeruginosa.* This was superior to activity displayed by the standard drug (ciprofloxacin) which had IZ 9.0±0.14mm at 200 µg/mL as shown in Table 10 than standard drug (ciprofloxacin) which displayed inhibition zone of 9.0±0.14mm at 200 µg/mL as shown in Table 8.

Table 10: Inhibition zone of synthesized compounds in mm (mean ± SD).

Conc .µg/L	86	87	88	89	Ciprofloxacin	Bacterial strains
100	11.0±0.72	9.33±0.33	10.5±0.55	11.6±0.25	20.0 ±0.76	*E.coli*
200	11.9±0.41	10.0±0.11	11.09±0.57	12.2±0.32	22.2±0.06	
100	12.2±0.54	11.1±0.32	9.76±0.44	11.0±0.72	9.0±0.14	*P. aeruginosa*
200	13.7±0.98	11.8±0.71	10.5±0.79	11.9±0.41	10.0±0.45	
100	11.2±0.71	9.0±0.64	9.3±0.60	10.7±0.67	11.8±0.91	*S. aureus*
200	12.0±0.01	10.4±0.60	9.7±0.52	11.0±0.56	12.3±0.53	
100	13.8±0.04	12.5±0.43	12.9±0.35	12.3±0.55	17.0±0.67	*S.pyogene*
200	14.7±0.04	13.0±0.53	13.2±0.3	12.9±0.33	18.2±0.34	
Conc .µg/L	**90**	**91**	**96**	**97**	**ciprofloxacin**	**Bacterial strains**
100	11.2±0.11	11.0±0.05	NA	NA	20.0 ±0.76	*E.coli*
200	11.2±0.13	11.1±0.07	7.0±0.80	7.5±0.65	22.2±0.06	
100	9.57±0.75	8.9±0.05	6.34±0.01	6.54 ±0.05	9.0±0.14	*P. aeruginosa*
200	10.4±0.66	9.0±0.02	7.9±0.45	8.0±0.55	10.0±0.45	
100	NA	8.88±0.54	7±0.22	7.1±0.22	11.8±0.91	*S. aureus*
200	NA	9.3±0.45	7.5±0.81	7.8±0.66	12.3±0.53	
100	9.77±0.33	6.6±0.87	7.1±0.33	7.3±0.77	17.0±0.67	*S.pyogene*
200	10.2±0.92	7.3±0.67	7.6±0.99	7.9±0.11	18.2±0.34	

NA: Not Applicable, no inhibition zone

The bacterial inhibition zone displayed by compounds synthesized were further elaborated in Figure 24.

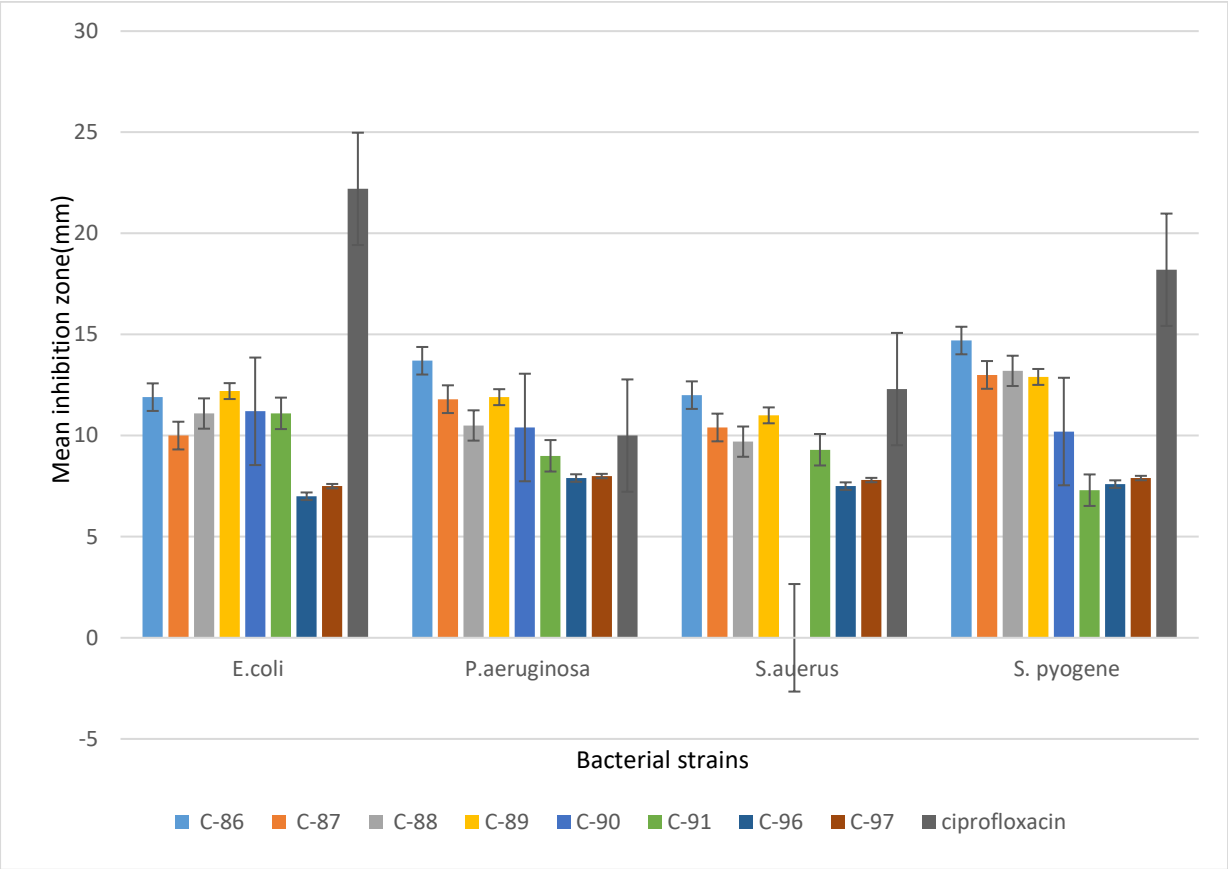

Figure 25: Inhibition zone (mm) of synthesized compounds at 200µg/mL.Error bar indicates standard deviation.

Table 11: Comparing inhibition zone (mm) of some synthesized compounds with similar compound from literature review

Concentration	Compounds	Bacterial strain			Structural difference	*Comments*
		E.coli	*P. aeruginosa*	*S. aureus*		
Synthesized compound at 200 µg/mL	**86**	11.9±0.41	13.7±0.98	12.0±0.01	Fluorine at 6 position	More active
Compounds from literature µg/mL 500	**53**	6. 67±0.89	9.0±0.67	7.0±0.67	No fluorine at 6 position	Less active
Synthesized compound at 200 µg/mL	**87**	10.0±0.11	11.8±0.71	10.4±0.60	Fluorine at 6 position	More active
Compounds from literature at µg/mL 500	**54**	No activity	9.33±0.44mm	6.33±0.44	No fluorine at 6 position	Less active
Synthesized compound at 200 µg/mL	**88**	11.09±0.57	10.5±0.79	9.7±0.52	Fluorine at 6 position	More active
Compounds from literature at µg/mL 500	**55**	No activity	9.67±1.11	7.67±0.44	No fluorine at 6 position	Less active
Synthesized compound at 200 µg/mL	**89**	12.2±0.32	11.9±0.41	11.0±0.56	Fluorine at 6 position	More active
Compounds from literature at µg/mL 500	**56**	11.33±1.11	8.33±0.44	6.33±0.44	No fluorine at 6 position	Less active
Synthesized compound at 200 µg/mL	**96**	7.0±0.80	7.9±0.45	7.5±0.81	Methoxy at 2-position	More active
Compounds from literature at µg/mL 500	**57**	No activity	6.33±0.44	7.33±0.44	Chlorine at 2-position	Less active

Table 11 shows quinoline derivatives containing fluorine substituent at 6-position shows greater inhibition zone than quinoline derivatives that have no fluorine at 6-position. Quinoline with carboxylic functional group at position-3 and methoxy at position-2 are more active than quinoline derivatives containing carboxylic acid at position-3 and chlorine at position-2.

4.4. Molecular Docking Studies of the Synthesized Compounds

4.4.1. Molecular docking studies of synthesized compounds against *E.coli* DNA gyrase B

DNA gyrase is Type II topoisomerases enzyme that reduces topological strain in an ATP dependent manner while double-stranded DNA is being unwound by elongating RNA-polymerase or by helicase and introduces negative supercoils into DNA(Drlica & Zhao, 2017). The molecular docking analysis of synthesized compounds was carried out to evaluate their binding pattern against *E.coli* DNA gyrase B and compared with standard clinical drug (ciprofloxacin). Binding affinity, H-bond and residual amino acid interaction of the synthesized compounds and ciprofloxacin were depicted in Table 12. Synthesized compounds displayed binding energy ranging from -6.0 to-7.2 kcal/mol (Table 12). From these, compound **91** showed comparable binding affinity with a minimum energy of -7.2 kcal/mol. Compound **91** has similar binding affinity with standard drug, ciprofloxacin. Compared ciprofloxacin the synthesized compounds showed similar residual interactions with amino acid residues Ile-78, Asn-46 Glu-50, Asp-73 and Gly-77 and H-bond Asp-73, Arg-76 and Thr-165. Compounds **89**, **90**, **91** and **97** have additional hydrogen bonding interaction with amino acid residue Asn-46. The compounds **89** (Asp-73, Asn-46, Gly-77), **90 (**Asp-73, Asn-46, Glu-50, Thr-165), **91 (**Asn-46**)** and **97 (**Asp-73, Asn-46, Thr-165**)** have additional hydrogen bonding interaction with amino acid residue. The compounds **86** (Asn-46, Ile-94, Ile-78, Ala-47)**, 87** (Asn-46, Ile-94, Ile-78, Ala-47)**, 88** (Asn-46, Ile-94, Ile-78, Ala-47) and **96** (Asn-46, Ile-94, Ile-78, Ala-47) have additional hydrophobic interaction with amino acid residue. The residual amino acid interactions of synthesized compounds with DNA gyrase (6f86) in this study were well in agreement with binding modes that include crucial interaction between the ligant, AS-73 and water molecules. **87** (-6.3 kcal/mol), **88** (-6.5 kcal/mol), **89** (-6.4 kcal/mol) and **90** (-6.3 kcal/mol) and **91** (-7.2 kcal/mol) showed good activity against *E.coli* DNA gyrase B, among which compound **91** (-7.2 kcal/mol) displayed best activity.

Table 12: Molecular Docking value of synthesized compounds against *E.coli* DNA gyrase B (PDB ID: 6F86):

Compounds	Affinity (kcal/mol)	H-bond	Residual Amino acid Interactions	
			Hydrophobic/Pi-Cation/Pi-Anion/ Pi-Alkyl interactions	Van-der Walls interactions
86	-6.1	Asp-73, Gly-77, Thr-165	Asn-46, Ile-94, Ile-78, Ala-47	Arg-76, Pro-79
87	-6.3	Asp-73, Gly-77, Thr-165	Asn-46, Ile-94, Ile-78, Ala-47	Glu-50, Ala-47, Arg-76, Pro-79
88	-6.5	Asp-73, Gly-77, Thr-165	Asn-46, Ile-94, Ile-78, Ala-47	Val-43, Glu-50
89	-6.4	Asp-73, Asn-46, Gly-77	Ile-78, Pro-79,	Ala-47, Thr-165, Glu-50, Gly-50, Arg-76
90	-6.3	Asp-73, Asn-46, Glu-50, Thr-165	Ile-78, Ile-94, Gly-77	Gly-75, Val-167
91	-7.2	Asn-46	Ala-47, Glu-50, Asp-73, Thr-165, Gly-77, Arg-76	Asp-49, Val-43
96	-6.2	Asp-73, Gly-77, Thr-165	Asn-46, Ile-94, Ile-78, Ala-47	Pro-79, Arg-76, Gly-75
97	-6.0	Asp-73, Asn-46, Thr-165	Glu-50, Arg-76, Ile-78	--
Ciprofloxacin	-7.2	Asp-73, Arg-76, Thr-165	Glu-50, Gly-77, Ile-78, Asn-46	Ala-47

The result was compared with literature review that, synthesized compound of **86** (-6.1 kcal/mol) have comparable binding affinity with compound **53** (-6.2 kcal/mol) of literature review. Synthesized compound **89** and **55** from literature have the same binding affinity which is -6.3 kcal/mol. Synthesized compound 87(-6.3 kcal/mol) and 53(-6.2 kcal/mol) a from literature review have comparable value.

4.4.2. Molecular docking value of synthetic compounds against Human Topoisomerase IIα

Topoisomerases are target for cancer therapy, by selectively cleaving, rearranging, and relegating DNA strands, topoisomerases can both alter the super helical state of DNA and help disentangle interlinked chromosomes. Topoisomerases fall in to two general categories, termed type I or type II(Wendorff *et al*., 2016). In this project, molecular docking interaction against Human Topoisomerase IIα was studied and compared with anticancer drug vosaroxin. The synthesized compounds were found to have binding affinity ranging from -6.8 to -7.5 (kcal/mol) as shown in Table 3, with best result **87** (-7.2 kcal/mol),**88** (-7.2 kcal/mol), **91** (-7.4 kcal/mol) and **97** (-7.5 kcal/mol). Compound **87** and **88** have similar binding affinity with standard drug Vosaroxin (-7.2 kcal/mol). Compound **91** and **97** have better binding affinity than vosaroxin. Compared vosaroxin the synthesized compounds showed similar residual interactions with amino acid residues Leu-705, Ile-577, Pro-593, Glu-682, Tyr-684, Arg-672, and Gln-542 and H-bond with Leu-705, Ile-577 and Pro-593. Compounds **88, 91** and **97** have additional hydrogen bonding interaction with amino acid residue Leu-705. Synthesized compounds showed similar residual interactions with vosaroxin against Human Topoisomerase IIα (PDB ID: 4fm9). The residual amino acid interactions of synthesized compounds in this study were well in agreement with binding modes that include crucial hydrogen interaction between the ligand and amino acids residues (Ser-591 and Leu-685). Compounds **88, 91** and **97** might have better anti-cancer agents than other synthesized compounds.

Table 13: Molecular docking value of synthetic compounds against Human Topoisomerase IIα (PDB ID: 4fm9)

Compounds	Affinity (kcal/mol)	H-bond	Residual Amino acid Interactions	
			Hydrophobic/Pi-Cation/Pi-Anion/ Pi-Alkyl interactions	Van-der Walls interactions
86	-6.8	Ser-547	Ile-577, Gln-542, Tyr-686, Leu-685, Leu-705, Lys-701	Ser-591, Pro-593, Leu-592, Tyr-590, Gln-544, Asp-543, Glu-702
87	-7.2	Ser-547, Glu-702, Gln-542, Leu-592, Tyr-684	Asp-683, Leu-685, Leu-705	Asp-543, Ile-577, Lys-701
88	-7.2	Ser-547, Leu-685	Leu-705, Lys-701	Tyr-684, Glu-702, Tyr-686, Gln-542, Asp-543, Gln-544, Ile-577
89	-7.1	Ser-547, Asp-543, Leu-685	Leu-705, Lys-701	Asp-683, Tyr-684, Glu-702, Gln-542, Ile-577, Gln-544, Tyr-590
90	-7.0	Ser-547, Ser-591, Asp-543, Gln-542, Pro-593, Leu-685	Asp-683, Lys-701, Leu-705, Glu-702	Gly-546, Asp-541, Ile-577, Tyr-684
91	-7.4	--	Asp-541, Gln-542, Asp-543, Leu-592, Pro-593, Leu-705	Ser-547, Glu-702, Tyr-686, Asp-683, Lys-701, Leu-685, Tyr-684, Gln-544
96	-6.9	Ser-547, Gln-542, Leu-685	Leu-705	Asp-543, Glu-702, Tyr-686, Lys-702, Tyr-684, Tyr-590, Ile-577
97	-7.5	Ser-547, Glu-702, Asp-543, Leu-685, Gln-542, Leu-592	Ile-577, Leu-705, Pro-593	Lys-701, Tyr-684, Tyr-590
Vosaroxin	-7.2	Ser-591, Leu-685, Leu-592	Leu-705, Ile-577, Pro-593	Glu-682, Tyr-684, Arg-672, Gln-542

Table 14: Molecular docking value of synthetic compounds against human peroxidoxin (PDB ID: 1HD2)

Compounds	Affinity (kcal/mol)	H-bond	Residual Amino acid Interactions	
			Hydrophobic/Pi-Cation/Pi-Anion/ Pi-Alkyl interactions	Van-der Walls interactions
89	-5.0	Thr-147	Pro-45, Arg-127	Thr-44, Gly-46, Gly-148, Leu-149
Ascorbic Acid	-4.9	Cys-47, Thr-44, Gly-46, Thr-147	Pro-40, Pro-45, Phe-120, Arg-127, Leu-149	--

Compound **89** (-5.0 kcal/mol) have better binding affinity than standard drug ascorbic acid (-4.9 kcal/mol).

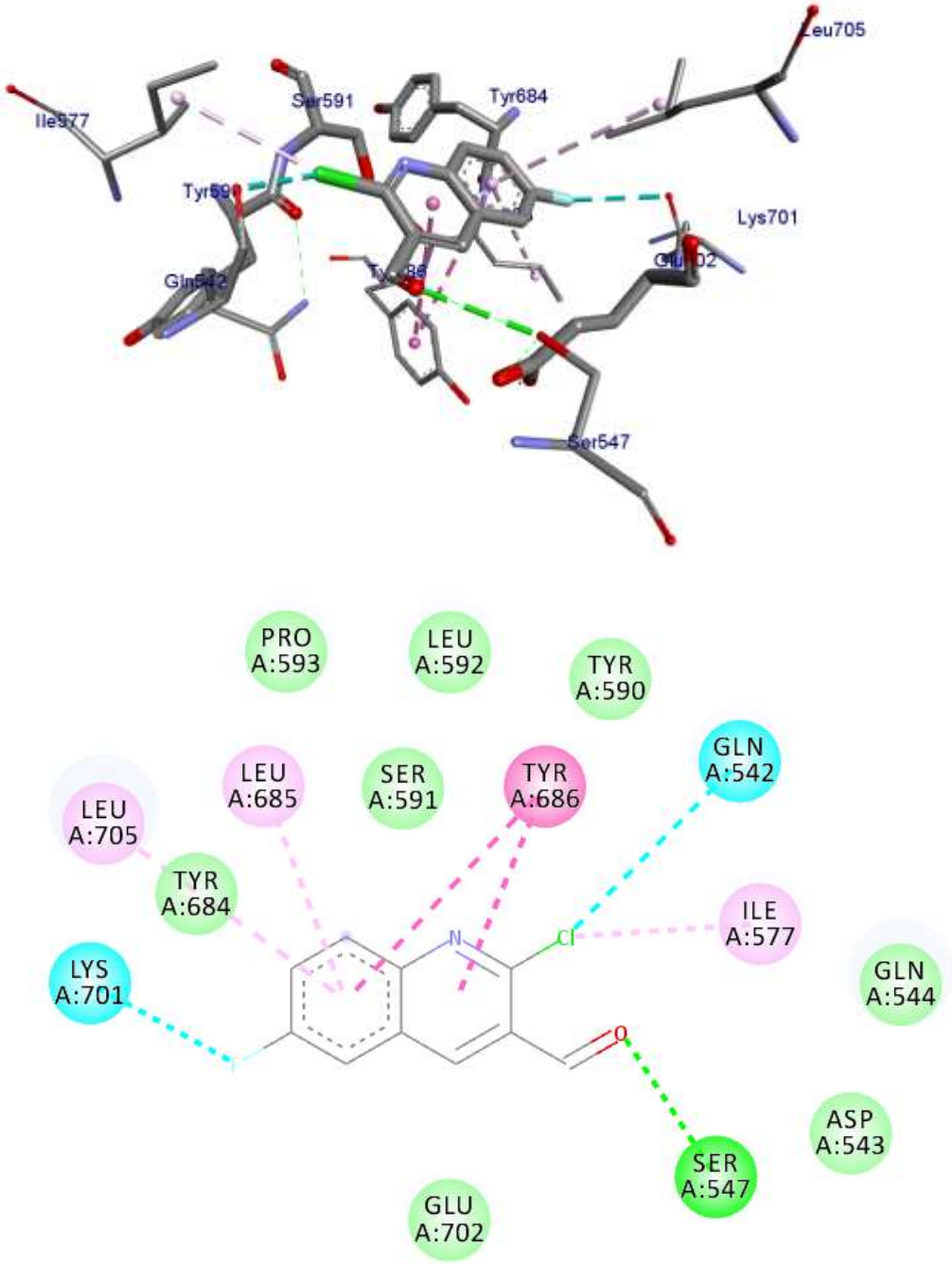

Figure 26: The binding interactions compound **86** against Human Topoisomerase IIα (PDB ID: 4fm9).

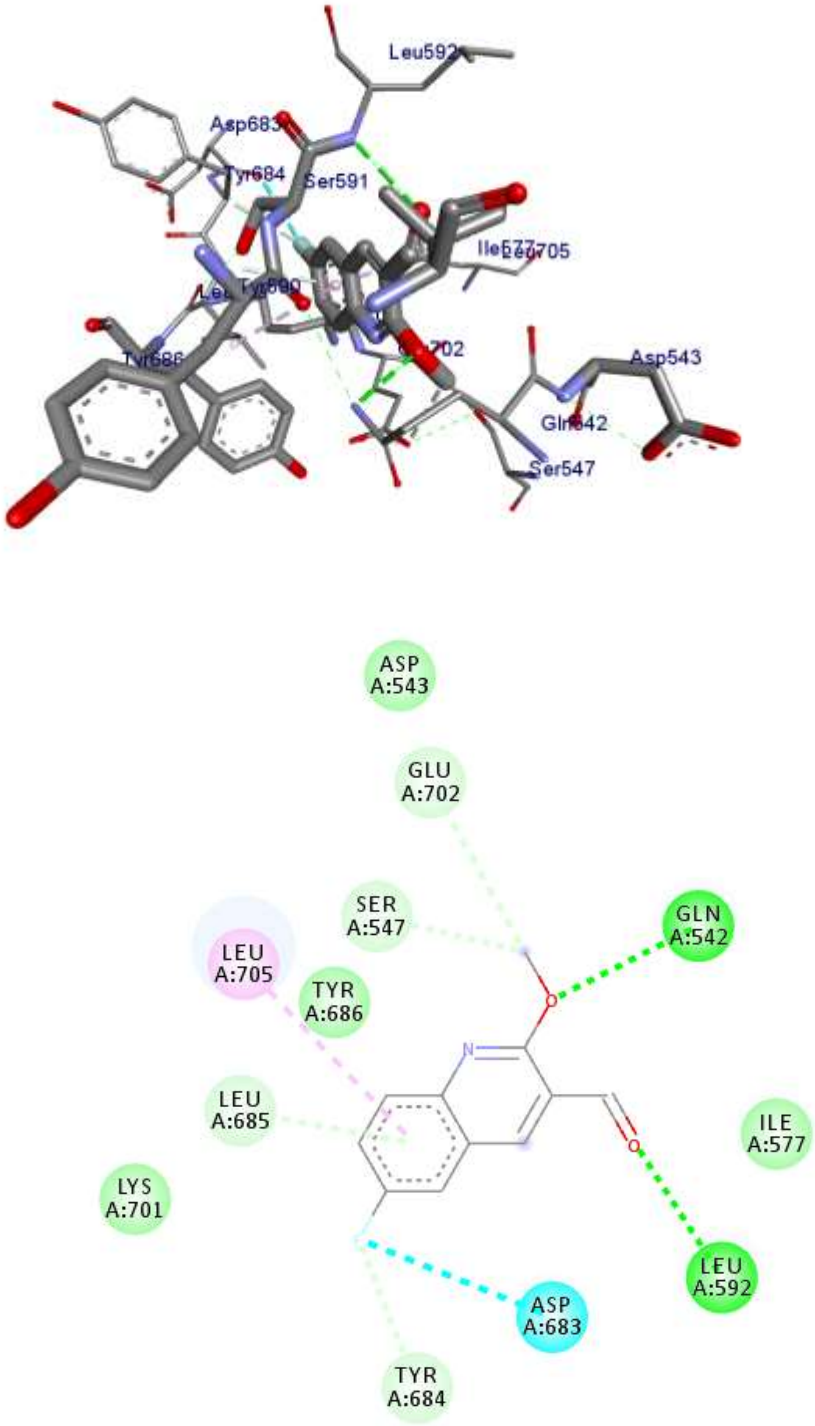

Figure 27: The binding interactions compound **87** against Human Topoisomerase IIα (PDB ID: 4fm9).

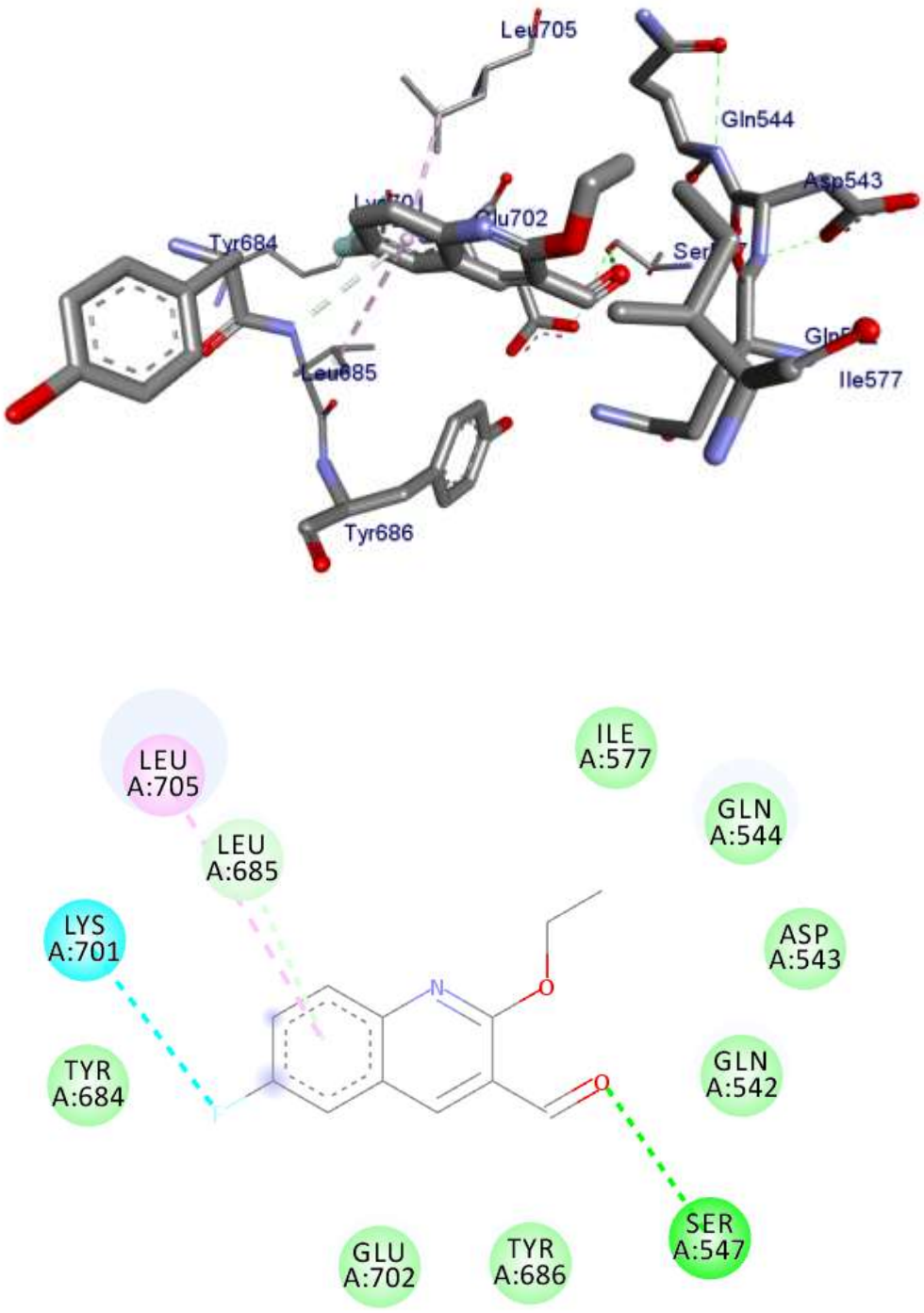

Figure 28: The binding interactions compound **88** against Human Topoisomerase IIα (PDB ID: 4fm9).

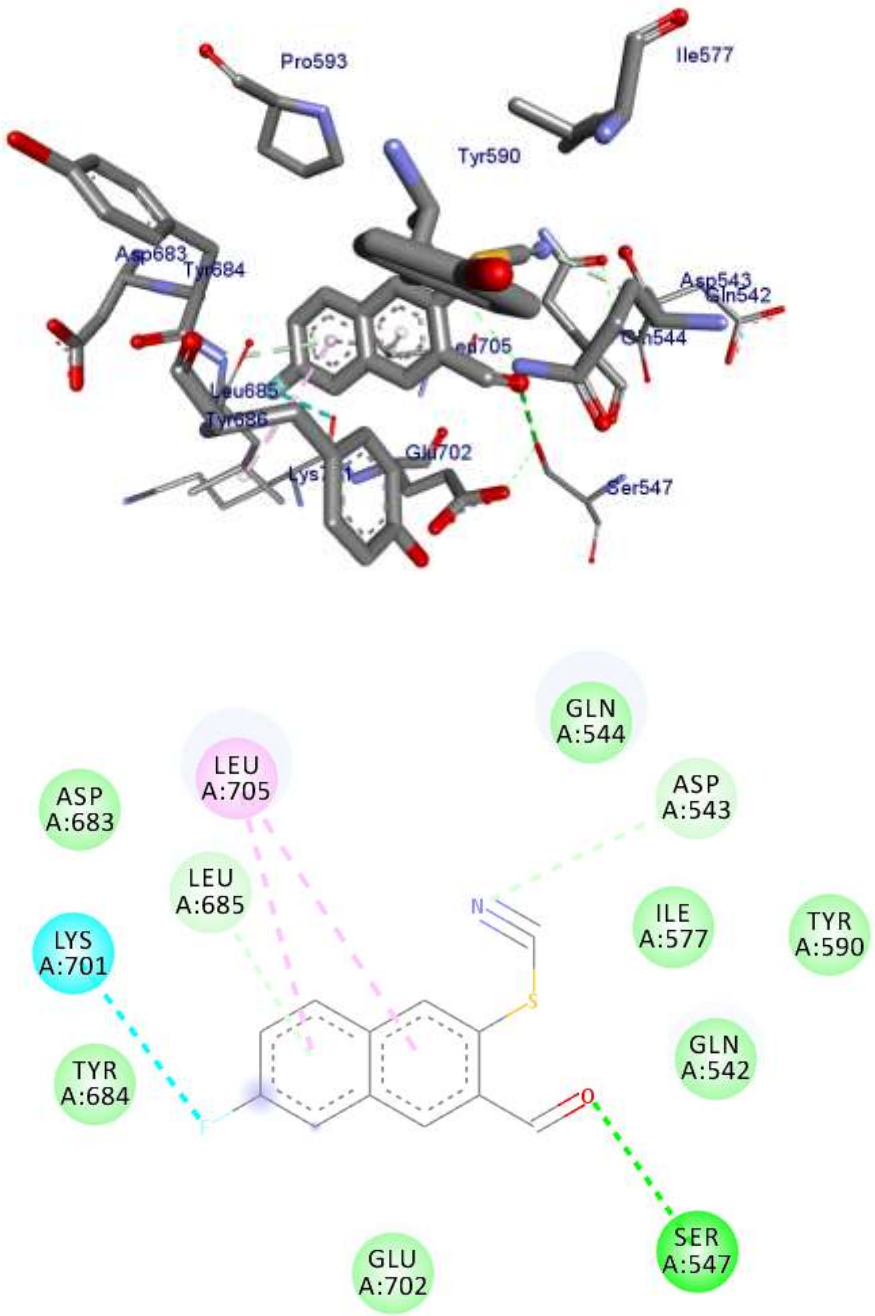

Figure 29: The binding interactions compound **89** against Human Topoisomerase IIα (PDB ID: 4fm9).

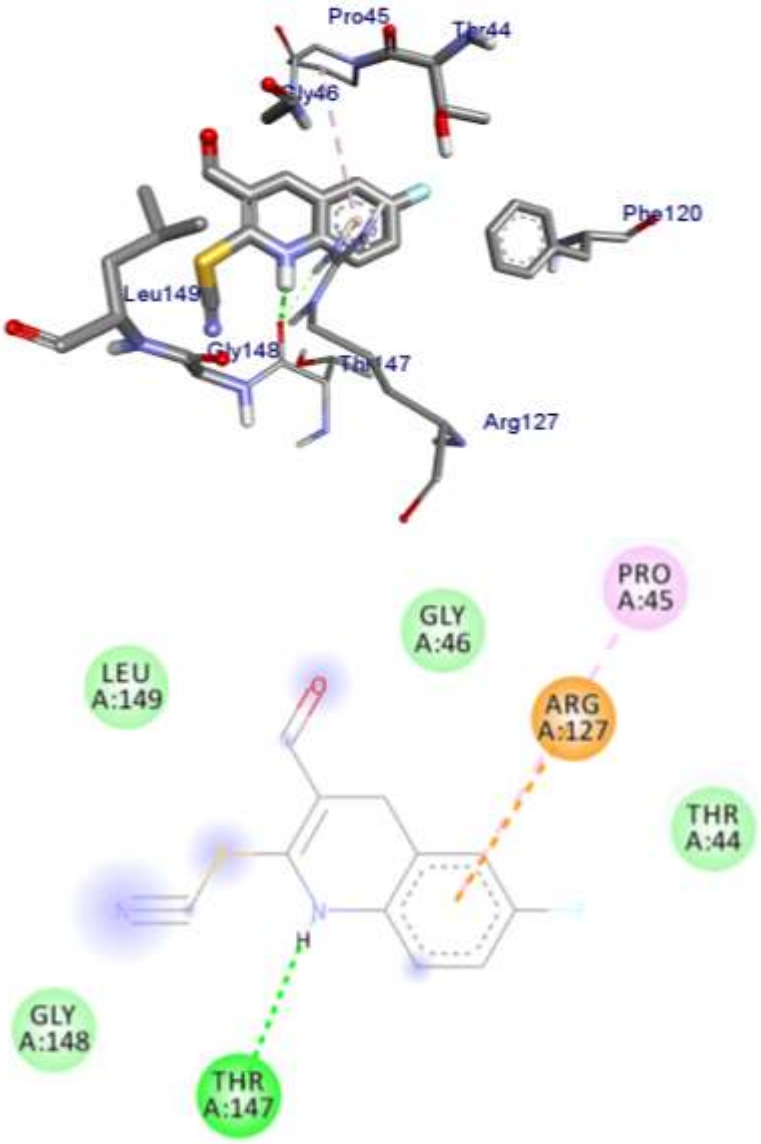

Figure 30: The 2D and 3D binding interactions of compound **89** against Human peroxiredoxin 5 (PDB ID: 1HD2).

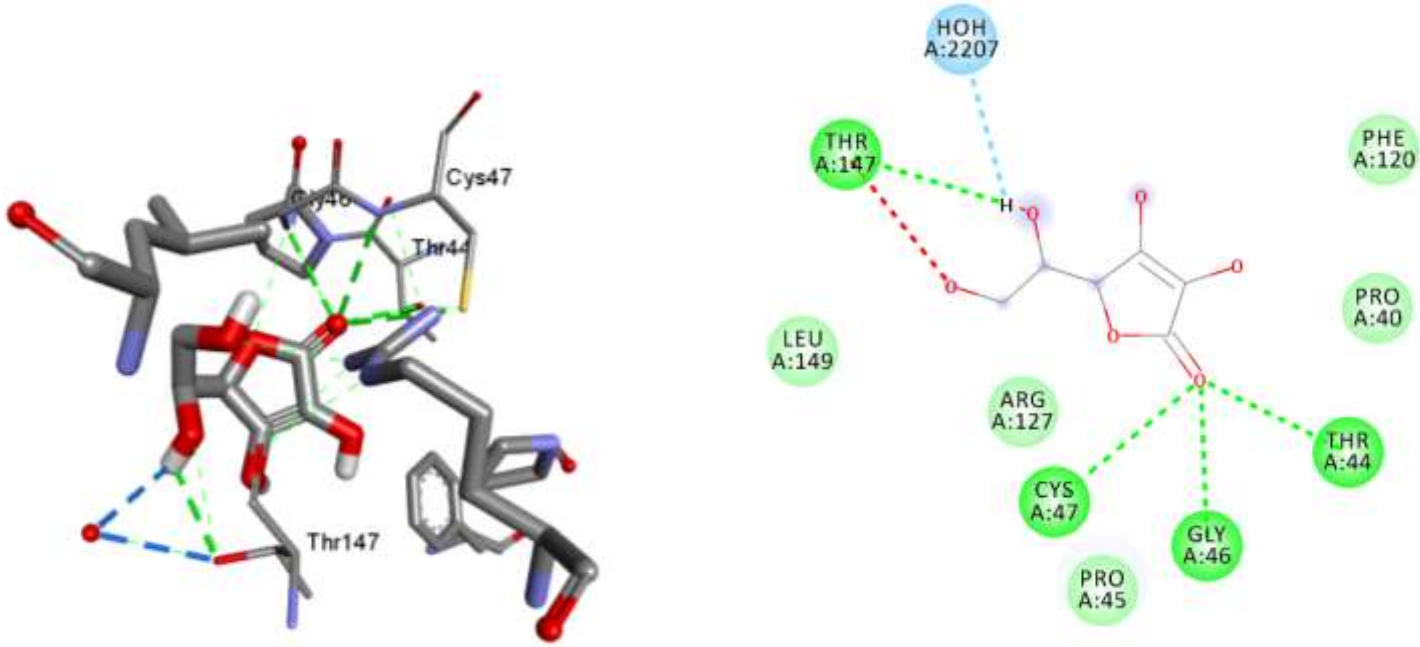

Figure 31: The 2D and 3D binding interactions of Ascorbic Acid against Human peroxiredoxin 5 (PDB ID: 1HD2).

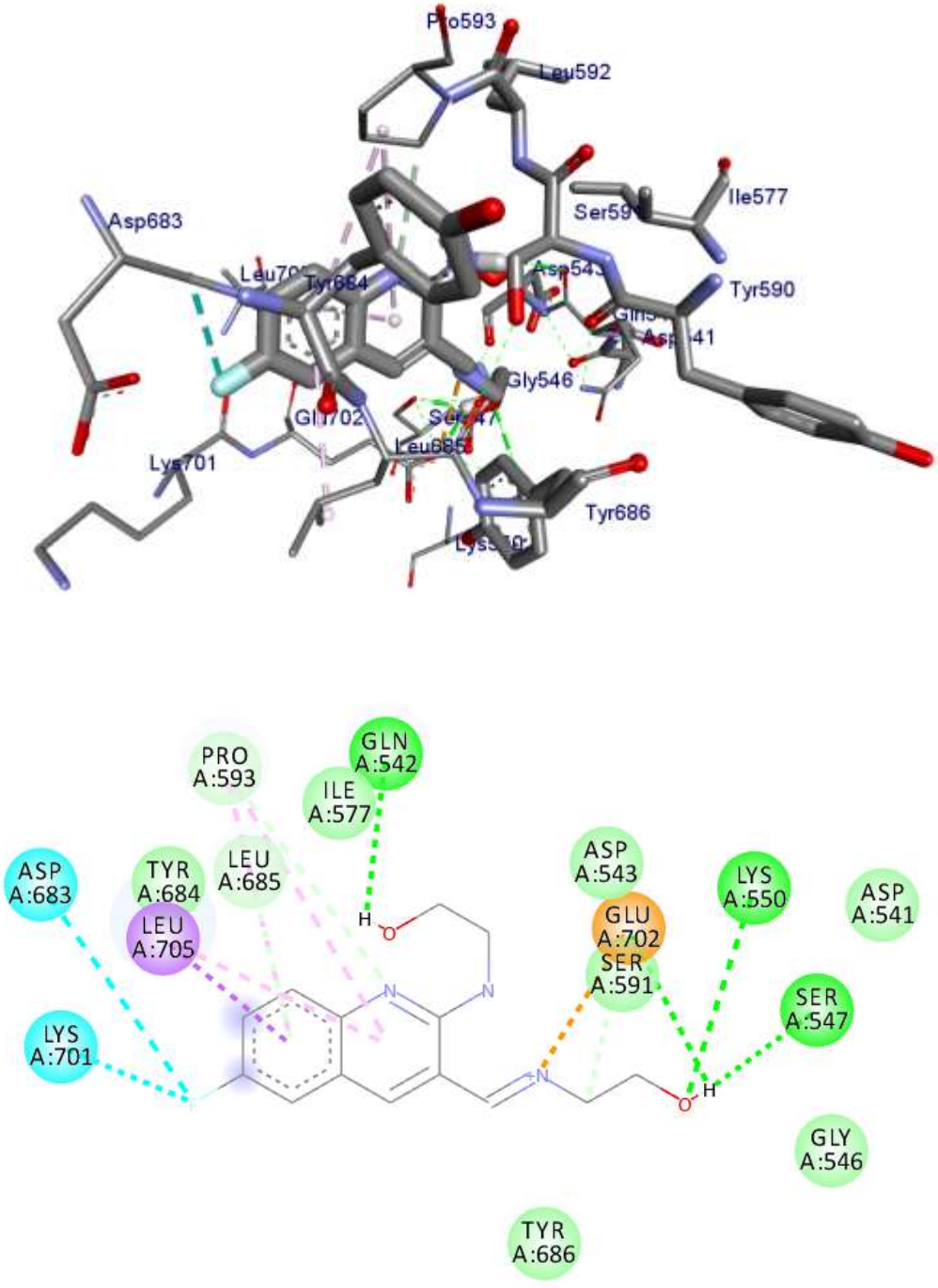

Figure 32: The binding interactions compound **90** against Human Topoisomerase IIα (PDB ID: 4fm9).

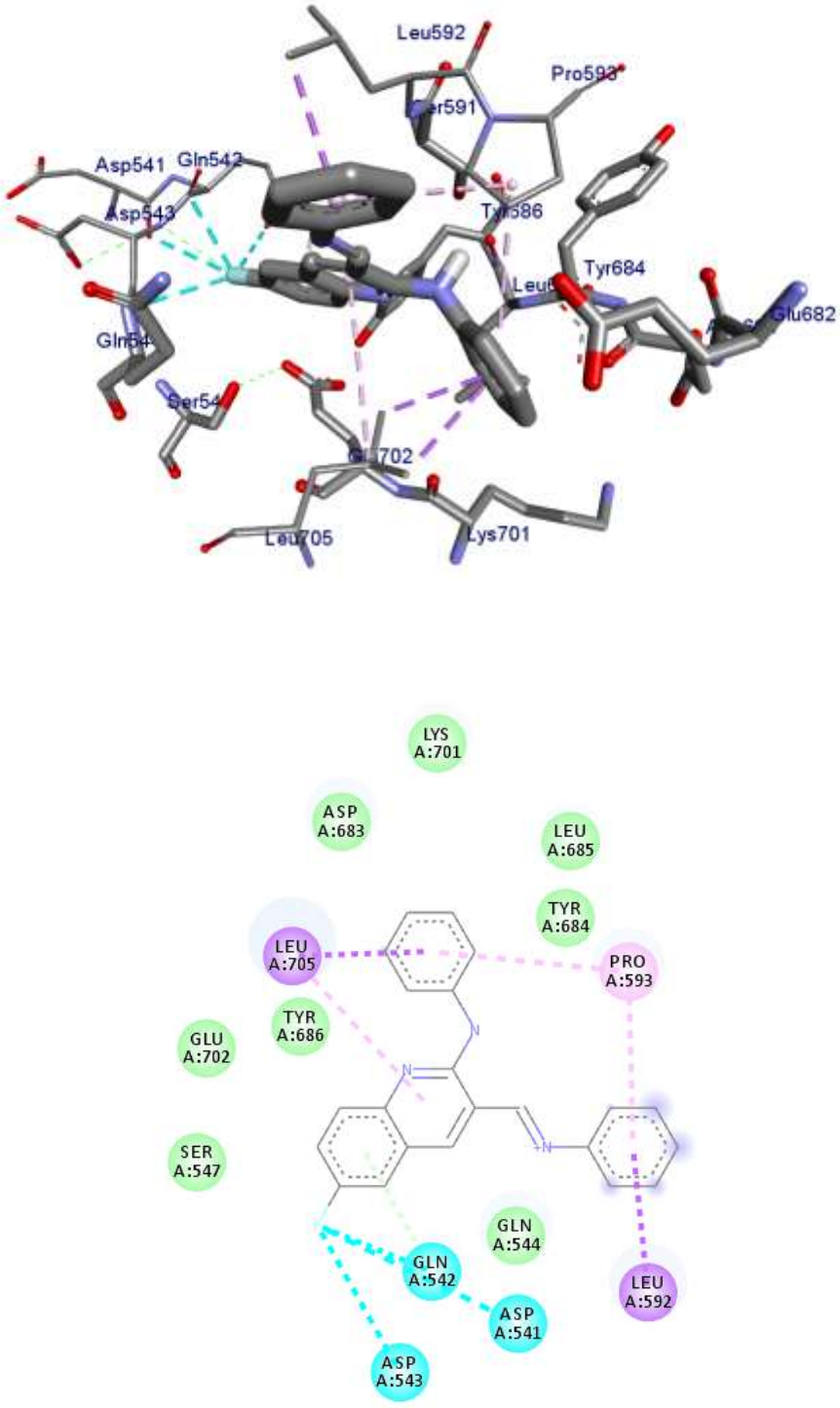

Figure 33: The binding interactions compound **91** against Human Topoisomerase IIα (PDB ID: 4fm9)

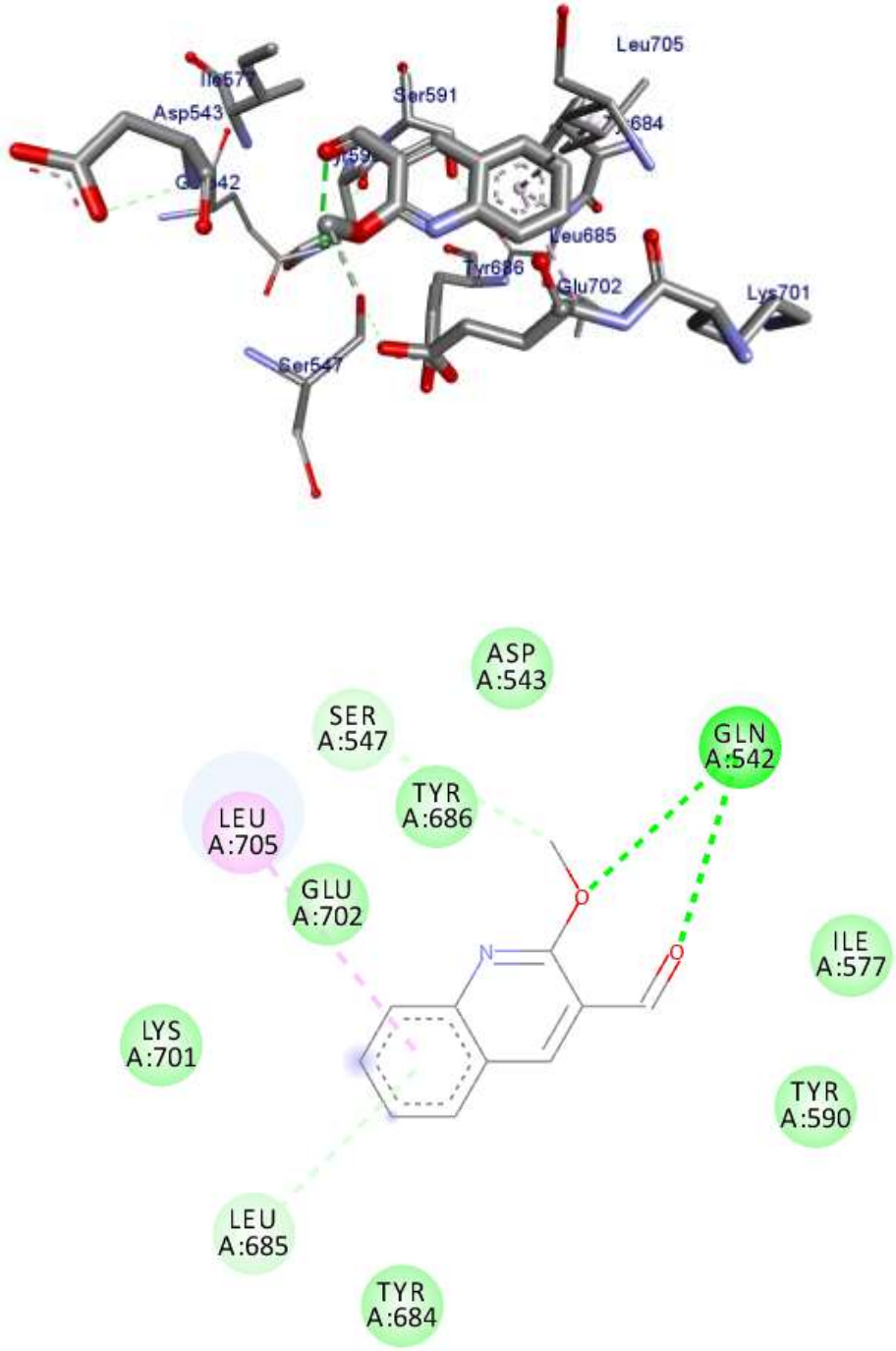

Figure 34: The binding interactions compound **96** against Human Topoisomerase IIα (PDB ID: 4fm9).

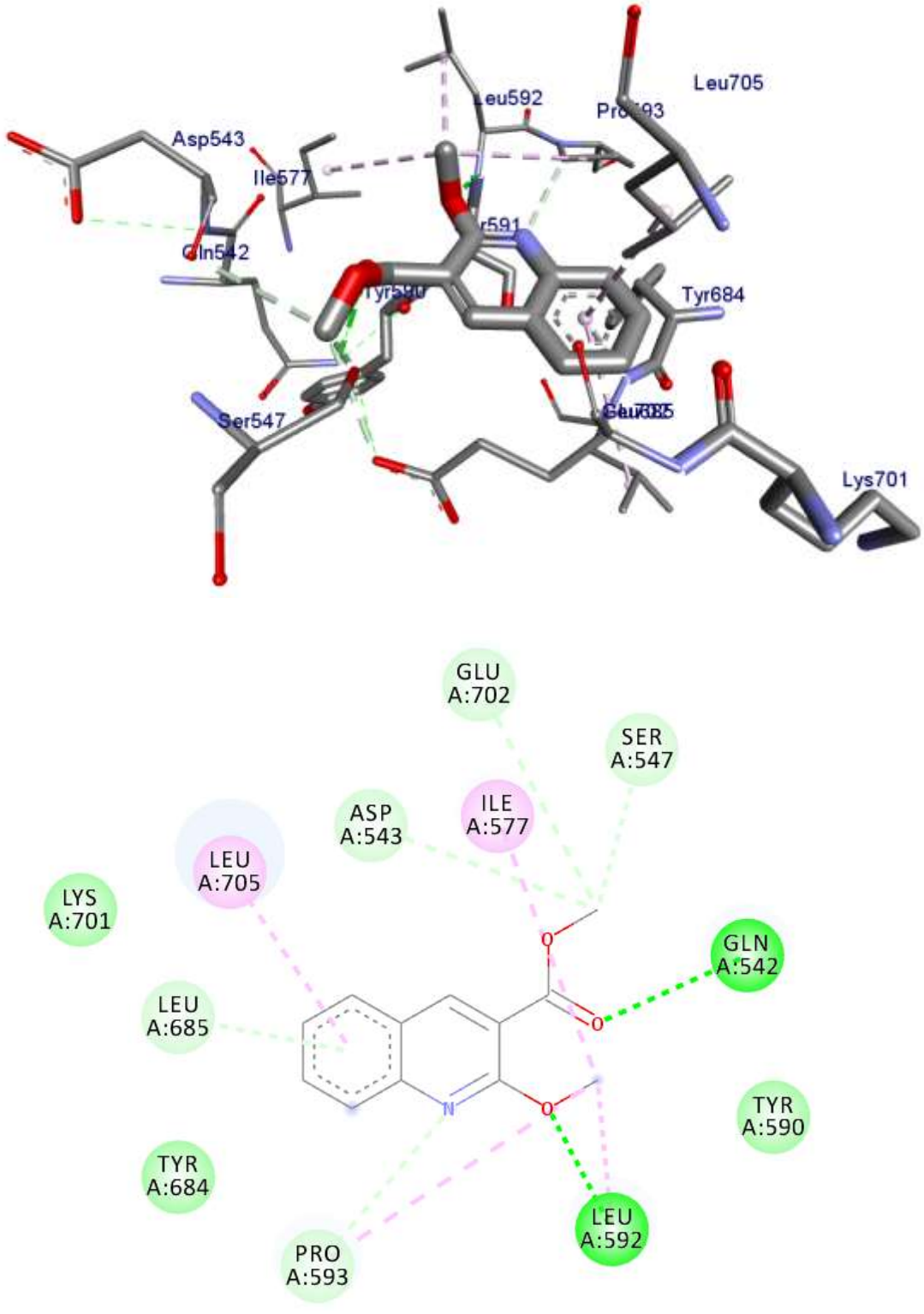

Figure 35: The binding interactions compound **97** against Human Topoisomerase IIα (PDB ID: 4fm9).

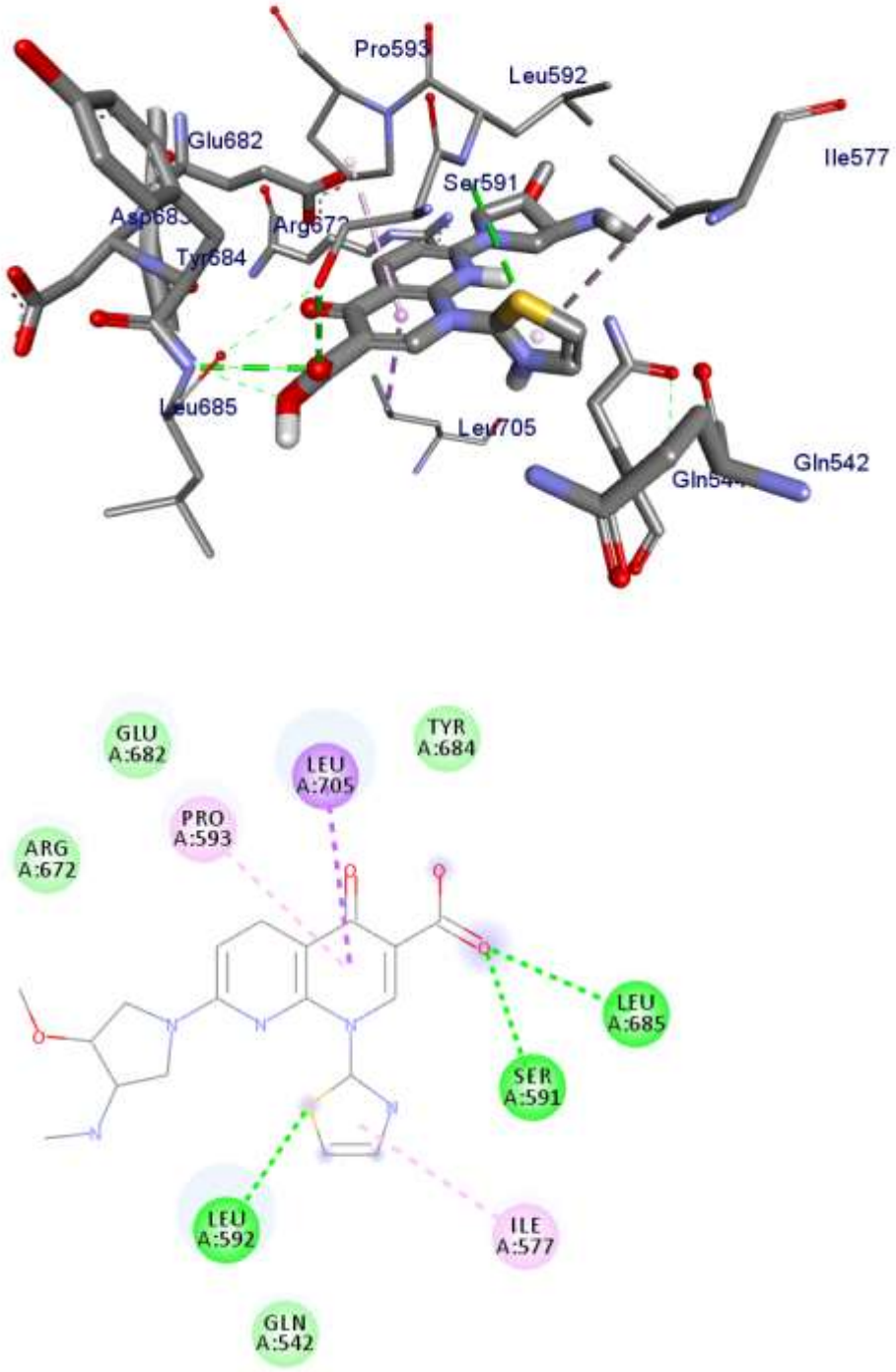

Figure 36: The binding interactions of vosaroxin against Human Topoisomerase IIα (PDB ID: 4fm9).

4.5. *In silico* drug likeness prediction

The drug like compounds are molecule which contain functional groups and/or have physical properties consistent with the majority of known drugs, and hence can be inferred as compounds which might be active biologically or might show therapeutic potential. Lipinski defines those compounds as drug like which have sufficiently acceptable ADME/T properties to survive through the Phase I clinical trials. However, drugs as well as drug-like compounds are distributed extremely meagerly through chemical space (Kadam & Roy, 2017).

Lipinski rule of 5 helps in distinguishing between drug like and non-drug like molecules. It predicts high probability of success or failure due to drug likeness for molecules complying with 2 or more of the following rules, Molecular mass less than 500 Dalton, High lipophilicity (expressed as LogP less than 5), Less than 5 hydrogen bond donors, Less than 10 hydrogen bond acceptors and Molar refractivity should be between 40-130(Suhud *et al*., 2019).

SwissADME predictions shows that all synthesized compounds satisfy Lipinski's rule of five with zero violation (Table 14). From the results obtained, C log p values of all the synthesized compounds were found to be less than five, molecular weight of all the derivatives were less than five hundred Daltons, hydrogen bond donor and acceptor is not more than five and 10 respectively which all satisfies Lipinski's rule of five, which is used to evaluate drug likeness and drug development. The Skin Permeation Value (log Kp) of synthesized molecules are in the range of (-4.5 to -7.2 cm/s) shows low skin permeability. The predicted logP values revealed that compounds have optimal liphophiliciy (ranging from 1.89 to 3.47). SwissADME predictions parameters showed that all the compounds have high gastrointestinal (GI) absorption, blood brain barriers (BBB) permeation (except compound **90** and **91),** no compounds are substrate of permeability glycoprotein (except compound **90**). All the compounds have inhibitor interaction (CYP1A2 inhibitor) (except compound **90).** All the compounds haven't inhibitor interaction (CYP2C9, CYP2D6 and CYP3A4 inhibitor) (except compound **91).** All synthesized derivatives were computed by Pro-Tox II and OSIRIS Property to evaluate for toxicity like Hepatotoxicity, Carcinogenicity, Immunotoxicity, Mutagenicity, and Cytotoxicity and found to be less toxic.

Table 15: Drug-likeness predictions of compounds, computed by SwissADME

S. No.	Formula	Mol. Wt. (g/mol)	NRB	NHA	NHD	TPSA ($A^{\circ 2}$)	LogP (cLogP)	Lipinski's rule of Five Violation
86	$C_{10}H_5ClFNO$	209.6	1	3	0	29.96	1.89	0
87	$C_{11}H_8FNO_2$	205.19	2	4	0	39.19	2.2	0
88	$C_{12}H_{10}FNO_2$	219.21	3	4	0	39.19	2.19	0
89	$C_{12}H_6FNOS$	231.25	2	3	0	66.16	2.1	0
90	$C_{14}H_{16}FN_3O_2$	277.29	6	5	3	77.74	2.31	0
91	$C_{22}H_{16}FN_3$	341.38	4	3	1	37.28	3.47	0
96	$C_{11}H_9NO_2$	187.19	2	3	0	39.19	2.12	0
97	$C_{12}H_{11}NO_3$	217.22	3	4	0	48.42	2.52	0
Vosaroxin	$C_{18}H_{19}N_5O_4S$	401.45	5	9	2	136.13	0.963	0

NHD = Number of Hydrogen donor, NHA = Number of Hydrogen acceptor

NRB = Number of rotatable bonds, and TPSA = total polar surface area

Table 16: ADME predictions of compounds, computed by SwissADME and PreADMET

S. No.	Chemical Formula	Skin Permeation Value (log Kp) cm/**s**	GI Absorption	BBB Permeability	Inhibitor (SwissADME/PreADMET**)** Interaction					
					P-gp substrate	CYP 1A2 inhibitor	CYP2C19 inhibitor	CYP 2C9 inhibitor	CYP 2D6 inhibitor	CYP 3A4 inhibitor
86	$C_{10}H_5ClFNO$	-5.65	High	Yes	No	Yes	No	No	No	No
87	$C_{11}H_8FNO_2$	-6.09	High	Yes	No	Yes	No	No	No	No
88	$C_{12}H_{10}FNO_2$	-5.92	High	Yes	No	Yes	Yes	No	No	No
89	$C_{12}H_6FNOS$	-5.37	High	Yes	No	Yes	Yes	No	No	No
90	$C_{14}H_{16}FN_3O_2$	-7.42	High	No	Yes	No	No	No	No	No
91	$C_{22}H_{16}FN_3$	-4.5	High	No	No	Yes	Yes	No	Yes	Yes
96	$C_{11}H_9NO_2$	-6.05	High	Yes	No	Yes	No	No	No	No
97	$C_{12}H_{11}NO_3$	-5.96	High	Yes	No	Yes	No	No	No	No
Vosaroxin	$C_{18}H_{19}N_5O_4S$	-8.98	High	No	Yes	Yes	No	No	No	No

GI = Gastro-Intestinal, BBB = Blood Brain Barrier, P-gp = P-glycoprotein, CYP = Cytochrome-P

Table 17: Toxicity prediction of compounds, computed by Pro-Tox II and OSIRIS Property Explorer.

S. No.	Formula	LD_{50} (mg/kg)	Toxicity Class	Organ Toxicity				
				Hepatotoxicity	Carcinogenicity	Immunotoxicity	Mutagenicity	Cytotoxicity
86	$C_{10}H_5ClFNO$	2190	5	Inactive	Inactive	Inactive	Inactive	Inactive
87	$C_{11}H_8FNO_2$	1000	4	Active	Active	Active	Inactive	Inactive
88	$C_{12}H_{10}FNO_2$	800	4	Inactive	Active	Inactive	Inactive	Inactive
89	$C_{12}H_6FNOS$	80	3	Active	Inactive	Inactive	Inactive	Inactive
90	$C_{14}H_{16}FN_3O_2$	756	4	Inactive	Inactive	Active	Inactive	Active
91	$C_{22}H_{16}FN_3$	250	3	Active	Inactive	Inactive	Active	Inactive
95	$C_{11}H_9NO_2$	1000	4	Inactive	Active	Inactive	Inactive	Inactive
96	$C_{12}H_{11}NO_3$	800	4	Inactive	Active	Inactive	Inactive	Inactive
Vosaroxin	$C_{18}H_{19}N_5O_4S$	500	4	Active	Inactive	Inactive	Inactive	Inactive

4.6. Radical Scavenging Activity of the Synthesized Compounds

DPPH assay was used to assess antioxidant ability of synthesized compounds. Compounds exhibiting antioxidant activity reduced the absorbance at 517nm. Most of synthesized compounds have good antioxidant activity relative to ascorbic acid as shown in (Table 17, Figure 26)

Table 18: Percentage inhibition of compound and ascorbic acid and IC_{50}

Con. µg/mL	Compound code **86**	**87**	**88**	**89**	**90**	**91**	**96**	**97**	**Ascorbic acid**
1.25	35.86	30.45	47.15	48.01	37.67	43.21	20.17	17.30	81.32
2.5	47.70	42.54	55.95	56.51	45.13	55.24	23.75	23.22	83.87
5	51.56	50.42	62.41	63.11	55.53	60.22	26.60	26.81	85.25
10	62.46	61.43	71.12.	73.32	57.78	66.09	35.55	35.12	87.06
IC_{50}	6.35	6.65	5.48	5.31	6.54	5.75	16.71	11.09	4.12

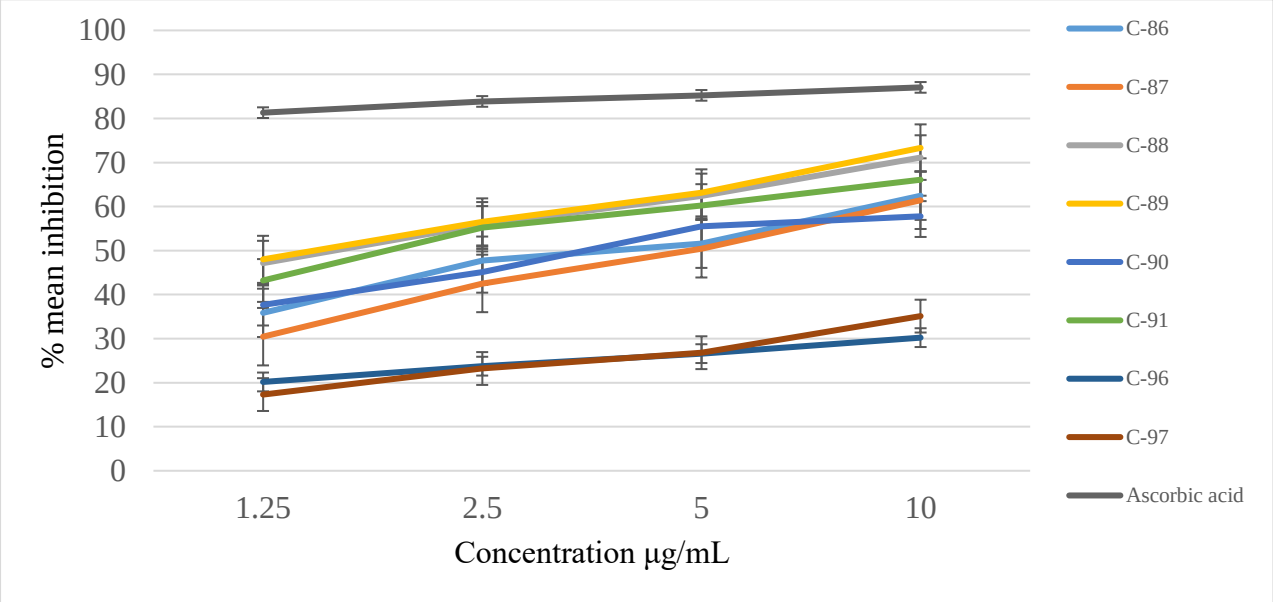

Figure 37: The percentage inhibition of the compounds and standard (Ascorbic acid)

Compounds **86, 87,88,89,90** and **91** exhibited percentage inhibition that is related to ascorbic acid suggesting having strong antioxidant activity. From synthesized compounds compound **89** have strong antioxidant activity. The IC_{50} value of synthesized compounds were calculated. Lower IC_{50} indicates higher antioxidant activity. IC_{50} varies from 5.31 µg/mL for compound **89** to 16.71 µg/mL for compound **96**. Synthesized compounds displayed comparable IC50 value compared with ascorbic acid. This indicates that activity shown by synthesized compounds are strong as radical scavengers. This is in good agreement with literature reported for closely of related compounds.

Table 19: Radical scavenging activity comparism of compounds with similar compounds from literature

Concentration	Compounds	Percentage inhibition	Structural difference	*Comments*
Synthesized compound at 100 µg/mL	**86**	62.46	fluorine at 6 position	More active
Compounds from literature at 100 µg/mL	**53**	32.64	No fluorine at 6 position	Less active
Sythesized compound at 100 µg/mL	**87**	61.43	Fluorine at 6 position	More active
Compounds from literature at µg/mL 500	**54**	31.53	No fluorine at 6 position	Less active
Synthesized compound at 200 µg/mL	**88**	71.12.	Fluorine at 6 position	More active
Compounds from literature at µg/mL 500	**55**	35.44	No fluorine at 6 position	Less active
Synthesized compound at 200 µg/mL	**89**	73.32	Fluorine at 6 position	More active
Compounds from literature at µg/mL 500	**56**	67.02	No fluorine at 6 position	Less active
Synthesized compound at 200 µg/mL	**96**	35.5	Methoxy at 2-position	More active
Compounds from literature at µg/mL 500	**57**	33.76	Chlorine at 2-position	Less active

5. CONCLUSION AND RECOMMENDATION

5. 1. Conclusion

In this project 8 novel quinoline derivatives, compounds **86, 87, 88,89,90,91, 96**, and **97** were synthesized. All synthesized compounds were evaluated for their *in-vitro* antibacterial activities against *S. aureus, E. coli, S. pyogene* and *P. aeruginosa using* disk diffusion method. The maximum inhibition zone was displayed by compound **86** with inhibition zone 14.7±0.04mm against *S. Pyogene* and minimum inhibition zone was displayed by compound **96** with inhibition zone 6.34±0.01 against *P. aeruginosa*.

DPPH assay was used to assess antioxidant ability of synthesized compounds. Compounds exhibiting antioxidant activity reduced the absorbance at **517nm**. Most of synthesized compounds have good antioxidant activity relative to ascorbic acid that is used as positive control. Compounds **86, 87,88,89,90** and **91** have strong antioxidant activity. This suggesting further evaluation of these compound might be used to get lead compound for drug design and development. From these compounds compound **89** have strong antioxidant activities. The IC_{50} value of synthesized compounds were calculated. IC_{50} varies from 5.31 μg/mL for compound **89** to 16.71 μg/mL for compound **96.**

In silico drug likeness prediction evaluation were best agreed with results of *in vitro* antibacterial activity. Molecular docking analysis of synthetic compounds was carried out to evaluate their binding pattern against *E.coli* DNA gyrase B and compared with standard clinical drug (Ciprofloxacin). Binding affinity, H-bond and residual Amino acid interaction of eight synthesized compound and ciprofloxacin was done. Compounds (**86-97**) displayed binding energy ranging from -6.0 to-7.2 kcal/mol showed in Table 12. From these, compound **88**, **89** and **91** showed best results of -6.4, -6.5 and -7.2 kcal/mol respectively. Compound **91** has similar binding affinity with standard drug, ciprofloxacin. Compound **86, 87** and **88** have shown hydrogen bonding interaction with amino acid residue Asp-73, Gly-77and Thr-165 and have hydrogen bonding interaction with Asp-73 and Thr-165 similar to ciprofloxacin.

5.2. Recommendation

Based on the present study the following were forwarded:

- It is better if synthesis of more derivatives of quinoline is carried out.
- Synthesis of heterocyclic substituted quinoline derivatives and studying their structure-activity relationship (SAR).
- Most of the tested compounds displayed good antibacterial activity; therefore it is better if mechanism of action be studied.
- The antibacterial activity was carried out on four strain (*S. aureus*, *E. coli*, *P. auroginosa* and *S. pyogene*), therefore it is better if synthesized compounds be investigated on other strain.
- It is better if further biological activity will be studied.

Research Fund Acknowledgment

This research project is funded by Adama Science and Technology University under the grant number ASTU/SM-R/014/19, Adama, Ethiopia.

6. REFERENCES

Adam, D. (2019). Quinoline antibacterials : An update of their pharmacology and therapeutic use. June. https://doi.org/10.1007/BF03260131

Al, J.-S. et. (2017). Synthesis , characterization and anti-inflammatory activity of 3-formyl 2-hydroxy quinoline thiosemicarbazides. Journal of Pharmacy Research, 5(5), 2735–2737.

Andersson, M. I. (2018). Development of the quinolines. https://doi.org/10.1093/jac/dkg212

As, T., & Sal, S. (2017). Synthesis and characterisation of substituted quinoline by Vilsmeier-Haack reagent. 5(1), 1–4.

Azam, S. S., & Abbasi, S. W. (2013). Molecular docking studies for the identification of novel melatoninergic inhibitors for acetylserotonin-O-methyltransferase using different docking routines. Theoretical Biology and Medical Modelling, 10(1), 1–16. https://doi.org/10.1186/1742-4682-10-63

B. Fernandes, T., C. F. Segretti, M., C. Polli, M., & Parise-Filho, R. (2016). Analysis of the Applicability and Use of Lipinski`s Rule for Central Nervous System Drugs. Letters in Drug Design & Discovery, 13(10), 999–1006. https://doi.org/10.2174/1570180813666160622092839

Beteck, R. M., Smit, F. J., Haynes, R. K., & Da, D. D. N. (2019). Recent progress in the development of anti-malarial quinolines. September. https://doi.org/10.1186/1475-2875-13-339

Clinton, S. N. (2015). VCU Scholars Compass A.

Divo, A. A. (2018). Activity of quinoline Antibiotics against Plasmodium falciparum In Vitro. 32(8), 1182–1186.

Drlica, K., & Zhao, X. (2017). DNA gyrase, topoisomerase IV, and the quinolines. Microbiology and Molecular Biology Reviews : MMBR, 61(3), 377–392. https://doi.org/10.1128/.61.3.377-392.1997

Edijane. (2017). Recent Studies About Synthesis and Biological Activity of recent studies about Synthesis And Biological Activity of Quinolines and derivatives : A Review. October. Https://Doi.Org/10.20959/Wjpps20168-7411

El-Gazzar, A. B. A., Hafez, H. N., & Nawwar, G. A. M. (2019). New acyclic nucleosides analogues as potential analgesic, anti-inflammatory, anti-oxidant and anti-microbial derived from pyrimido[4,5-b]quinolines. European Journal of Medicinal Chemistry, 44(4), 1427–1436. https://doi.org/10.1016/j.ejmech.2008.09.030

Faisal, M., Raauf, A., & Shafeeq, S. (2018). Synthesis , Characterization and Antimicrobial Study of New Nalidixic Acid Mannich Base Derivatives CODEN (USA): PCHHAX Synthesis , Characterization and Antimicrobial Study of New Nalidixic Acid Mannich Base Derivatives. December.

Gaba, M., Shaheed, A., Ajit, B., Jujhar, S., & Memorial, S. (2015). An overview on Molecular Docking International Journal of Drug Development & Research. 02(February 2010), 1–14.

Gao, F., Xiao, J., & Huang, G. (2019). European Journal of Medicinal Chemistry Current scenario of tetrazole hybrids for antibacterial activity. European Journal of Medicinal Chemistry, 184, 111744. https://doi.org/10.1016/j.ejmech.2019.111744

Giardinieri, A., Prof, S., Ballini, R., Palmieri, P. A., Sampaolesi, C. S., Prof, S., & Palmieri, A. (2017). A new practical and efficient one-pot synthesis of polyfunctionalized quinolines from β - nitroacrylates under heterogeneous conditions Chemistry and Advanced Chemical Methodologies Examination Committee June 2017. June.

Harold, D. (2019). Annals of Pharmacology and Pharmaceutics Quinolones : Understanding the Drug Designing to Combat. 2(9), 9–11.

Horta, P. (2019). Quinolones for applications in medicinal chemistry: synthesis and structure. 260–297.

Hu, Y. Q., Gao, C., Zhang, S., Xu, L., Xu, Z., Feng, L. S., Wu, X., & Zhao, F. (2017). Quinoline hybrids and their antiplasmodial and antimalarial activities. European Journal of Medicinal Chemistry, 139, 22–47. https://doi.org/10.1016/j.ejmech.2017.07.061

Huang. (2019). QUINOLINE : its synthesis and biological activities. June.

Ishak, C. Y., Wahbi, H. I., & Mohamed, M. E. (2018). International Journal of Pharmaceutical and Synthesis and Characterization of some New 6-substituted-2 , 4-di (hetar-2-yl) Quinolines via Micheal Addition - Ring closure Reaction of Schiff base N- (hetar-2- yl) methylene aniline with

Hetarylketones. 2(6), 431–435.

Jabeen, F., Rahman, Q. I., & Zafar, S. (2019). Determination of rate of reaction and rate constant of the hydrolysis of ester (ethyl acetate) with alkali(sodium hydroxide). International Journal of Applied Chemistry, 6(3), 18–23.

Kadam, R., & Roy, N. (2017). Recent trends in drug-likeness prediction: A comprehensive review of in silico methods. Indian Journal of Pharmaceutical Sciences, 69(5), 609–615. https://doi.org/10.4103/0250-474x.38464

Kar, S., & Leszczynski, J. (2020). Open access in silico tools to predict the ADMET profiling of drug candidates. Drug Likeness Prediction, 15(12), 1473–1487. https://doi.org/10.1080/17460441.2020.1798926

Kaur, P., & Kaur, R. (2019). QUINOLINE : ITS SYNTHESIS AND PHARMACOLOGICAL ACTIVITIES. June.

Kaur, R., & Kumar, K. (2021). European Journal of Medicinal Chemistry Synthetic and medicinal perspective of quinolines as antiviral agents. European Journal of Medicinal Chemistry, 215, 113220. https://doi.org/10.1016/j.ejmech.2021.113220

Kouznetsov, V. V, Méndez, L. Y. V., & Gómez, C. M. M. (2018). Recent Progress in the Synthesis of Quinolines Recent Progress in the Synthesis of Quinolines. April. https://doi.org/10.2174/1385272053369196

Kumar, S., Singh, R. K., Patial, B., Goyal, S., Bhardwaj, T. R., Kumar, S., Singh, R. K., Patial, B., & Goyal, S. (2016). Recent advances in novel heterocyclic scaffolds for the treatment of drug-resistant malaria Recent advances in novel heterocyclic scaffolds for the treatment of drug-resistant malaria. 6366. https://doi.org/10.3109/14756366.2015.1016513

Ladani, N. K., Patel, M. P., & Patel, R. G. (2020). An efficient three component one-pot synthesis of some new octahydroquinazolinone derivatives and investigation of their antimicrobial activities. 2009(vii), 292–302.

Marella, A., Tanwar, O. P., Saha, R., & Ali, M. R. (2017). Quinoline : A Versatile Heterocyclic Quinoline : A versatile heterocyclic. January. https://doi.org/10.1016/j.jsps.2012.03.002

Matada, B. S., Pattanashettar, R., & Yernale, N. G. (2019). A comprehensive review on the biological interest of quinoline as anti oxidant and its derivatives. Bioorganic and Medicinal Chemistry, 32(August 2020), 115973. https://doi.org/10.1016/j.bmc.2020.115973

Mohammed, H. H. H., Abuo-rahma, G. E. A., Abbas, S., & Abdelhafez, E. M. N. (2018). Current Trends and Future Directions of quinolines Current Trends and Future Directions of Fluoroquinolones. February. https://doi.org/10.2174/0929867325666180214122944

Monte, R., Diedrich, D., Ruaro, T. C., Zimmer, A. R., Teixeira, M. L., Oliveira, L. F. De, Jean, M., & Weghe, P. Van De. (2020). Quinolines derivatives as promising new antifungal candidates for the treatment of candidiasis and dermatophytosis. 1691–1701.

Mura, C., & McAnany, C. E. (2014). An introduction to biomolecular simulations and docking. Molecular Simulation, 40(10–11), 732–764. https://doi.org/10.1080/08927022.2014.935372

Narwal, S., Kumar, S., & Verma, P. K. (2017). Synthesis and therapeutic potential of quinoline derivatives. Research on Chemical Intermediates, 43(5), 2765–2798. https://doi.org/10.1007/s11164-016-2794-2

Orhan Puskullu, M., Tekiner, B., & Suzen, S. (2013). Recent Studies of Antioxidant Quinoline Derivatives. Mini Reviews in Medicinal Chemistry, 13(3), 365–372. https://doi.org/10.2174/138955713804999793

Parminder, & Rajwant. (2019). Quinoline: its synthesis and pharmacological activities. Pramana Research Journal, 9(6), 1718–1748.

Patel, O. P. S., Beteck, R. M., & Legoabe, L. J. (2021). Antimalarial application of quinones: A recent update. European Journal of Medicinal Chemistry, 210, 113084. https://doi.org/10.1016/j.ejmech.2020.113084

Rahman, M. M., Islam, M. B., Biswas, M., & Khurshid Alam, A. H. M. (2015). In vitro antioxidant and free radical scavenging activity of different parts of Tabebuia pallida growing in Bangladesh. BMC Research Notes, 8(1), 1–9. https://doi.org/10.1186/s13104-015-1618-6

Riahifard, N., Tavakoli, K., Yamaki, J., Parang, K., & Tiwari, R. (2017). Synthesis and evaluation of antimicrobial activity of [R4W4K]-levofloxacin and [R4W4K]-levofloxacin-Q conjugates.

Molecules, 22(6), 1–11. https://doi.org/10.3390/molecules22060957

Secrieru, A. (2020). Antimalarial Agents as Therapeutic Tools Against.

Suhud, F., Tjahjono, D. H., Yuniarta, T. A., Putra, G. S., & Setiawan, J. (2019). Molecular docking, drug-likeness, and ADMET study of 1-benzyl-3-benzoylurea and its analogs against VEGFR-2. IOP Conference Series: Earth and Environmental Science, 293(1). https://doi.org/10.1088/1755-1315/293/1/012018

Valadbeigi. (2019). sciencedirect-topic-4-quinoline-derivative.pdf.

Wendorff, T. J., Schmidt, B. H., Heslop, P., Austin, C. A., & Berger, J. M. (2016). The structure of DNA-bound human topoisomerase II alpha: Conformational mechanisms for coordinating inter-subunit interactions with DNA cleavage. Journal of Molecular Biology, 424(3–4), 109–124. https://doi.org/10.1016/j.jmb.2012.07.014

Zeleke, D., Eswaramoorthy, R., Belay, Z., & Melaku, Y. (2020). Synthesis and Antibacterial , Antioxidant , and Molecular Docking Analysis of Some Novel Quinoline Derivatives. 2020.

Zhang, J., Wang, H., Chen, Y., Xie, H., Ding, C., Tan, J., & Xu, K. (2020). Electrochemical synthesis of selenocyanated imidazo[1,5-a]quinolines under metal catalyst- and chemical oxidant-free conditions. Chinese Chemical Letters, 31(6), 1576–1579. https://doi.org/10.1016/j.cclet.2019.11.037

7. APPENDICES

Appendix 1: ^{1}H NMR spectrum (400 MHz, $CDCl_3$) of 2-chloro-6-fluoroquinoline-3-carbaldehyde (**86**)

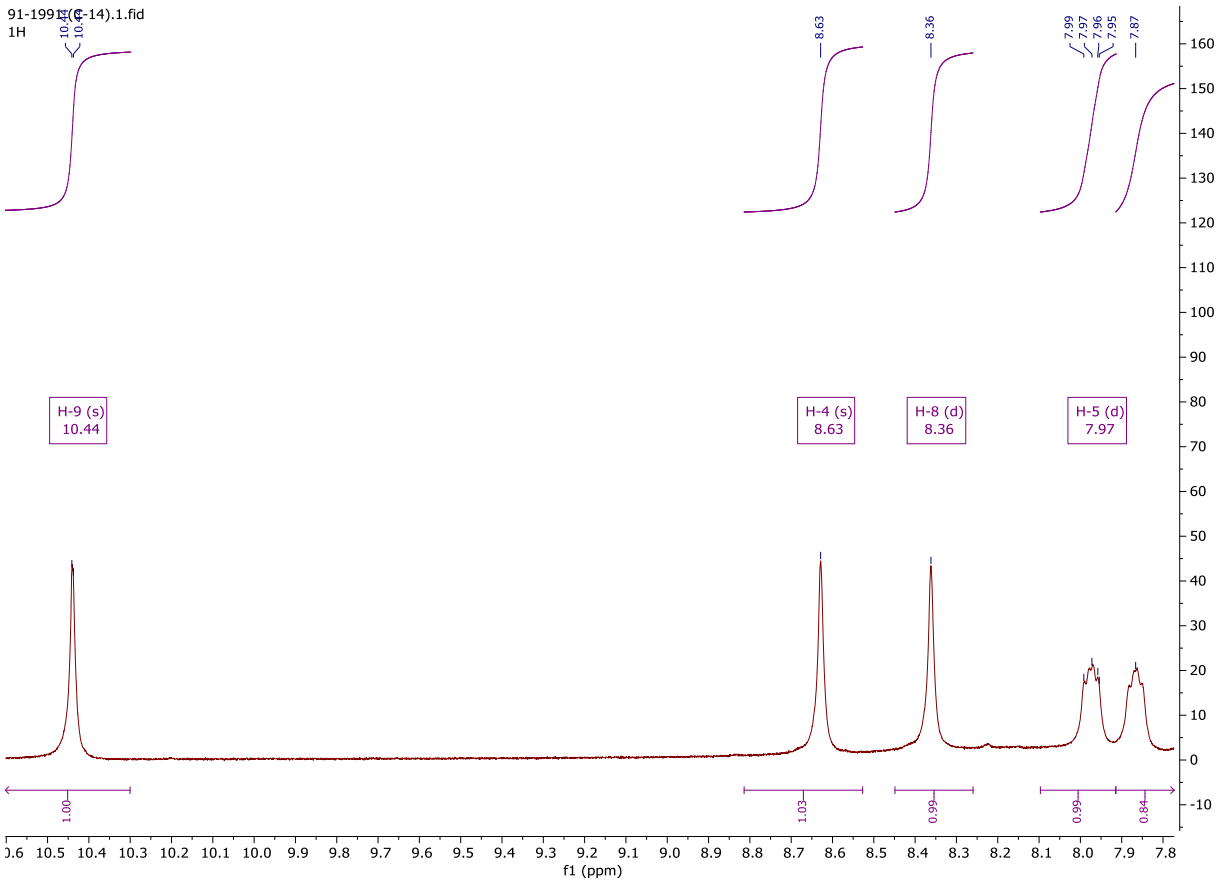

Appendix 2: ^{13}C NMR spectrum (100 MHz, $CDCl_3$) of 2-chloro-6-fluoroquinoline-3-carbaldehyde (**86**)

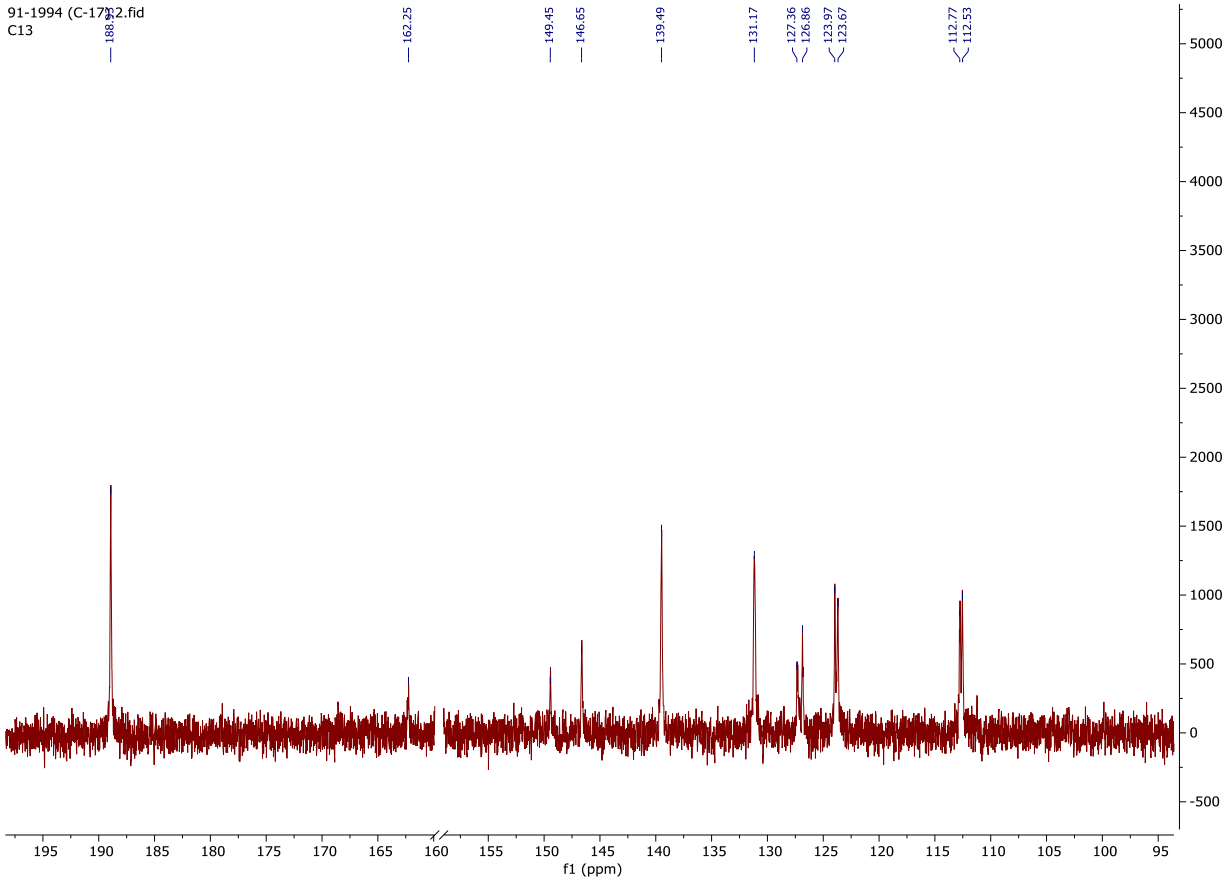

Appendix 3: The DEPT-135 NMR spectrum of 2-chloro-6-fluoroquinoline-3-carbaldehyde (**86**)

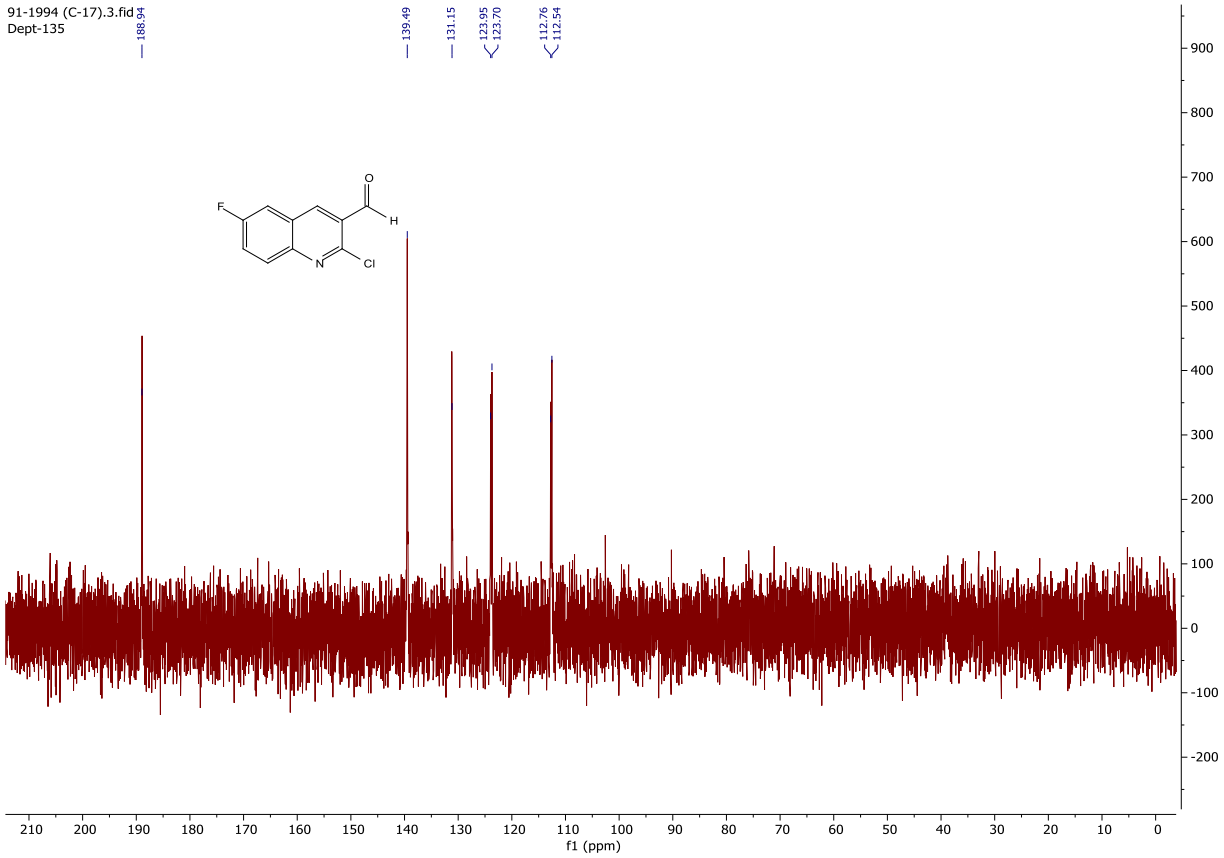

Appendix 4: ^{1}H NMR spectrum (400 MHz, $CDCl_3$) of 6-fluoro-2-methoxyquinoline-3-carbaldehyde (**87**)

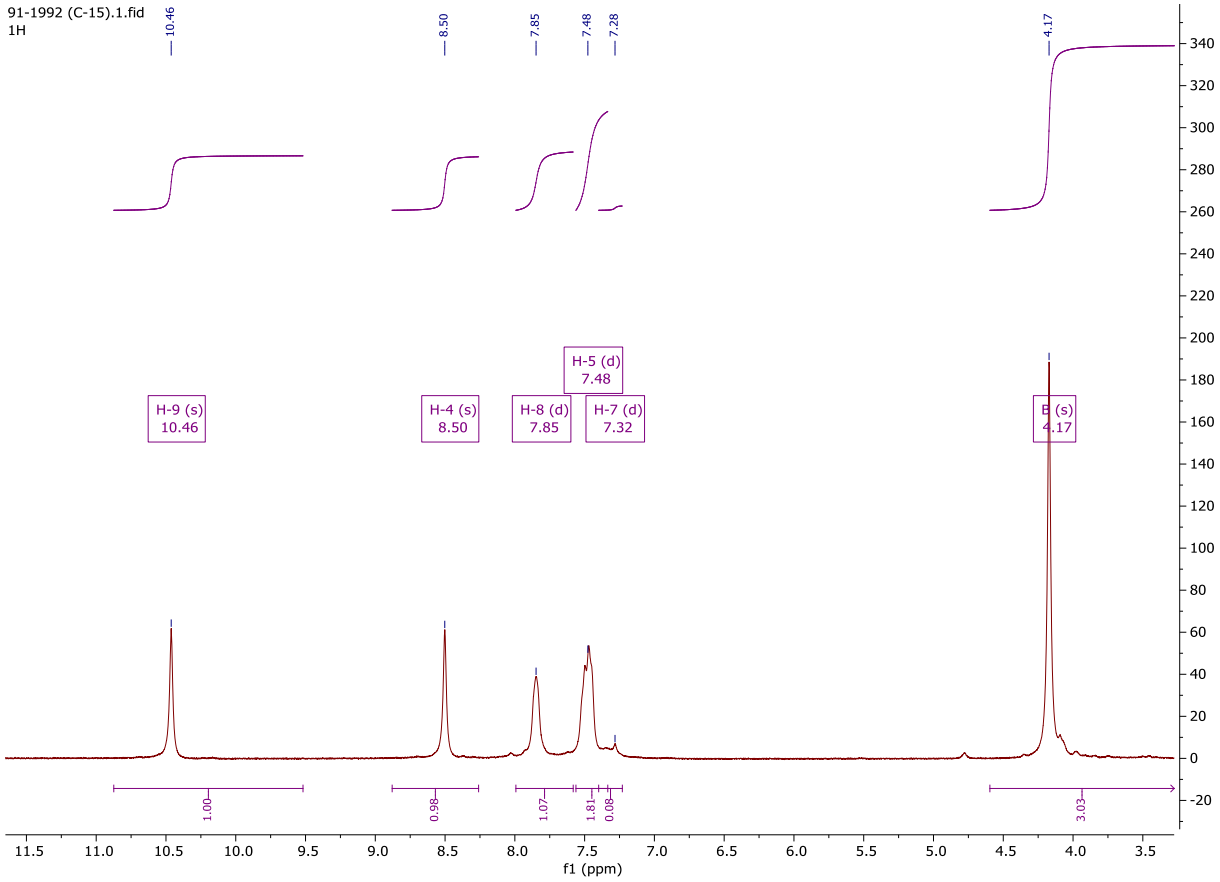

Appendix 5: ^{13}C NMR spectrum (100 MHz, $CDCl_3$) of 6-fluoro-2-methoxyquinoline-3-carbaldehyde (**87**)

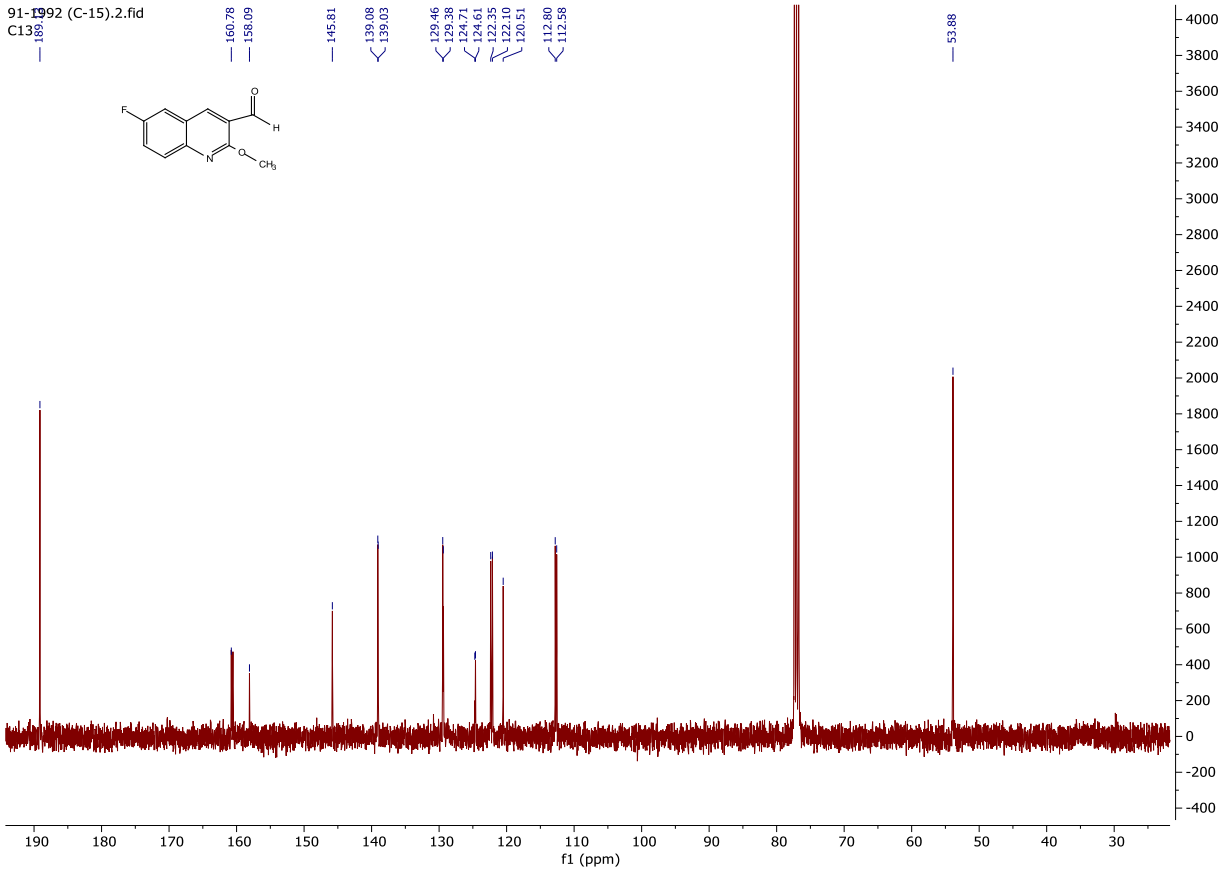

Appendix 6: DEPT-135 NMR spectrum of 6-fluoro-2-methoxyquinoline-3-carbaldehyde (**87**)

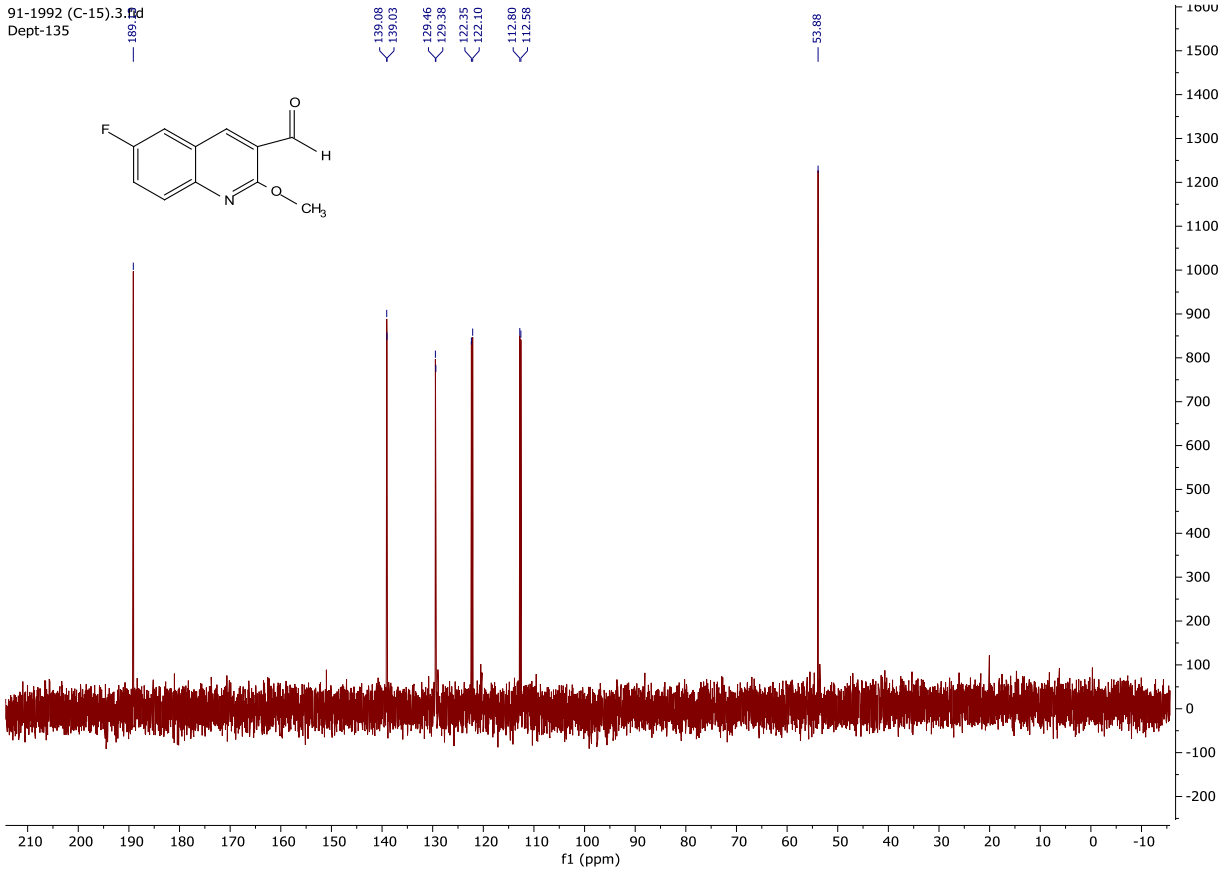

Appendix 7: ^{1}H NMR spectrum (400 MHz, $CDCl_3$) of 2-ethoxy-6-fluoroquinoline-3-carbaldehyde (**88**)

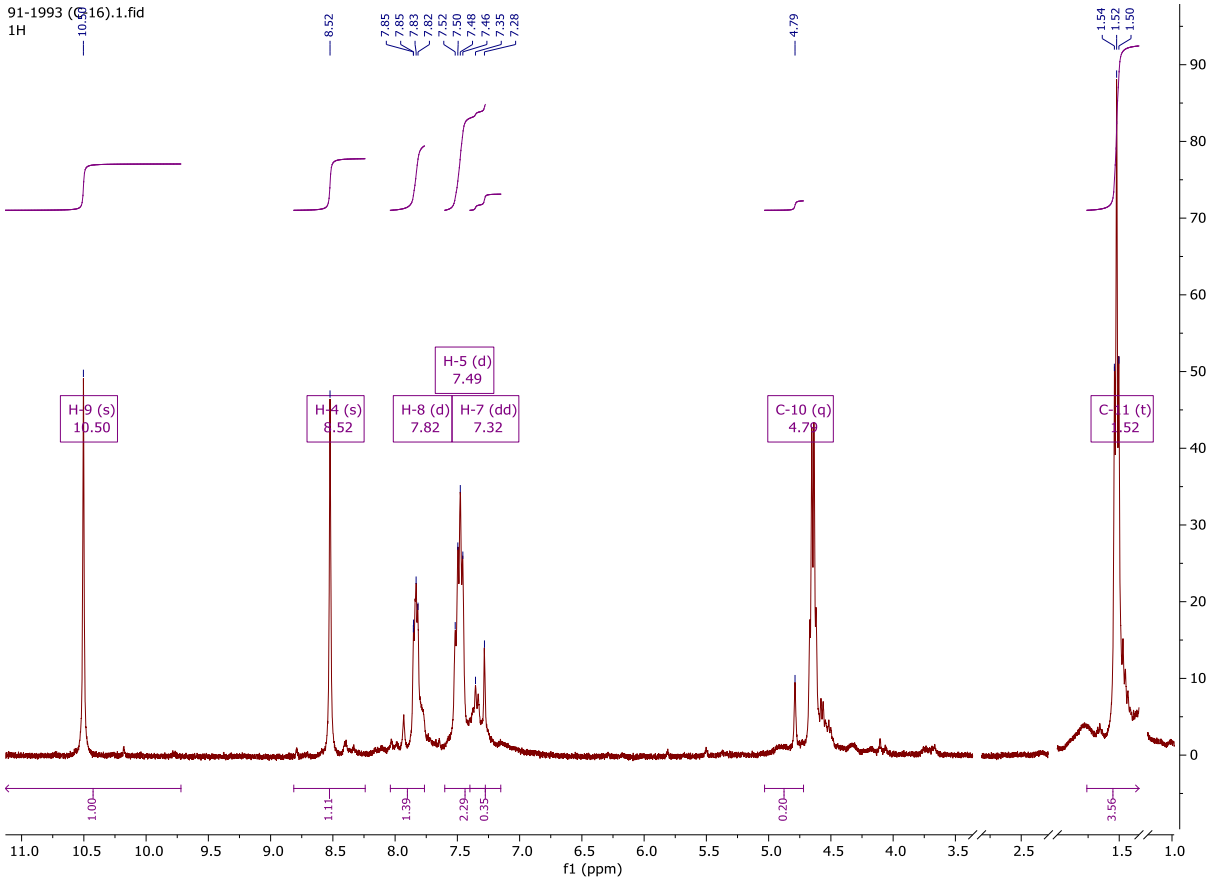

Appendix 8: ^{13}C NMR spectrum (100 MHz, $CDCl_3$) of 2-ethoxy-6-fluoroquinoline-3-carbaldehyde (**88**)

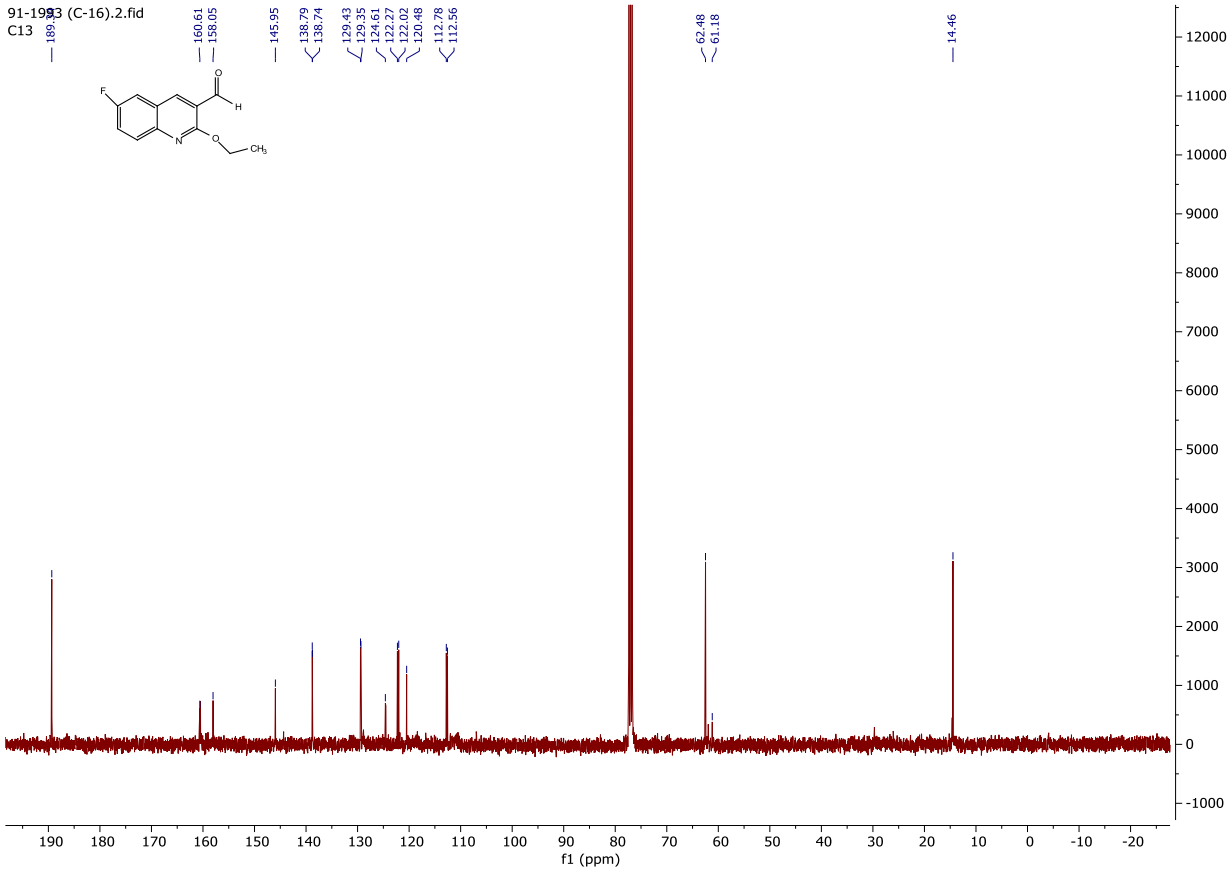

Appendix 9: DEPT-135 NMR spectrum of 2-ethoxy-6-fluoroquinoline-3-carbaldehyde (**88**)

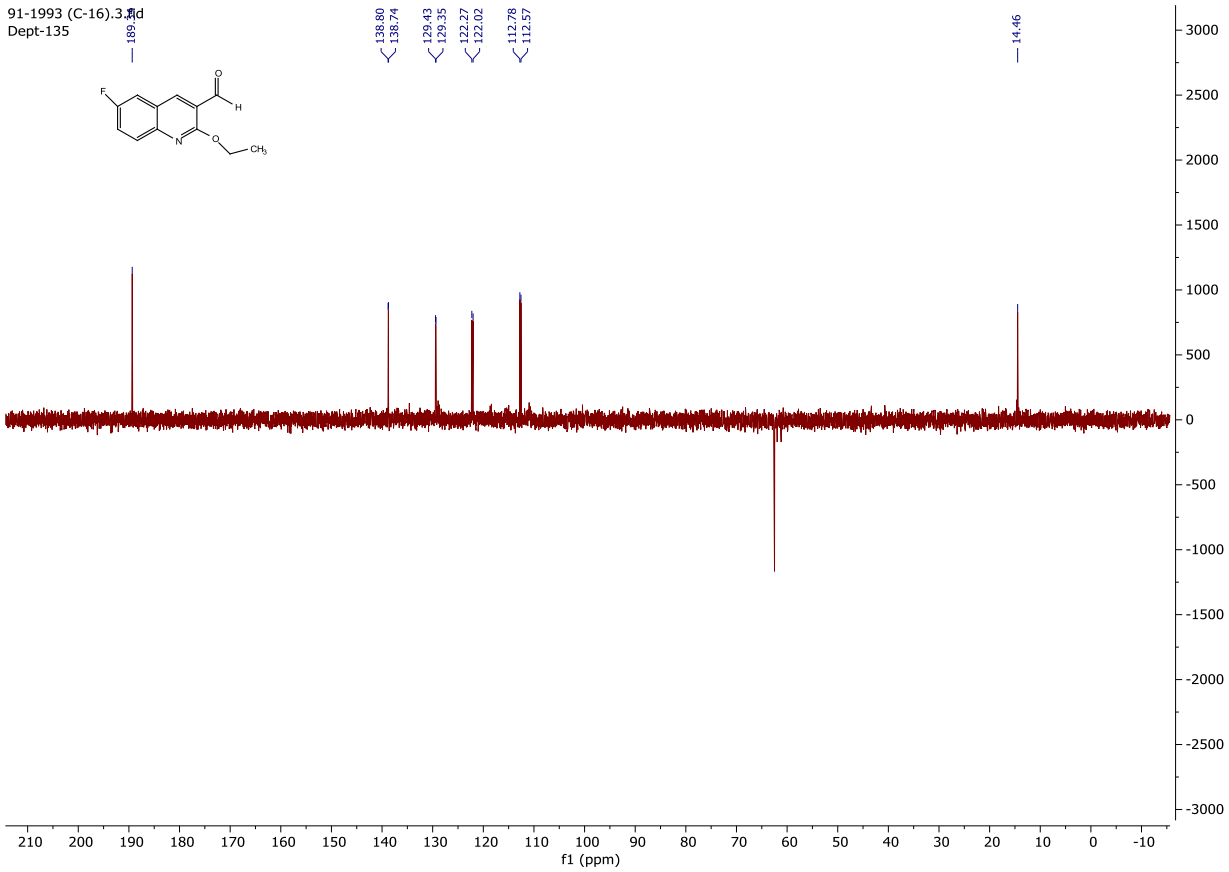

Appendix 10: ^{1}H NMR spectrum (400 MHz, $CDCl_3$) of 6-fluoro-2-thiocyanatoquinoline-3-carbaldehyde (**89**)

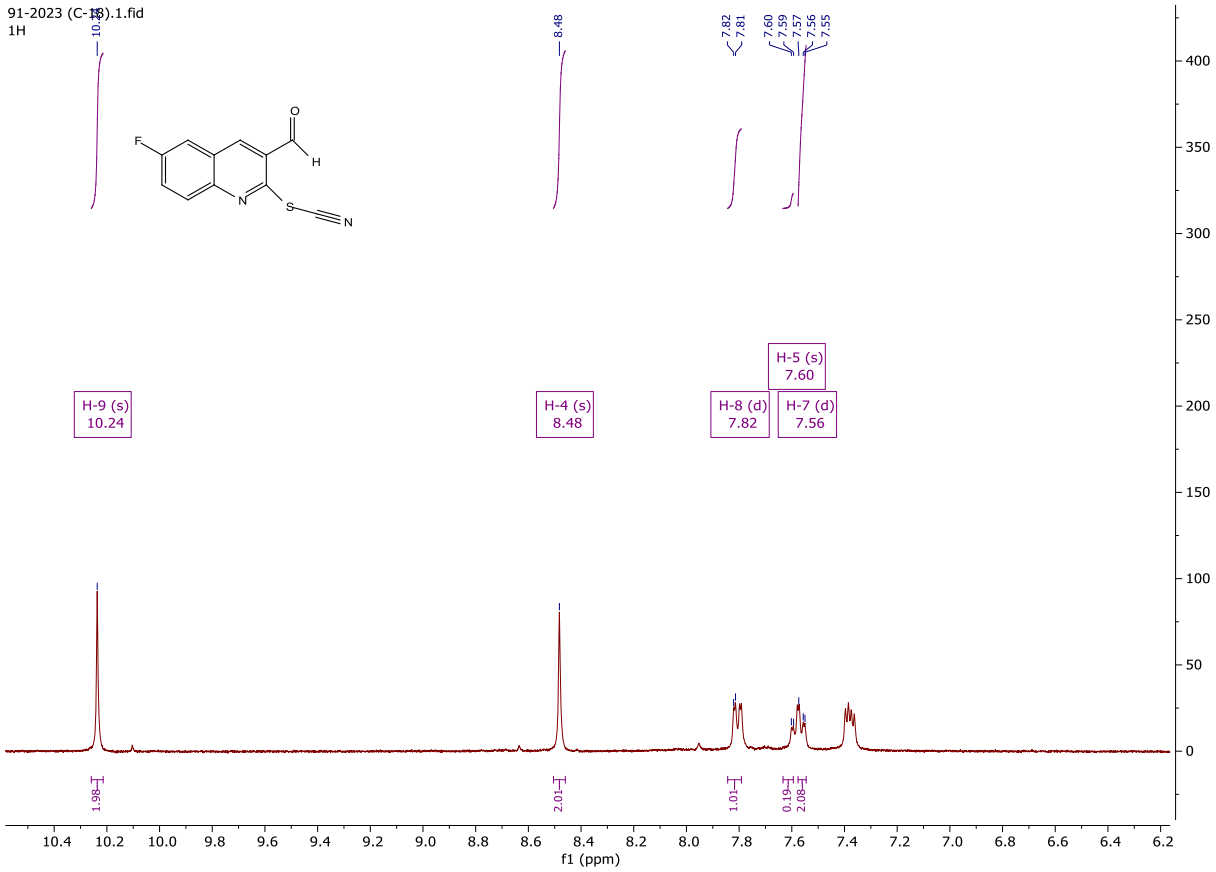

Appendix 11: ^{13}C NMR spectrum (100 MHz, $CDCl_3$) of 6-fluoro-2-thiocyanatoquinoline-3-carbaldehyde (**89**)

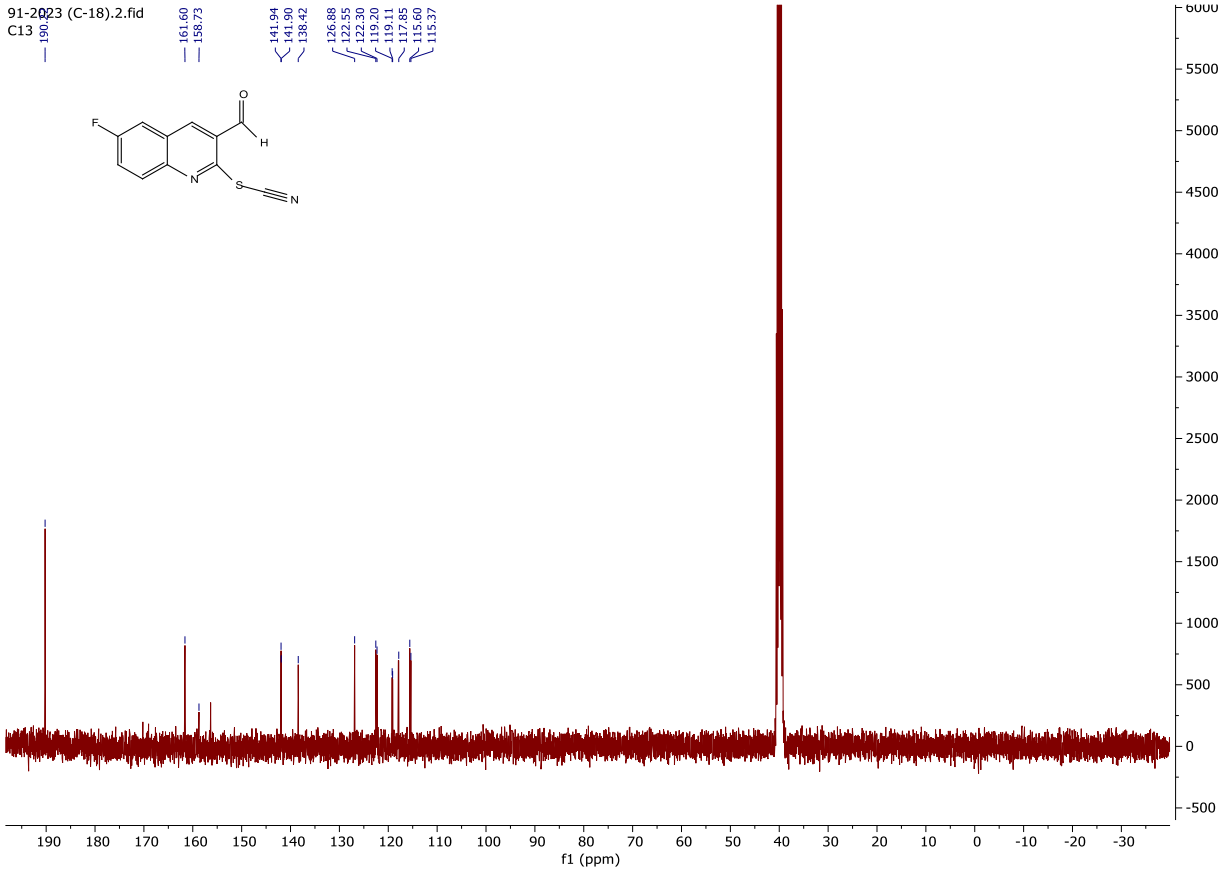

Appendix 12: DEPT-135 NMR spectrum of 6-fluoro-2-thiocyanatoquinoline-3-carbaldehyde (**89**)

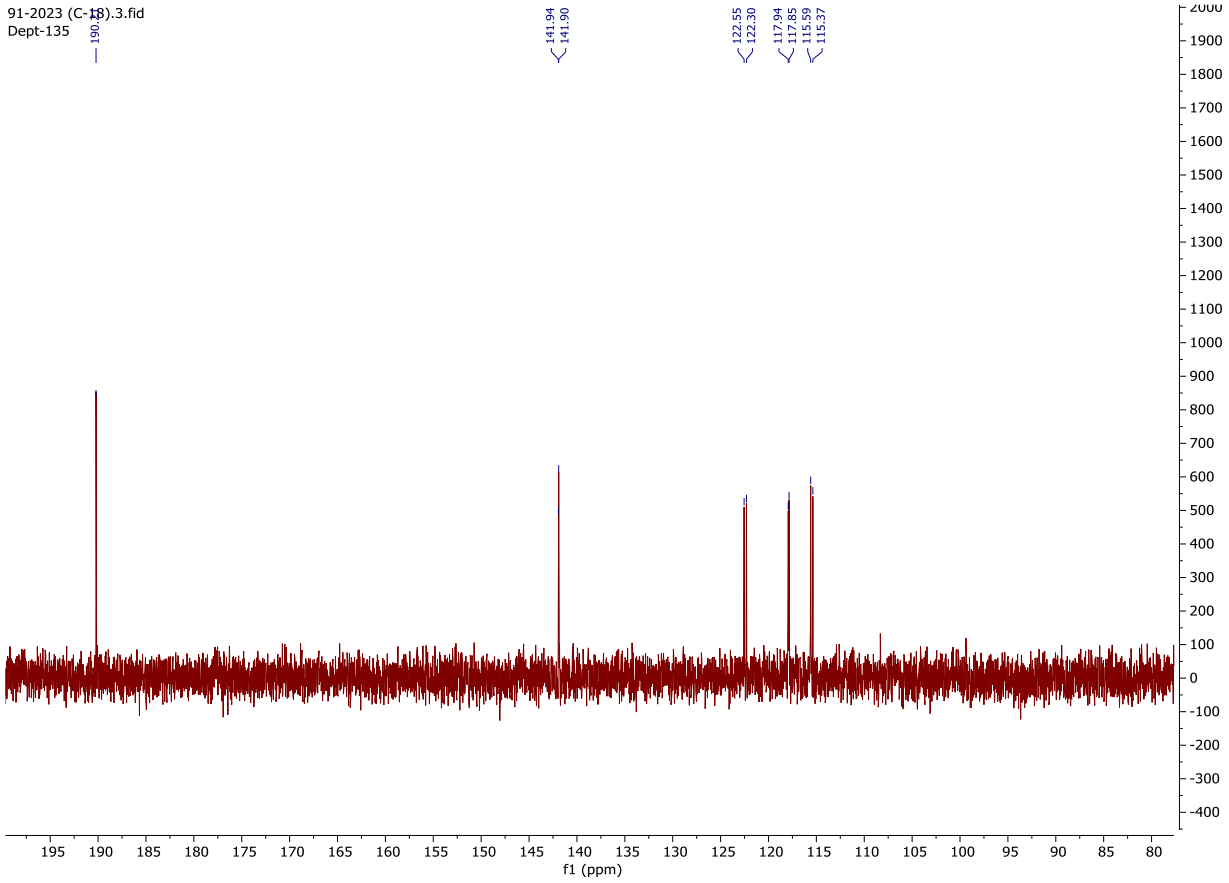

Appendix 13: ^{1}H NMR spectrum (400 MHz, $CDCl_3$) of 2-((2-hydroxyethyl) amino)-3-(-2-(ethylideneamino) ethanol quinoline (**90**)

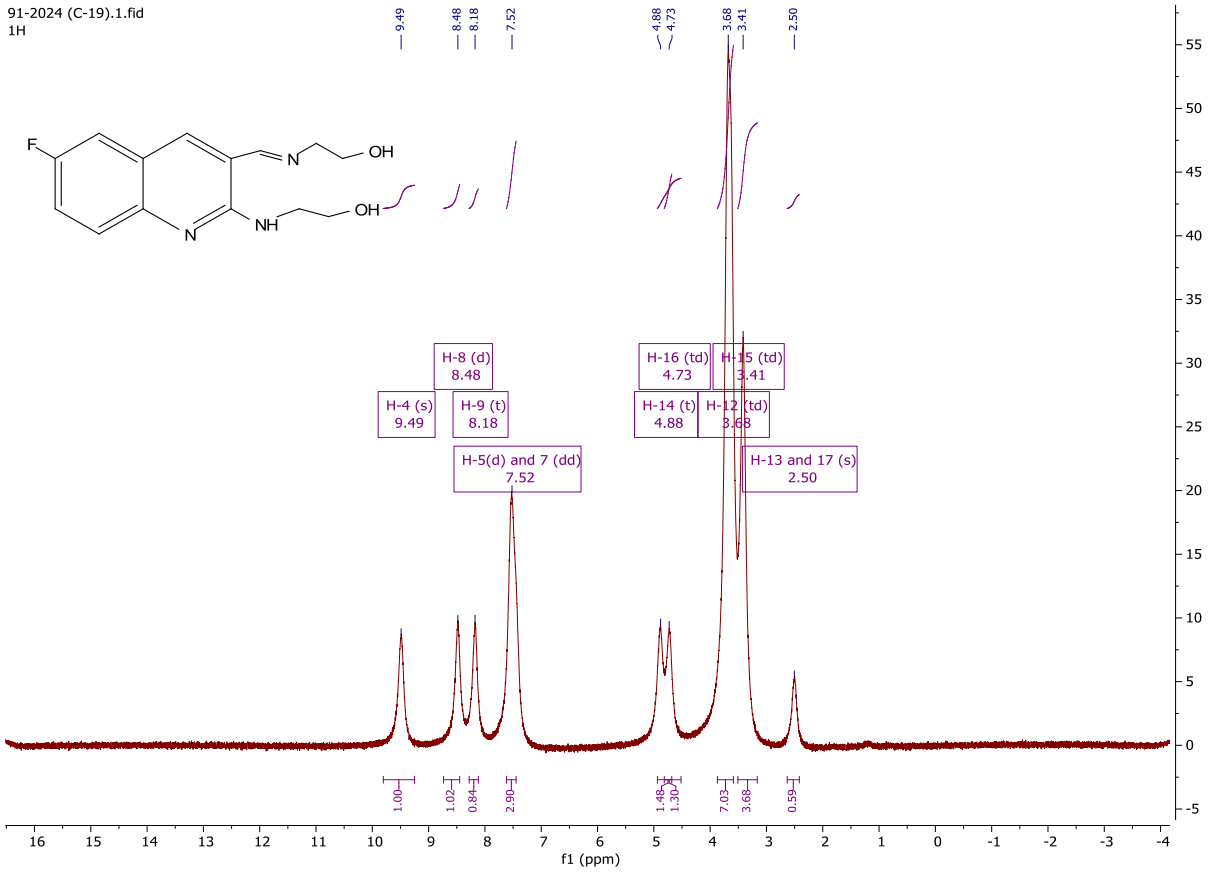

Appendix 14: ^{13}C NMR spectrum (100 MHz, $CDCl_3$) of 2-((2-hydroxyethyl) amino)-3-(-2-(ethylideneamino) ethanol quinoline (**90**)

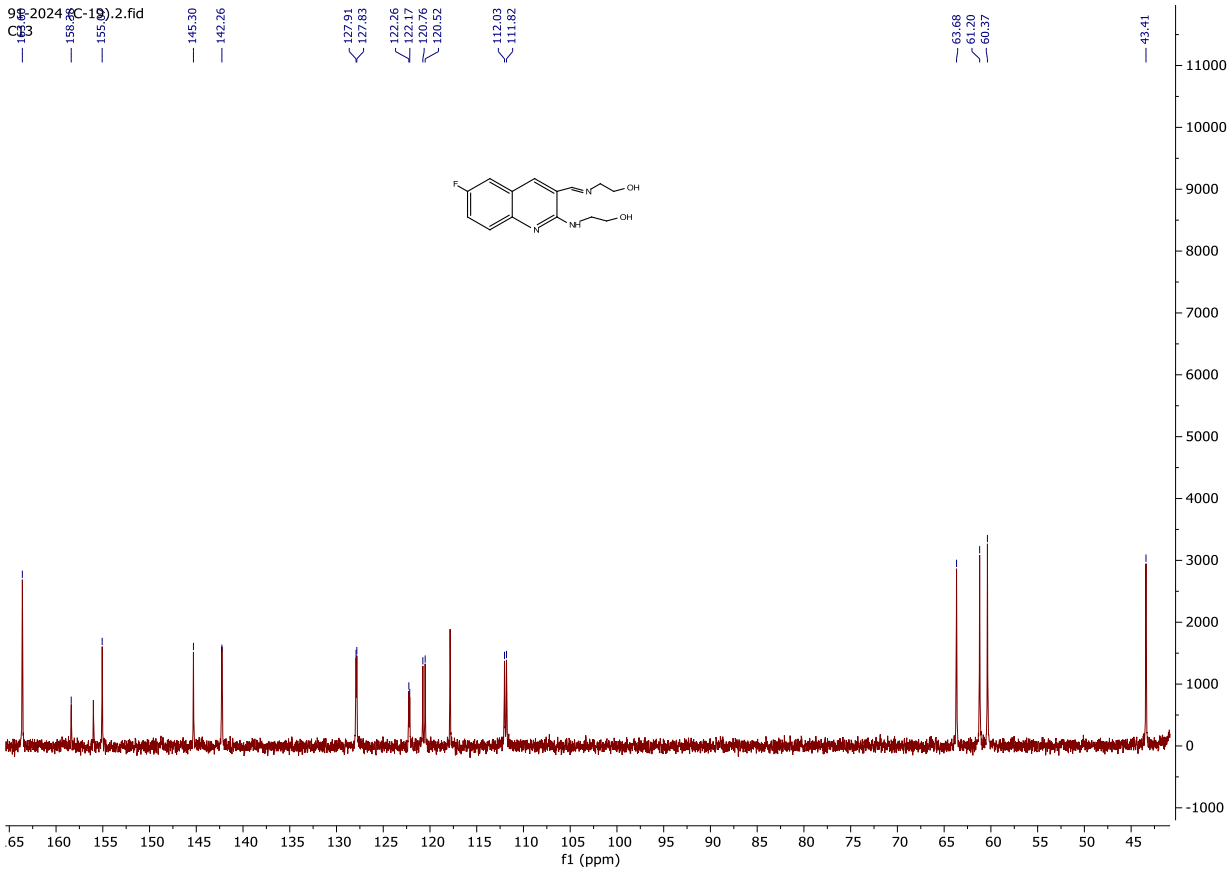

Appendix 15: DEPT-135 NMR spectrum of 2-((2-hydroxyethyl) amino)-3-(-2-(ethylideneamino) ethanol quinoline (**90**)

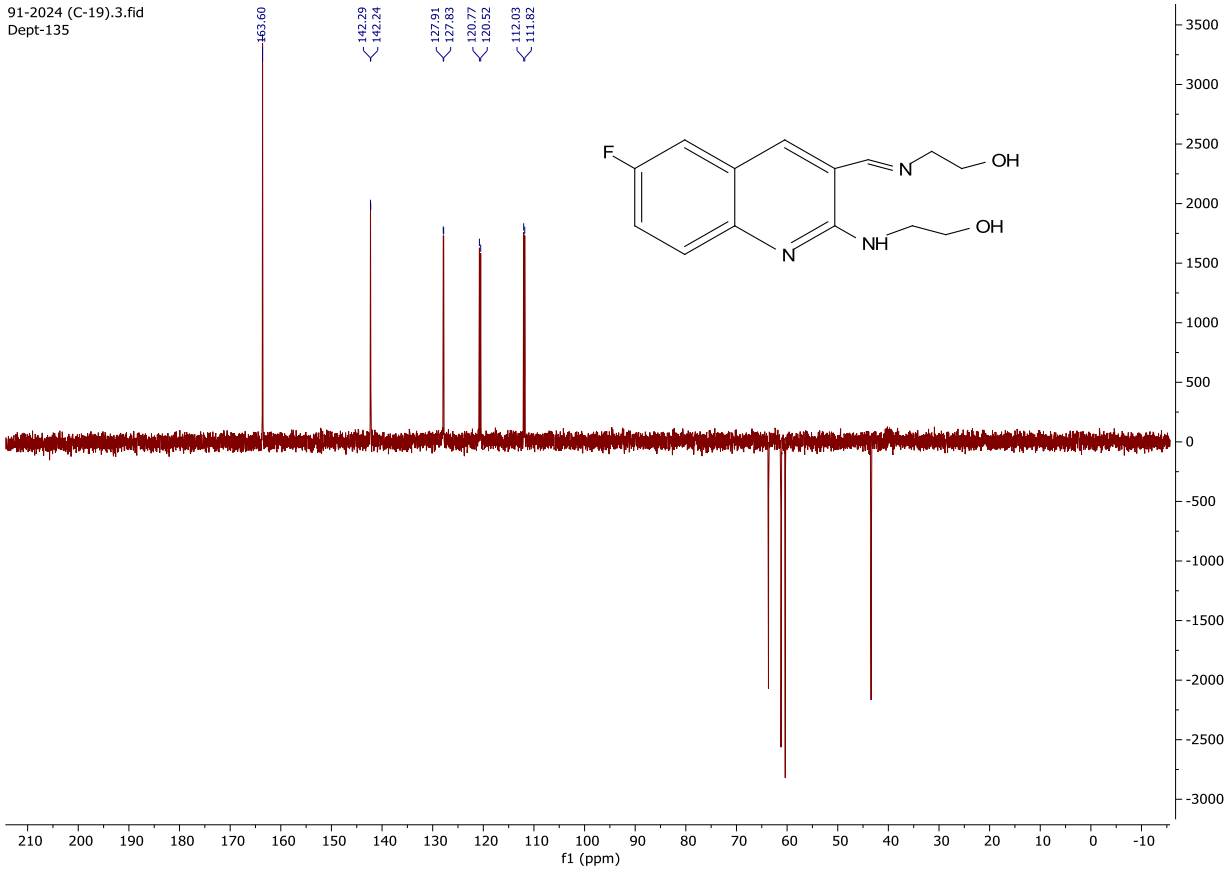

Appendix 16: ^{1}H NMR spectrum (400 MHz, $CDCl_3$) of 6-fluoro-N-phenyl-3-((phenylimino) methyl) quinolin-2-amine (**91**)

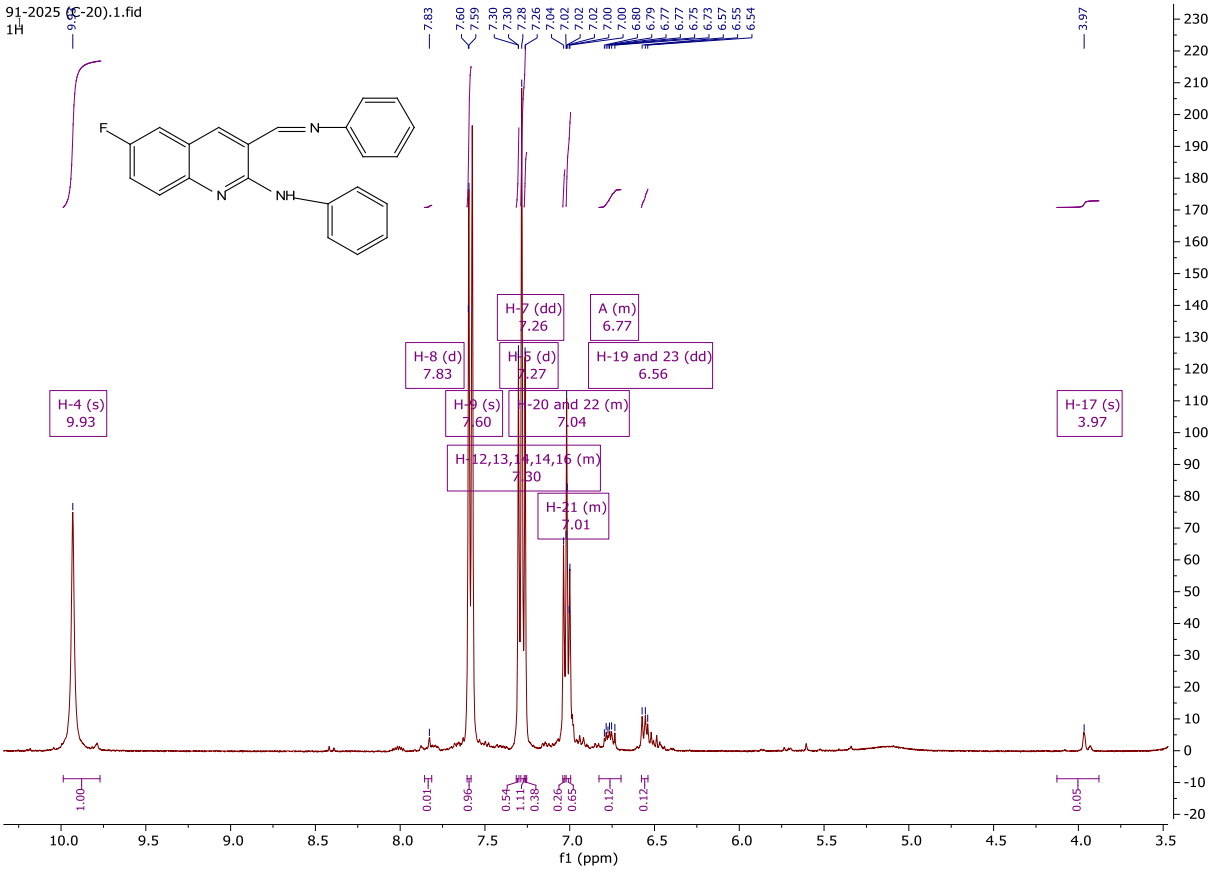

Appendix 17: ^{13}C NMR spectrum (100 MHz, $CDCl_3$) of 6-fluoro-N-phenyl-3-((phenylimino) methyl) quinolin-2-amine (**91**)

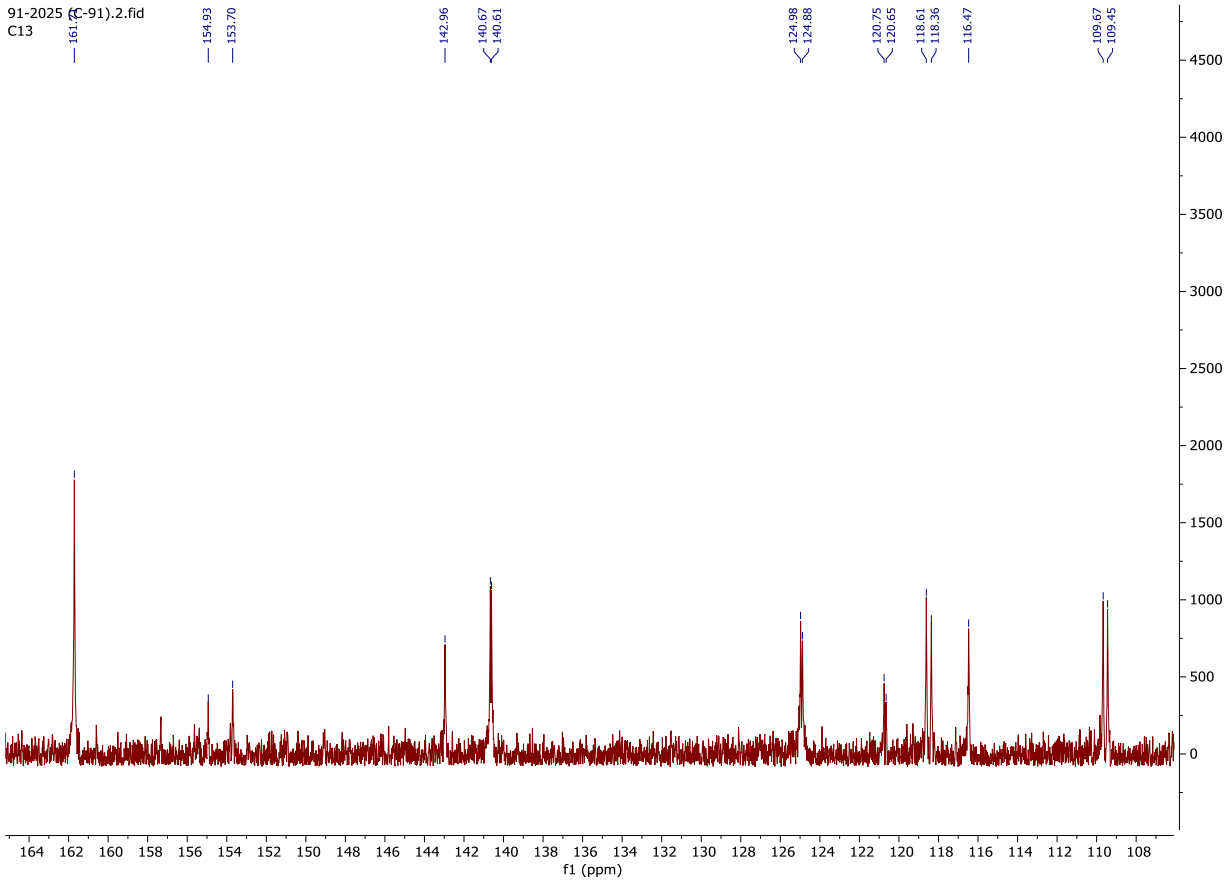

Appendix 18: DEPT-135 NMR spectrum of 6-fluoro-N-phenyl-3-((phenylimino) methyl) quinolin-2-amine (**91**)

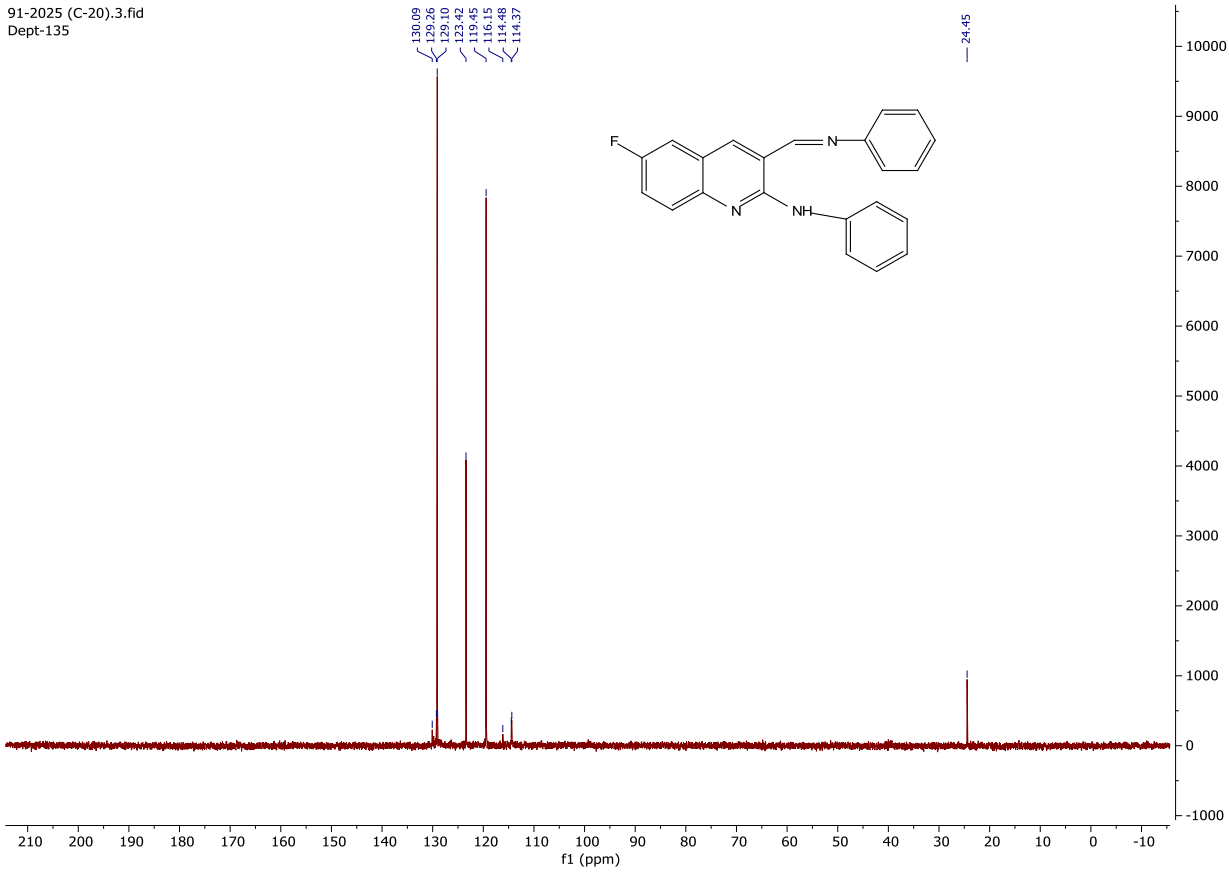

Appendix 19: ^{1}H NMR spectrum (400 MHz, $CDCl_3$) of 2-methoxyquinoline-3-carboxylic acid (**96**)

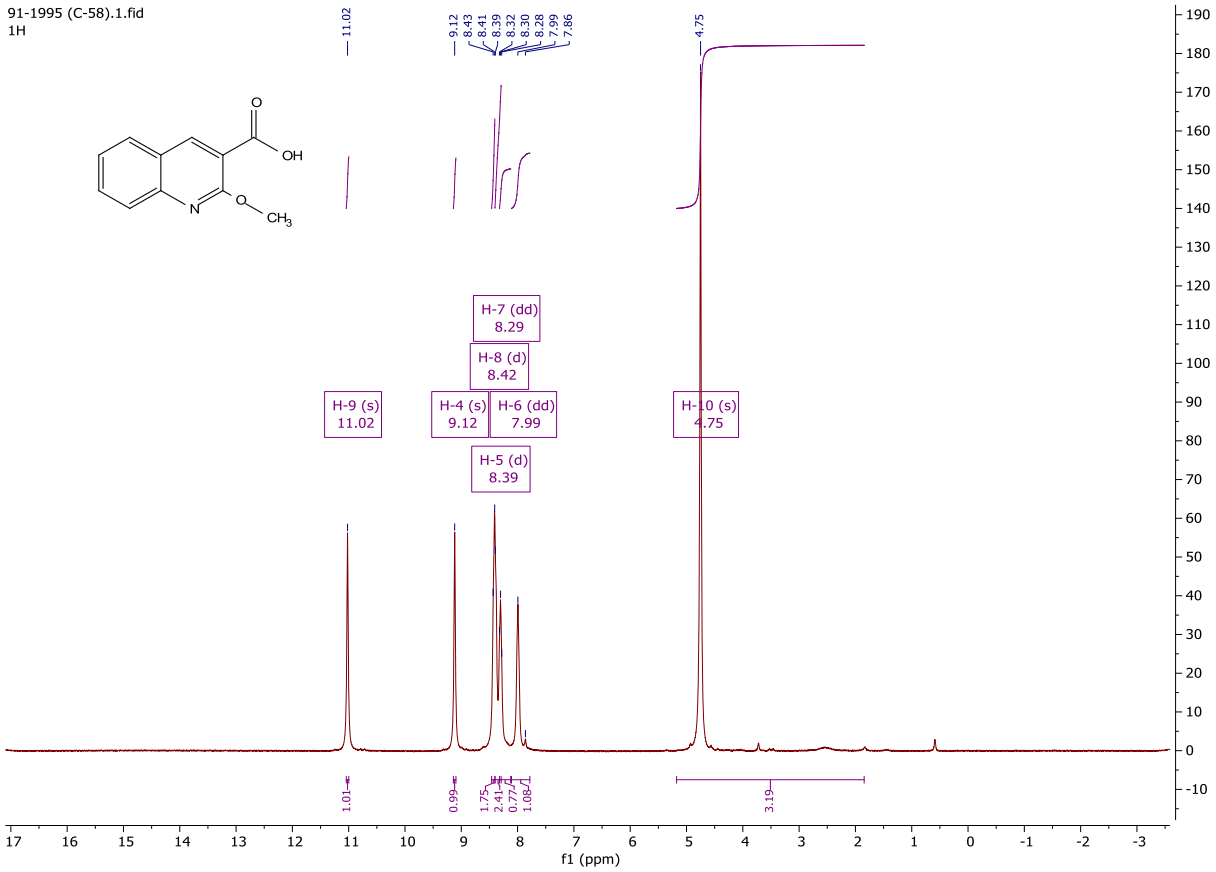

Appendix 20: ^{13}C NMR spectrum (100 MHz, $CDCl_3$) of 2-methoxyquinoline-3-carboxylic acid (**96**)

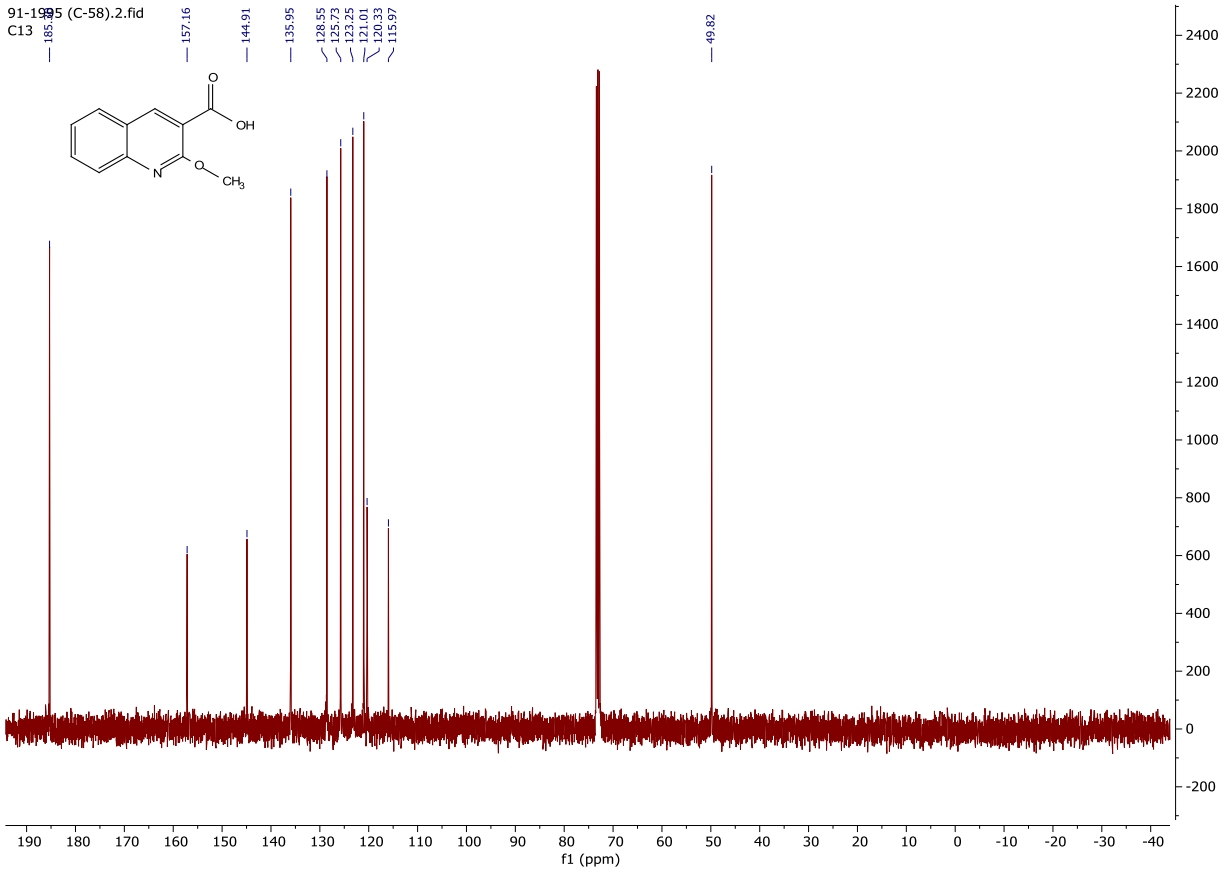

Appendix 21: DEPT-135 spectrum of 2-methoxyquinoline-3-carboxylic acid (**96**)

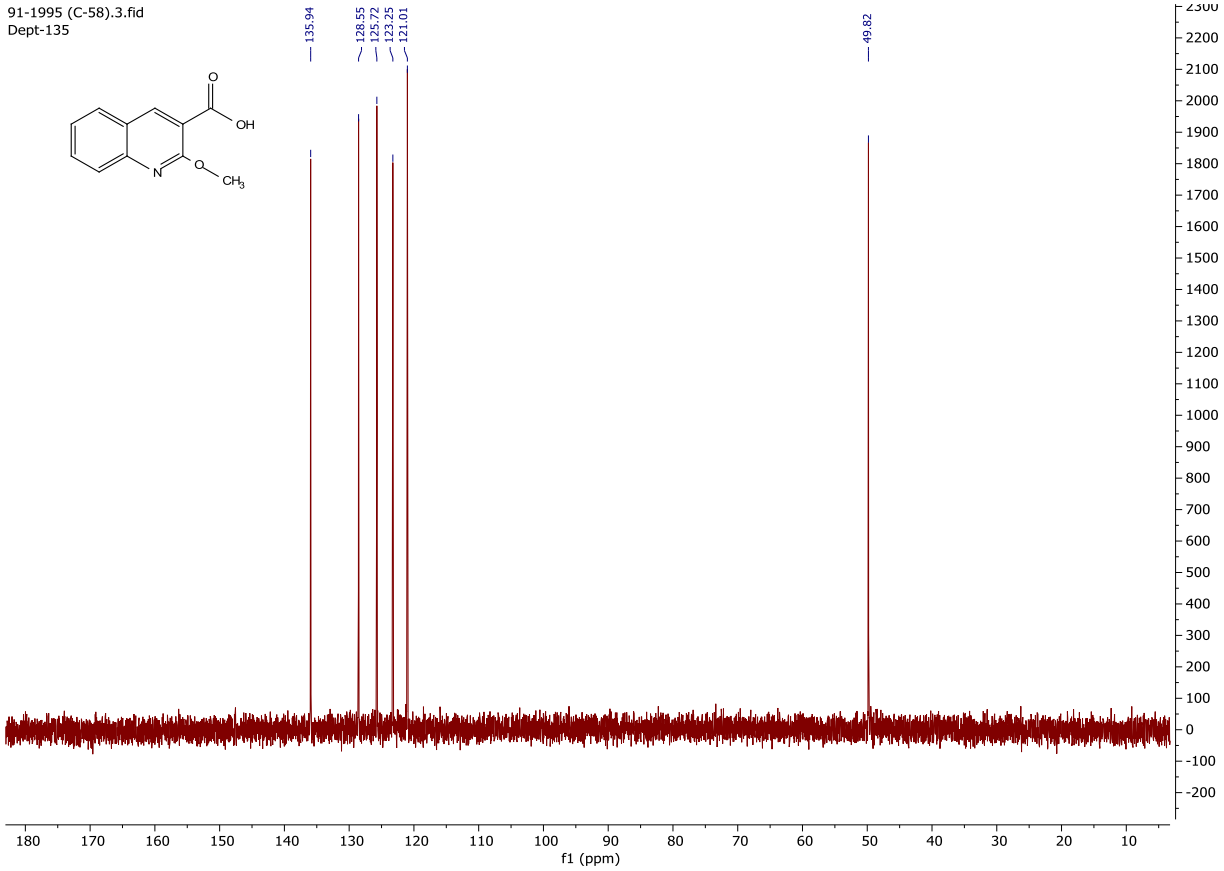

Appendix 22: ^{1}H NMR spectrum (400 MHz, $CDCl_3$) methyl 2-chloroquinoline-3-carboxylate (**97**)

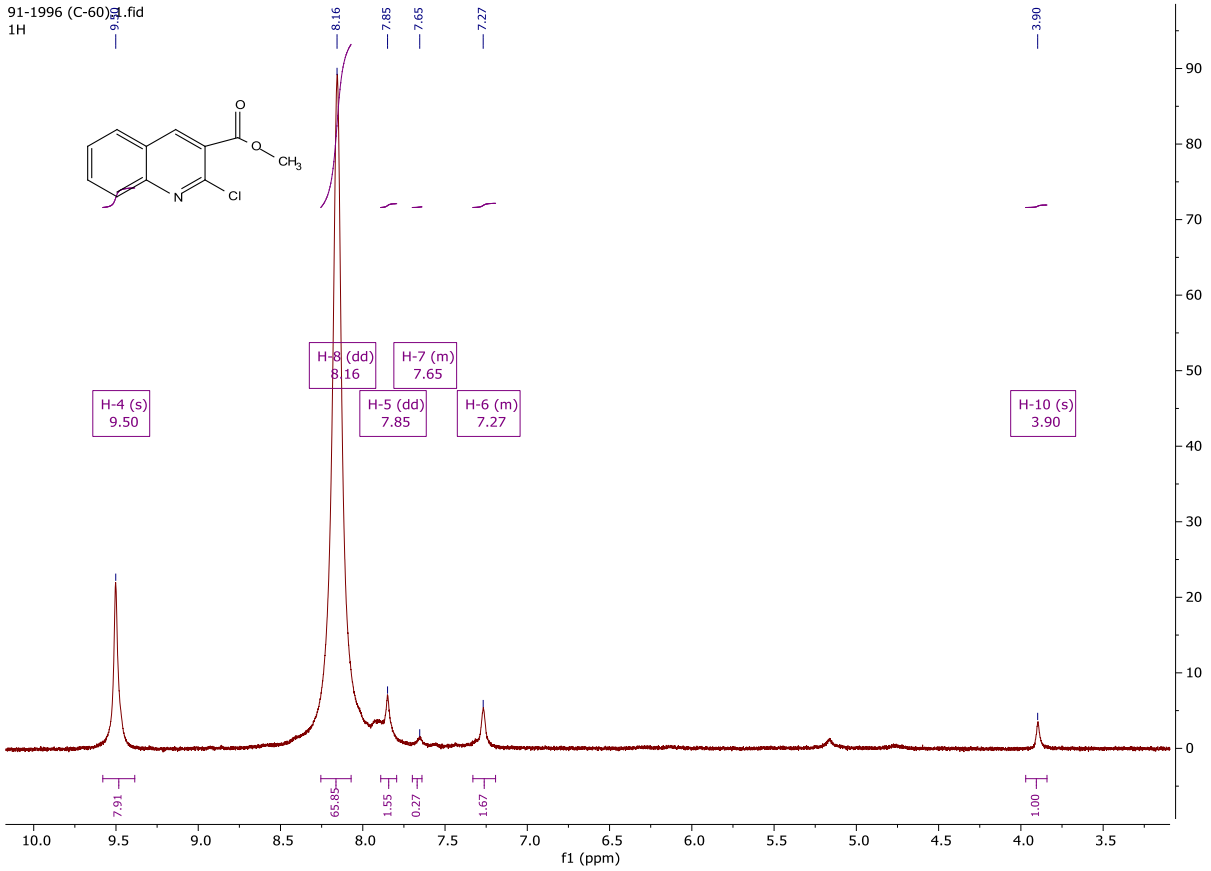

Appendix 23: ^{13}C NMR spectrum (100 MHz, $CDCl_3$) of methyl 2-chloroquinoline-3-carboxylate (**97**)

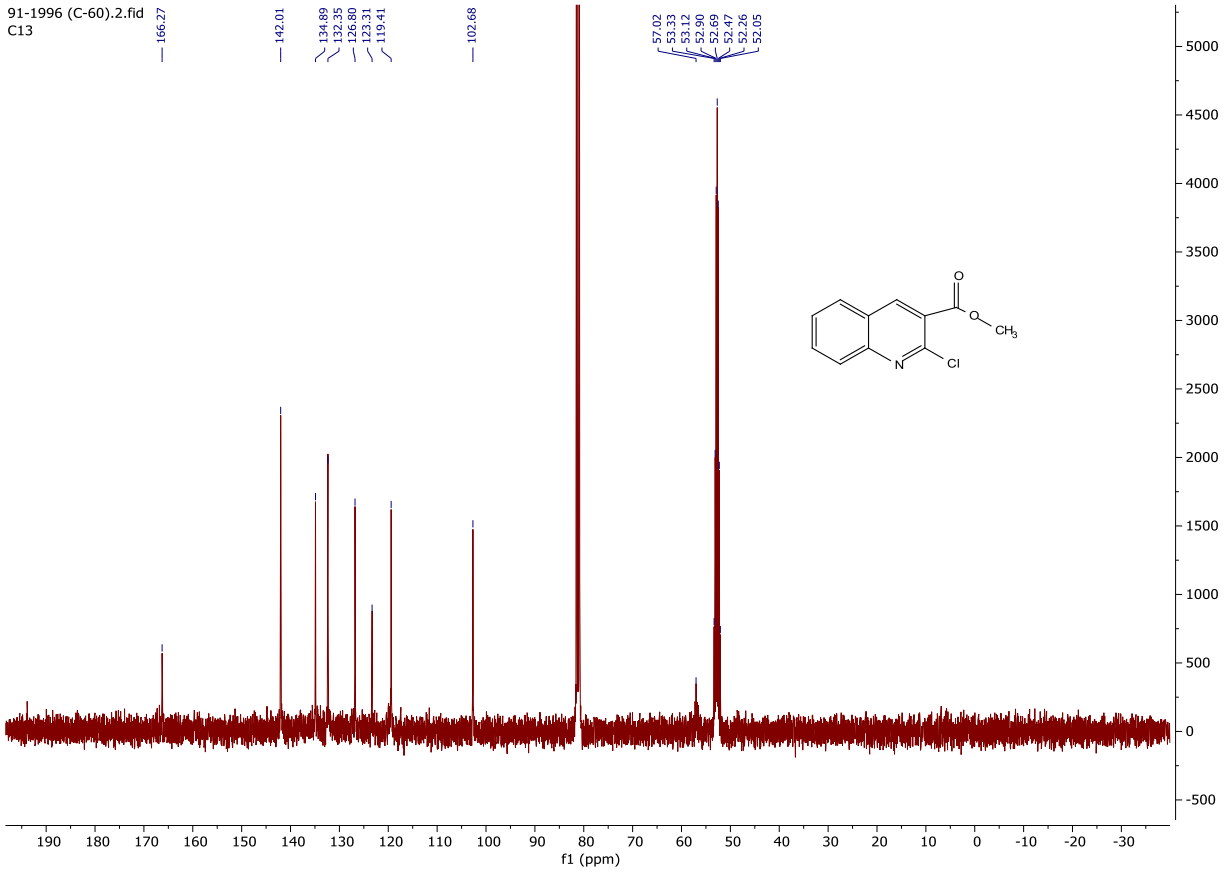

Appendix 24: DEPT-135 spectrum of methyl 2-chloroquinoline-3-carboxylate (**97**)